

Characterization of quality of railway track and train based on vibration analysis of track



Jyoti Kumar Barman

Department of Electrical Engineering

Assam Engineering College

Gauhati University

This thesis is submitted to

Gauhati University as requirement for the degree of

Doctor of Philosophy

I would like to dedicate this thesis to my teachers, parents, wife, family and friends.

Declaration

I hereby declare that this thesis is the result of my own research work which has been carried out under the guidance of Prof. (Dr.) Durlav Hazarika of Assam Engineering College. I further declare that this thesis as a whole or any part thereof has not been submitted to any university (or institute) for the award of any degree or diploma.

This thesis contains less than 90,000 (ninety thousand) words excluding bibliography and captions.

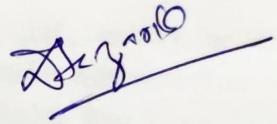


Jyoti Kumar Barman
December 2020

Certificate

This is to certify that the thesis titled "Characterization of quality of railway track and train based on vibration analysis of track" is the result of research work of Jyoti Kumar Barman, carried under my supervision, submitted to Gauhati University for the award of the degree of Doctor of Philosophy in Electrical Engineering.

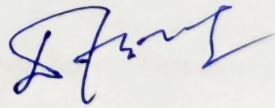
This thesis conforms to the standard of PhD Thesis under Gauhati University including the standard related to plagiarism and has a similarity index not more than 20% (twenty percent), excluding the bibliography.



Prof. (Dr.) Durlav Hazarika, Supervisor
December 2020

Members of the Research Advisory Committee:

Dr. D. Agarwal, Department of Electrical Engineering, AEC



Dr. A. Bardalai, Department of Electrical Engineering, AEC



Dr. A. Ganguly, Department of Electrical Engineering, AEC



Acknowledgements

I would like to show immense gratitude to my supervisor, Prof. (Dr.) Durlav Hazarika, Professor, Department of Electrical Engineering, Assam Engineering College. I sincerely thank him for his exemplary guidance and encouragement, without whose guidance and persistent help, this project would not have been materialized.

I am indebted to the Department of Electrical and Instrumentation Engineering, Assam Engineering College. I would like to acknowledge Prof. (Dr.) Damodar Agarwal, head of the department and all the faculty members of the department for their enthusiastic support and encouragement I received throughout this endeavor.

I would like to acknowledge the North-East Frontier Railway(NFR) authority, for their wholehearted support in carrying out the experiments. The experiments were carried out on the permission and supervision of NFR. I express my sincere thanks to Mr. Ajay Kumar, DEN, Guwahati for his permission and suggestion to carry out the project under the supervision of Mr. Gopal Das, Senior Section Engineer (P-Way), Bamunimaidan, Guwahati.

I would also like to acknowledge the Assam Don Bosco University, especially the department of Electrical and Electronics Engineering for constant help, support and encouragement I received throughout this endeavor.

I am indebted to my parents, family and friends for their belief in me and for being a constant source of encouragement.

Finally I would like to thank my wife Mrs. Pallabi Pathak for her constant support and encouragement.

Abstract

Railway safety is a major concern throughout the world. Unfortunately, railway accidents are common and a good number of them occur due to derailment of the train off the track. One way to minimize the accidents due to derailment, is to ensure proper health of the train and the track. This can be achieved by condition monitoring of the train and the track. Condition monitoring of railway vehicles and track has been a major thrust area of research. Although a lot of work is done towards this goal, still a lot needs to be done to achieve satisfactory results. In this work, a few trains of North-East Frontier Railway(NFR) are considered for analysis. A suitable live track at Chandmari, Guwahati, Assam, India is selected for sensor attachment; as suggested by the NFR authority. Two sensors viz. ADXL335 and MPU6050 are used as sensing devices while Arduino boards are utilized as development boards. The vibration signals generated by the trains while in motion over the track, are captured by the sensors attached to the fish-plate of the track. The captured vibration signals are transferred and stored in a laptop. Many signal processing techniques in time-domain, frequency-domain, time-frequency domain, statistical measures and Graph Signal Processing technique are utilized for the analyses of these signals. These vibration signals contain information regarding both the train and the track. By analyzing these vibration signals, modelling of railway track is achieved, faults are detected and also the trains are categorized in different categories.

Table of contents

List of figures	xvii
List of tables	xxi
1 Introduction	1
1.1 Importance of condition monitoring of a system	1
1.2 Vibration signal as an indicator of health of machine and railway tracks and trains	4
1.3 Literature survey	6
2 Development of a mathematical model for a railway track using a gray-box modelling technique	17
2.1 Introduction	18
2.2 Modelling of Railway track system	20
2.2.1 Determination of peak time t_p	26
2.2.2 Calculation of Rise Time t_r	27
2.2.3 Calculation of Delay Time t_d	28
2.3 Experimental Results and validation of the model	29
2.4 Discussion	33
2.5 Conclusion	35
3 Condition monitoring of NFR trains with measurements from a single wayside 3D vibration sensor	37
3.1 Introduction	38
3.2 Scheme for capturing vibration of a railway track using ADXL335 sensor: .	40
3.3 Information about the trains:	41
3.4 Experimental results and analysis:	43
3.4.1 Information from time-domain analysis:	43

3.4.2	Information from frequency domain analysis:	51
3.5	Discussion	56
3.6	Conclusion	56
4	Linear and Quadratic Time-Frequency Analysis of Vibration for Fault Detection and Identification of NFR Trains	57
4.1	Introduction	58
4.2	Theoretical background	60
4.2.1	Wavelet transform optimized for local extrema detection	60
4.2.2	Wigner-Ville transform for localization of impulses	63
4.3	Capturing of the vibration signal generated by a train running over a track, using an ADXL335 sensor	64
4.4	Experimental results and analysis:	66
4.4.1	Information from wavelet transform	68
4.4.2	Information from Wigner-Ville transform	70
4.5	Discussion	71
4.6	Conclusion	74
5	Health Monitoring of a few Passenger Trains Using Statistical Measures and Graph Signal Processing	75
5.1	Introduction	76
5.2	MPU6050 measurements of the different trains under study	77
5.3	Time-Domain Features	79
5.3.1	Definitions and mathematical formulae of the time-domain features considered	79
5.4	Experimental results and analysis	79
5.4.1	Selecting proper signals for correlation	82
5.4.2	Signal analysis	82
5.4.3	Calculation of the time-domain features	83
5.5	Graph Signal Processing on the vibration signal	83
5.5.1	Mathematical analysis of Graph Signal Processing (GSP)	90
5.6	Discussion	100
5.7	Conclusion	101
6	Conclusion	103
	References	105

Table of contents	xv
-------------------	----

Appendix A List of publication	113
---------------------------------------	------------

Appendix B List of papers communicated	115
---	------------

List of figures

1.1	The classic Bathtub Curve of a life cycle of a machine	3
1.2	Schematic of railway structure.	7
1.3	Classification of condition monitoring of railway structure.	10
2.1	Five subsystems of the vehicle/track system.	22
2.2	Track resting on a simple support.	22
2.3	Distributed sleeper model	23
2.4	Discrete sleeper model	23
2.5	Scheme adopted for development of model for railway track system	24
2.6	Block diagram for extracting vibration signals from the railway track	29
2.7	Experimental set-up for capturing 3-D vibration signals from railway tracks.	30
2.8	The orientation of the MPU6050 sensor axis with reference to the railway track	31
2.9	Vibration signal of Z axis of Rajdhani Express	31
2.10	Filtered Vibration signal of Z axis of Rajdhani Express	32
2.11	Filtered Vibration signal of Z axis of Rajdhani Express with Key Parameters	32
2.12	Filtered Vibration signal of Z axis of Kamrup Express	32
2.13	Filtered Vibration signal of Z axis of Kamrup Express with Key Parameters	33
3.1	Block diagram for extracting vibration signals from the railway track	40
3.2	Experimental set-up for capturing 3-D vibration signals from railway track.	41
3.3	The orientation of the ADXL335 sensor axis with reference to the railway track	42
3.4	Vibration Vs Time of Kamrup Express	44
3.5	Vibration Vs Time of Kopili Express	45
3.6	Vibration Vs Time of Kolangpar Express	46
3.7	Vibration Vs Time of Rajdhani Express	47
3.8	Vibration Vs Time of Rajendra Express	48
3.9	Concept of an impulse	50
3.10	Cross Power Spectrum Density for Kamrup Express	54

3.11	Total power of different trains at different frequency bands	55
4.1	Block diagram representation of the scheme to capture vibration signals generated by a train while in motion over a track.	64
4.2	Experimental set-up for capturing vibration signals from the railway track.	65
4.3	The orientation of the ADXL335 sensor axes with the reference to the railway track.	65
4.4	(a) Wavelet Transform applied to X-axis vibration signal of Kamrup Express with $p=2$. (b) Wavelet Transform applied to Y-axis vibration signal of Kamrup Express with $p=2$. (c) Wavelet Transform applied to Y-axis vibration signal of Kamrup Express with $p=2$	67
4.5	Vibration(Acceleration) of Rajdhani Express in Z-axis.	68
4.6	(a) Wavelet Transform applied to vibration signal of Rajdhani Express with $p=2$. (b) Wavelet Transform applied to vibration signal of Rajdhani Express with $p=4$. (c) Wavelet Transform applied to vibration signal of Rajdhani Express with $p=6$. (d) Wavelet Transform applied to vibration signal of Rajdhani Express with $p=8$	69
4.7	Wigner-Ville transform applied to vibration signal of Rajdhani Express. . .	70
4.8	Wheel-flat detection by calculating the distance and occurrence of the burst of energy.	71
4.9	Wigner-Ville transform applied to vibration signal of Kamrup Express. . .	72
4.10	Wigner-Ville transform applied to vibration signal of Kolongpar Express. .	72
4.11	Wigner-Ville transform applied to vibration signal of Kopili Express.	73
5.1	Vibration signal acquisition and sensor orientation	78
5.2	ECDFs of Rajdhani Express.	81
5.3	Gyroscope orientation	82
5.4	The 3-axis vibrations of Rajdhani Express	83
5.5	Gyroscope signal obtained from Rajdhani Express	90
5.6	Velocity signal obtained from Rajdhani Express	91
5.7	Correlated signals obtained from Rajdhani Express	92
5.8	Graph generated from the weight matrix of the statistical parameters. . . .	97
5.9	Graph Fourier Transform (GFT) of the graph obtained from the vibration signals of the database	98
5.10	Graph Fourier Transform (GFT) of the vibration signal on the graph of the Rajdhani Express.	98

5.11 Graph Fourier Transform (GFT) of the vibration signal on the graph of the Kamrup express.	99
5.12 Graph Fourier Transform (GFT) of the vibration signal on the graph of the Kolongpar express.	99

List of tables

1.1	Summary of previous works on mathematical modelling of railway system .	11
2.1	Key contributions to the railway track modelling	21
3.1	Slip tendency and derailment tendency	49
3.2	Power w.r.t Frequency analysis: X-axis	51
3.3	Power w.r.t Frequency analysis Y-axis:	52
3.4	Power w.r.t Frequency analysis Z-axis:	52
3.5	Total Power from Frequency analysis	52
3.6	Power calculations of different trains along X-Z directions	53
3.7	Power calculations of different trains along Y-Z directions are tabulated below:	53
4.1	Detection of wheel-flat.	71
5.1	Time-domain features	80
5.2	Time-domain features of Rajdhani Express	84
5.3	Time-domain features of Kamrup Express	85
5.4	Time-domain features of Kolongpar Express	86
5.5	Comparison along X-Axis and Yaw correlated signal	87
5.6	Comparison along Y-Axis and Pitch correlated signal	88
5.7	Comparison along Z-Axis and Roll correlated signal	89
5.8	Statistical parameters of vibration signals from the database	95
5.9	Correlation coefficient	96
5.10	Quantification of health condition of the trains in comparison with the database	100

1

Introduction

1.1 Importance of condition monitoring of a system

The assessment of system features for estimating the system condition is generally called condition monitoring. Condition monitoring of a system is a process to monitor one or more key parameters such as vibration, temperature etc. so as to find out the operating condition, efficiency etc. of the system that enables one to estimate the overall health of the system. Condition monitoring helps one collect all the necessary data that can ensure timely maintenance of any system thereby reducing overall cost of repairing and downtime. Once a machine is installed, it is important to monitor its health. Smooth operation of a plant depends on smooth operation of its different components; where different machines, machine-trains and other components become very important. Proper maintenance of these components ensures smooth running of the plant and operation. With proper maintenance, sudden breakdown of different machines can be avoided. Also proper monitoring ensures timely repair of faulty parts and replacement of damaged parts. Hence a proper schedule for different activities can be maintained and a smooth transition of plant status from working to shutdown and shutdown to working can be achieved. Same philosophy may be extended to the railways. By proper monitoring of train and track condition one can achieve timely repair of different train components as well as the tracks. The purpose of condition monitoring is to

achieve timely detection of different deterioration and rectify different faults before any major breakdown occurs. Proper condition monitoring in railways will ensure minimum downtime of track or different trains. Passenger comforts can also be taken care of by condition monitoring of railways. Good health of tracks and trains will ensure minimum accidents by minimizing derailment incidents. Railways are one of the most common, economical and widely used modes of transport throughout the world. In India, it is very widely used, Indian Railways run more than 20,000 passenger trains daily. In India, lakhs of people use trains daily for their commute. Hence maintaining the trains and track at their best of health is very necessary. Condition-based maintenance for railways can ensure minimum downtime and safety for the passengers. Condition Based Maintenance(CBM) is a well researched field especially in application to rotating machines. As far as CBM is considered for railways, although a lot of work has been reported but mostly it is restricted to finding wheel defects, suspension and bearing faults. For maintenance, generally three schemes are followed; viz. Breakdown maintenance, Preventive maintenance and condition-based maintenance [1]. Breakdown maintenance is used when the machine under consideration is of non-critical nature. If the machine or the components under consideration are not costly, easily available, then this type of maintenance can be considered. Also downtime of the plant or the process due to this type of maintenance should not be very large i.e. the machinery under consideration is not only cheap and available but also should be easily replaceable. For the plant and the processes where downtime due to particular machinery can bring significant loss, or there are safety issues, this type of maintenance is not acceptable. Preventive maintenance is the kind of maintenance, where a fixed schedule of maintenance is maintained. Generally this schedule is fixed based on experience or some industry standards. A fixed interval such as 3000 operating hours or once a year is common [1]. Although this type of maintenance is quite common in many industries it may not be the best type of maintenance as there may be some sudden breakdown if all the components are not monitored properly and consistently. Sudden breakdown may increase loss of production time, also it will be time consuming to find out the fault, whether to repair or replace etc. Without proper monitoring the quality of products may deteriorate and simply replacing the machinery at a regular interval can not guarantee that there will be no sudden breakdown and in many cases replacing all the components after a fixed interval may not be necessary. Condition-based maintenance is superior compared to the previous two schemes especially if the process or machinery under condition is of critical nature. As mentioned before, replacing everything at a regular interval may not be necessary and again some components may break down before their lifespan. Hence condition based maintenance is a good approach for critical applications. Also regular monitoring may indicate when some machinery can break down

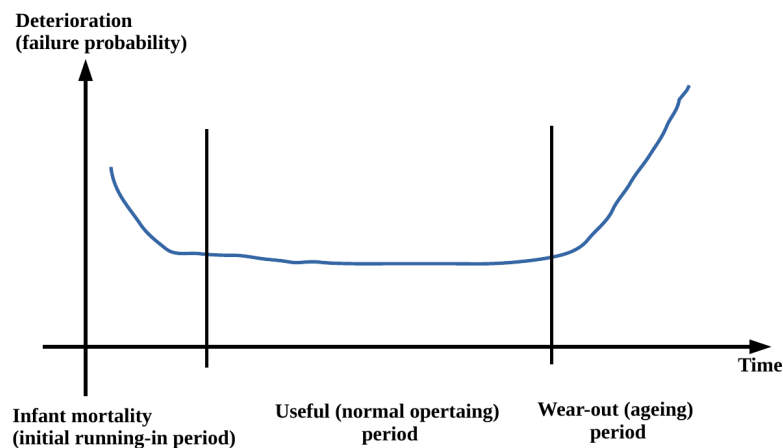


Fig. 1.1 The classic Bathtub Curve of a life cycle of a machine [1]

and the operators can be prepared to replace or repair beforehand. Overall condition-based maintenance is a good approach to prevent sudden breakdown and also useful in increasing overall safety. Generally a machine's life can be indicated by the classic *bathtub curve* as shown in fig. 1.1 [1].

Railway system is complex and various factors affect their aging process and thereby changing their behavior pattern over time. Smooth operation of a railway system depends on the components such as rolling stock(the vehicle) and the infrastructure(the tracks, signaling, power supply and passenger facilities) [2]. Again in the vehicle there are many components such as the wagon itself, primary and secondary suspensions, the bogie and the wheels. The track system consists of the track which sits upon sleepers which are in turn spread over ballast and the entire structure is on the properly made substrate on the ground. It is of the utmost importance to keep these components at their best health to ensure passenger comfort and safety. In this type of system such as railway system breakdown maintenance is not acceptable at all while preventive maintenance may not yield the best result. *Condition-based maintenance is the best option for such critical systems to operate smoothly.* Condition monitoring can be achieved by different methods such as aural, visual, operational variables, temperature, wear debris and vibration [1]. Aural and visual methods are quite simple and used by personnel with quite experience in their field. Aural method involves simply listening to the sound produced by the machine or machine component and estimating any change in operating condition of the machine. Sometimes a microphone can be used for a better observation. Visual inspection may include observing the amplitudes of the vibration produced and/or any change noticeable. Visual inspection also involves monitoring for any color change in the hot area of the system which may be an indicative of unusual heat production. For electrical systems, monitoring of currents and voltages are very important.

Operational variable methods involve measuring of different variables associated with the process. Constant monitoring of current, voltage, temperature etc. falls under this category. Wear debris is generally generated where there is any moving component. This can be found in lubricating oils, grease etc. *Vibration monitoring is most widely used because of its reliability and ability to find out the condition of different components of a system.*

1.2 Vibration signal as an indicator of health of machine and railway tracks and trains

Vibration analysis as a tool for diagnosis and predictive health maintenance is based on the fact that all mechanical equipment while in motion generates some vibration. This generated vibration is unique for different machines and is an indicator of its operating conditions. This is also called the signature of that machine as the generated vibration profile is unique for different machine and machine components. Whether the motion is linear, rotating or reciprocating, vibration analysis can be used for diagnosis and preventive measures. The major advantages of vibration analysis are that *it is non-destructive and can be used online, that is when the system is operating.* The system need not to be shut down nor does it require any opening of the system and system components. Properly implemented vibration based condition monitoring can be a very reliable and efficient mode of condition monitoring. It promises to provide data that is sufficient to analyze and find out any shift in operating condition, probable failures in near future or if there is any urgent action to be taken. The dynamics of a railway vehicle represents a balance between forces acting at the wheel-rail interaction, suspension forces and inertia forces. The excessive response of the rail vehicle to track irregularities can result in poor guidance and ride quality which may increase wear on the wheel and rail, and can lead to derailment [3]. Vibration analysis for railways is a popular technique. By properly utilizing the analysis of vibration signals generated by the train running over a track one can design a simple yet effective condition monitoring technique for the train track system. An increase in vibration indicates aging. Vibration may increase due to wear-out, axle bend, change of damping due to aging etc. Thus monitoring the vibration level proves to be a good condition monitoring technique. Vibration based condition monitoring approach can be classified in the following categories:

- Time domain
- Frequency domain
- Time-Frequency domain

- Quefrequency domain

Time domain analysis and frequency domain analysis are the most discussed approaches in literature [4].

Time domain: Time domain approaches aim to compute signal statistics and signal shape factors characterizing periodic behavior. Since time domain data rely on historical perspective of the vibration data it is important to normalize the collected data so as to remove influence of variables such as load etc. Reference or baseline data may be prepared for each machine during installation when the machine is certified to be of good condition. The most used time domain features are: *Root Mean Square(RMS)*, *mean*, *peak value*, *crest factor*, *skewness* and *kurtosis*. The RMS is used to compute the average power of the system's vibrations. The mean is estimated in the rectified vibration signal because in raw signals the mean remains close to zero. These features are expected to increase when machines deteriorate. Peak value and crest factor catches instantaneous accelerations or burst closely related with cracks and indentations. Skewness and kurtosis are respectively the third order and the fourth order signal's statistical moment. *For normally distributed data, skewness = 0 and kurtosis = 3*; these reference values allow to track shifts in the condition. Force generated by the machines or different components of the machine may be captured by the accelerometer data. RMS value of the acceleration is the best measure for this type of analysis [5]. While the vibration data may be compared with the baseline data to find out its condition another method of comparison is to compare the data with industrial standards. The International Standards Organization (ISO) established the vibration-severity standards (ISO 2372 is such a standard). These data are applicable for comparison with filtered narrow-band data taken from machine-trains with true running speeds between 600 and 12,000 rpm. The values from the table include all vibration energy between a lower limit of 0.3X of true running speed and an upper limit of 3.0X. For example, an 1,800-rpm machine would have a filtered narrow-band between 540 (1,800 X 0.3) and 5,400 rpm (1,800 X 3.0) [5].

Frequency-domain: Only time-domain analysis is not sufficient for proper diagnosis of a machine or structure. Time-domain only provides limited information. However in frequency analysis we can find out the concentration of energy around distinct frequency components. Since the dynamic characteristics of individual components of the system are usually known, we can relate the distinct frequency components (of the frequency response) to specific components [6]. FFT is one of the most widely used method to find out frequency spectrum of a vibration signal and that help us finding energy components of the signal about different

specific frequencies. The phrase full Fast Fourier Transform (FFT) signature is usually applied to the vibration spectrum that uniquely identifies a machine, component, system, or subsystem at a specific operating condition and time [5]. The vibration signal generated depends on the machines, machine components, mounting, installation and operation. The peaks of the spectrum represent various machine components. Various frequencies regarding different components like bearings, gearbox, pumps, fans, pulleys may be calculated and can be used to relate these frequencies to the different peaks of the spectrum. Similarly other frequencies for misalignment, looseness, unbalance etc can be calculated.

1.3 Literature survey

Railway structure is a complex system. A schematic of this massive structure is shown in fig. 1.2. The car is connected to the bogie by a suspension system known as the *secondary suspension*. The bogie and wheel are connected via another suspension known as the *primary suspension*. Wheels are in direct contact with the rail, while the rail is placed on the sleepers with *rail-pads* in between. Sleepers are generally placed on the stone ballast, which in turn is placed over the subgrade. Subgrade is prepared in accordance with the soil conditions.

From a mathematical modelling point of view this structure is studied as single components or as a group of components as a *subsystem*. The vehicle itself is modelled by Discrete Elements Methods (DEM). The track is modelled as a Timoshenko beam or Euler-Bernoulli beam resting on discrete support. Analysis of the track is generally carried out by Finite Element Methods (FEM) technique. Rail-pads are generally modelled as mass-less spring-dampers. Sleepers are modelled as rigid elements connected by spring dampers in some cases while in some cases they are modelled as continuous distribution of mass. Ballasts are sometimes modelled as vibrating mass connected by spring-damper in both horizontal and vertical directions. Sometimes again ballasts are modelled as continuous dampers. Generally FEM technique is used for analysis. These are described in detail in the next paragraph.

In 1926, Timoshenko published "Method of analysis of statistical and dynamical stresses in rail", which is one milestone literature in railway structure especially the rail [7]. Grassie et al. in their work presented the shortcomings of the existing models and proposed a new model to overcome these shortcomings. The Euler beam model of the railway track resting on a continuous uniform, damped elastic foundation is not sufficient in the frequency range of 50-1500 Hz. A new continuous model was developed where rail-pads and ballast were considered as continuous dampers; sleepers were considered as continuous distribution of

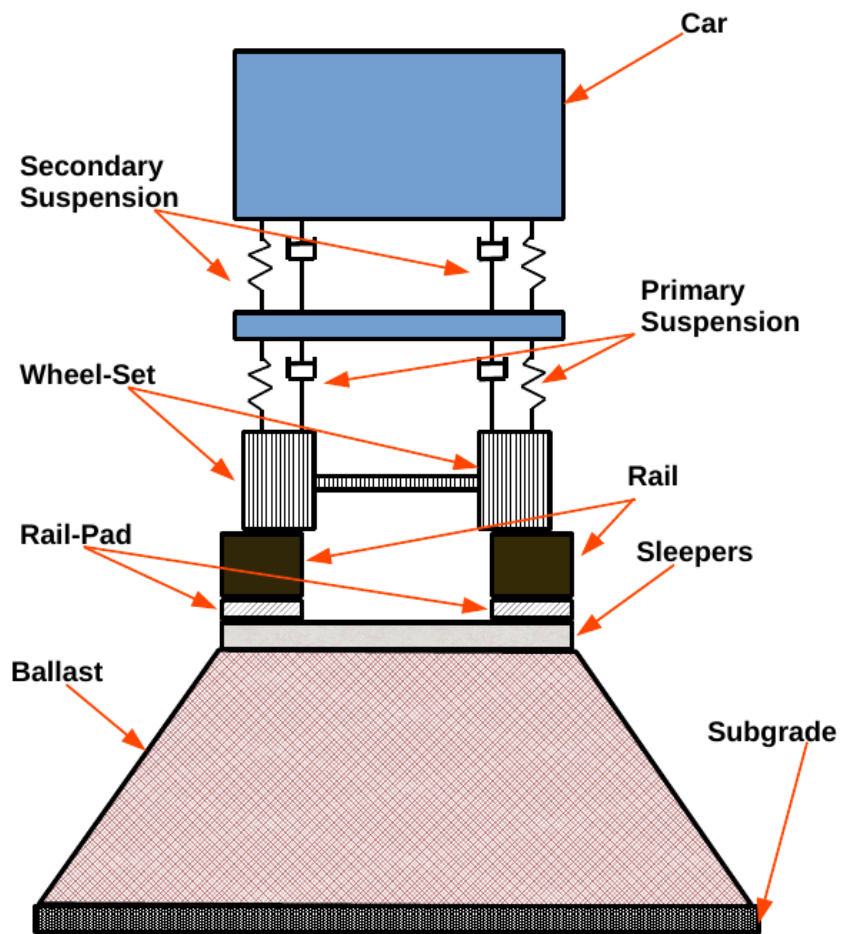


Fig. 1.2 Schematic of railway structure.

mass. The shear and rotational inertia were incorporated by considering the track as a Timoshenko beam rather than a Euler beam. The wheel was represented by a concentrated mass in contact with the rail through a linearized Hertzian spring. The model was utilized to understand the contact force on the track especially with corrugation [8]. Knothe et al. in their review work emphasized the fact that the modelling of railway structure is to solve practical problems. The problems can be classified into problems of vehicle dynamics, problems involving components of the bogie and unsprung mass, deterioration of wheel and rail surfaces, deterioration of track components and noise. To study these problems the railway system can be subdivided into five subsystems viz. i) the vehicle, including the car body, bogie and wheel-set ii) wheel rail contact and representation of excitation iii) the rail iv) the fastening system, including the rail fastening itself and the rail pad and v) the sleeper. The remaining components are the sleeper support including the ballast and the substrate. These subsystems can be modelled individually to study deep into the structures. Solutions of these models can be achieved in either frequency or time-domain techniques [9]. In the work of Dong et al., railway track was modelled with Finite Elements Methods (FEM). The rail was considered as long and represented by a Timoshenko beam on discrete pad-tie-ballast supports. The model developed considered a lot of factors such as loss of wheel-rail contact, rail lift-off from the tie and tie lift-off from the ballast etc. The model also considered the impact loads due to wheel flats [10]. Luo et al. presented a FEM model to study the ballast dynamics of a ballasted railway track, where the rail was modelled as a Timoshenko beam. The outcome of the study may be divided into three parts, viz. dynamics of the ballast due to slow moving, intermediate and fast moving trains. The results also indicate that the propagation of the vibration wave goes deep in the vertical direction, while the same gets attenuated in the horizontal direction [11]. Ferreira. et. al. suggested that the railway track modelling can be classified mainly in three categories, viz. microscopic, deterioration and macroscopic models. While microscopic models are aimed at detailed engineering analysis, macroscopic models are utilized for decision making in operation and maintenance. Deterioration models sit somewhere in between the microscopic and macroscopic models and are useful in condition monitoring, analyzing current engineering status and judging future life and maintenance schedule. While microscopic and deterioration models study the single track or single track components; macroscopic models are used for multi-component, multi-segment analysis. Macroscopic models are fully utilized for network analysis, maintenance planning, investment appraisal etc [12]. Dahlberg in his work suggested that the railway system could be described in three main parts: the train system, track system and the sub-structure. The train or the vehicle itself is a complex dynamic system whereas the track system with the rail, rail-pads and the sleepers is another complex

system. The sub-structure consists of the ballast and the subgrade. When one dynamic system interacts with another dynamic system, the dynamic effects in the compound system become pronounced. If the train is a fast moving one, then these effects are even greater. These interactions produce oscillations and vibrations that decrease the ride comfort and develop the settlements of the track. Settlement of a track is loss of the track level and or alignment. Generally these settlements are not uniform throughout the track although they are exposed to the same kind of loading. Therefore the settlements must be dependent on the track and sub-structure system rather than the loading by the train system. Hence modelling these systems and understanding is necessary to understand these settlements better. Dahlberg described theoretical modelling of track and sub-structure systems in different contexts such as static and dynamic loading, time-domain and frequency-domain modelling and also modelling of the track under track settlements [13]. Zhai et al. modelled ballast vibration considering the load transmission from sleeper to ballast. Shear stiffness and shear damping of the ballast were also considered in the model [14]. In the paper by El Kacimi et al. modelling was based on 3D FEM. The rail was considered as a 3D beam-column element in this model. A quarter train model was considered which was connected to the track based on the nonlinear Hertzian contact theory. The main aim of this model was to study the ground induced vibration due to passage of the train vehicles [15]. Azoh et al. mentioned that the vibration is inevitable in structural dynamics. Railway system is a complex structure which can be mainly classified as the vehicle and the track system. For modelling of the vehicle, Discrete Elements Method (DEM) is used whereas for the modelling of the track, Finite Elements Method (FEM) is used. The track is placed over the sleepers with rail-pads in between. The rail-pads are modelled as mass-less spring-dampers connected between the track and the sleepers. Subgrade provides a damping and stiffness effect. Authors modelled the sleepers as rigid elements connected by spring damper while the ballast was modelled as separate vibrating mass connected by spring-damper coupled together vertically and horizontally. The wheel-rail contact was modelled by massless springs. The vehicle was considered as a harmonic load vertically applied on the track structure and the dynamic effects of the train track components were studied during starting and steady state response [16]. Zygiene et al. developed a mathematical model of wheel-track considering the wheel-flat. For rail dynamics FEM was employed and linear, nonlinear, elastic and damping discrete elements were considered for the modelling [17]. Thompson et al. modelled the system keeping the noise in mind. Wheel and rail surface roughness is the major source of noise from railways. Authors had developed a mathematical model for better understanding of this phenomenon. The model revealed that the vibrations of both the wheel and rail are significant from a noise point of view [18]. For electrified rail track, Hill et al. presented a finite element

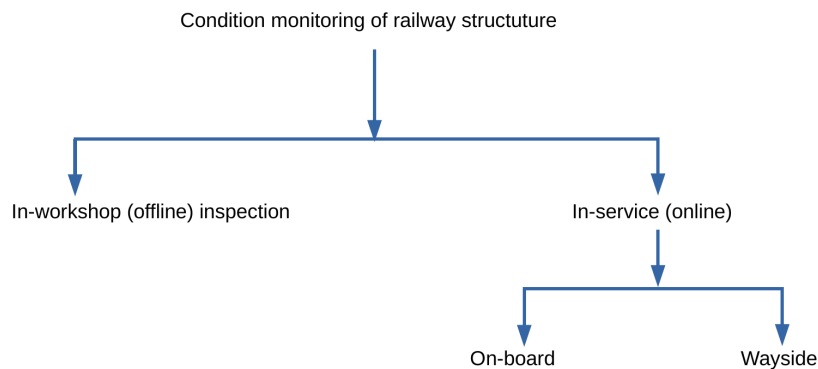


Fig. 1.3 Classification of condition monitoring of railway structure.

method that had been applied to establish the validity of the analytical models, and a practical method was described for the measurement of the mutual impedance between the individual rails [19]. Again, Berova presented a method for Audio Frequency Jointless Track Circuits (AFJTC) [20]. Cantieni discussed Forced Vibration Testing (FVT) and Ambient Vibration Testing (AVT) as the two methods used to identify the dynamic characteristics of a structure experimentally. While in FVT, the structure is excited with an artificial excitation, the AVT depends on natural excitation such as winds or seismic micro-tremors. The excitation and response is converted to frequency domain to understand the dynamics of the structure [21]. System identification in frequency-domain, obtained using arbitrary signals was developed by Pintelon et al. [22]. While de los Santos et al. talked about the convolution method with variable kernel where a moving vertical excitation produces deflection of the track so that the response to this excitation could be found out, Oyama et al. investigated railway track surface irregularities and an all-integer linear programming (AILP) optimization model was developed to obtain an optimal schedule of multiple tie tamper (MTT) operation [23], [24]. A summary of these works are presented in the table 1.1.

Condition monitoring of railway structure is mainly carried out in terms of Fault Detection and Identification (FDI). Condition monitoring of railway structure can be classified into in-workshop and in-service monitoring; again in-service monitoring is classified into on-board and wayside monitoring.

In on-board condition monitoring techniques, *different sensors such as accelerometers, thermocouples, strain sensors etc. are mounted on different components of the structure such as axle, bearing, suspension systems etc.* In wayside monitoring, *all the detection devices are installed along the side track or the rail. There has been a lot of work done in condition monitoring of railway structures.* Bencat utilized vibration from railway train track interaction to understand the ground vibration and soil characteristics [25]. Signal

Table 1.1 Summary of previous works on mathematical modelling of railway system

Sl.No.	Component	Modelling technique	Goal	Reference
1	Vehicle	Discrete Element Method (DEM), Harmonic load vertically applied on the track structure	Maintenance	[16]
2	Track	FEM, AFJTC, Timoshenko beam, Euler-Bernoulli beam	Maintenance, Development of software tools, Wheel-flat problem, High frequency response	[16], [10], [20], [8]
3	Rail-pad	Mass-less spring dampers, continuous dampers	Maintenance, High frequency response	[16], [8]
4	Sleepers	Rigid elements connected by spring dampers, continuous distribution of mass	Maintenance, high frequency response	[16], [8]
5	Ballast	Vibrating mass connected by spring dampers both in vertical and horizontal directions, continuous dampers, FEM, Five parameters vibration model	Maintenance, High frequency response, Vibration propagation	[16], [8], [11], [14]
6	Subgrade	Damping and stiffness	Maintenance	[16]
7	Wheel-rail contact	Mass-less spring, Wheel as concentrated mass in contact with the track with springs	Maintenance, High frequency response	[16], [8]
8	Train system (the car, secondary suspension, bogie, primary suspension, wheel)	Modelled as one complex dynamic system	To understand track settlements	[13]
9	Track system (rail, rail-pads and the sleepers)	Modelled as one complex dynamic system	To understand track settlements	[13]
10	Sub-structure (Ballast and subgrade)	Modelled as one complex dynamic system	To understand track settlements	[13]

processing techniques were utilized by Bracciali et al. to detect and classify wheel defects. While high energy analysis allowed the detection of wheel corrugation, cepstrum analysis was used to detect wheel-flat precisely. They also pointed out that velocity of the trains had a strong influence on the peak amplitudes [26]. Steets et al. commented that wayside condition monitoring devices can prevent incidents such as derailment of the train off the track due to degraded health of the components by raising alarms at appropriate times. Their paper summarizes the freight car failure detection devices which were available in service [27]. Suhairy presented a work on prediction of ground vibration from railways. Wave propagation due to the movement of trains not only affects the structures such as buildings, but also the human body. In this paper, an empirical formula was developed to predict the ground vibrations from the railways. It was also mentioned that the Z-direction (i.e. perpendicular to the ground) is the most significant compared to the other two directions viz. X-axis(perpendicular to the track and parallel to the ground) and Y-axis(parallel to the ground). It was also mentioned that heavy, long and slow trains such as freight trains behave as a line source rather than a point source and generate low frequency vibrations which causes more problems to the human body rather than the fast moving short trains [28]. Combination of field measurements, experimental modal analysis and finite element methods were utilized by Kaewunruen et al. for the study of the dynamic characteristics of a railway track and its components [29]. The same authors studied the track system components and stated that track system components can be classified into superstructure and substructure. While superstructure is the visible part such as the rail, rail-pads, sleepers and fastening system, the substructure consists of ballast, sub ballast and subgrade. The dynamic testing of these components lead to a dynamic model which gives a better insight into the rail track behavior [30]. Chong et al. also discussed wayside condition monitoring which is a dominant condition monitoring technique for railway structures while advanced integrated sensor methods are used for advanced train health and operation management [31]. Vibration behavior of timber sleepers vs concrete sleepers and also good ballast vs degraded ballast was studied by Sadeghi et al., modal analysis of the track system were also carried out for better understanding [32]. Liu et al. studied the derailment causes of railway vehicles track-wise and speed wise. Generally, tracks are classified as main, yard and siding tracks. While in the main track component failures such as broken wheel or bearing failure caused most derailment, in the yard and siding tracks, human factors such as improper use of switches caused the damage. Speed-wise a broken rail or weld was the main cause of derailment in all the speed range while the second cause for derailment varied with speeds. For speed below 10mph, human factor was predominant, above 25mph, equipment failures caused the damage [33]. Ngigi et al. reviewed the condition monitoring techniques for railway system dynamics.

Condition monitoring in terms of Fault Detection and Identification (FDI) was carried out by advanced filtering, system identification and signal analysis method [4]. Consensus Principal Components Analysis (CPCA) was used for Fault Detection and Identification (FDI) of railway vehicle suspension systems by Wei et al. [34]. Inexpensive sensor system was deployed in the axle bearing box to capture acoustic emission and vibration. Analysis of these signals provided information related to wheel and axle bearing defects [35]. Time-frequency slice technique was utilized to detect fault from wheel-rail vibration signals by Yuejian et al. [36]. Alemi et al. studied the different condition monitoring approaches for identifying wheel-defects. The importance of in-workshop inspection for periodic maintenance was emphasized and also further development of wayside monitoring was stressed so that the transition from diagnostic to prognostic approach is possible [37]. Ground Penetrating Radar (GPR) data was used for the health monitoring of railway ballast conditions [38]. Li et al. reviewed the present condition monitoring techniques for railway structure that can be classified into signal-based and model-based techniques. While signal-based methods suffer from the shortcomings of the requirement of a pre-existing database with all the faults, the model-based methods demand linearization which introduces error [39]. Statistical analysis based methods were implemented for condition monitoring of railway vehicle suspension systems by Melnik et al. [40]. Health monitoring of electrical components in railway structure was discussed by Tobon-Mejia et al. [41]. Atamuradov et al. used time-domain features to construct a health indicator. A support vector machine classifier was used for fault detection [42].

Apart from railways there are another three areas where condition monitoring techniques are used extensively viz. bearing health monitoring, rotating machines health monitoring and health monitoring of large structures. Studying the techniques used in these areas are important as a new development in the field of condition monitoring can be used for the improvement of condition monitoring techniques of the railway structures. Few notable works in these areas are discussed here. Extracting time-domain features, power spectral density, statistical measures and training ANN, SVM etc. is a common practice in fault detection; fuzzy classifiers, fuzzy support vector data are also common [43], [44], [45], [46], [47]. Motor current analysis is utilized along with the vibration for condition monitoring of induction motors [48], [49]. Modal analysis and principal component analysis are carried out for structure health monitoring [50], [51], [52]. Feature extraction and vibration signature analysis for fault detection is also widely used [53]. Advanced signal processing techniques such as wavelet, empirical wavelet transform, Hilbert-Huang transform, improved spectral kurtosis, generalized frequency response, energy kurtosis, orthogonal Hilbert-Huang

transform, multivariate statistical signal processing etc. are common in literature for condition monitoring approaches [54], [55], [56], [57], [58], [59], [60], [61]. Statistical analysis is another popular method and RMS based probability density function is also used for fault detection [62], [63], [64]. The recent trend is towards deep learning, k-mean clustering approach etc [65] [66].

Objective of the work The objective of this work is to *collect vibration signals of a railway track while a train is under motion over the track; process this signal to extract information of the train and track and thereby quantify the quality of a few trains and estimate the health of the track by its mathematical modelling.* This is achieved by using a data acquisition system designed with an Arduino based embedded system with a laptop. The embedded system utilized, composed of Arduino microcontroller development boards, 3-D vibration sensors ADXL335 and MPU6050. While ADXL335 provides 3D acceleration, MPU6050 provides 3D acceleration and 3D gyroscope signals. The sensors are attached to the rail track to capture different signals. Using these vibration data, the mathematical model of the track is developed and some limiting conditions are found out. Advanced signal processing techniques in both time-domain and frequency-domain are carried out for the condition monitoring of the railway structure. A sensor based system is developed to achieve the objectives of *modelling, diagnosis and monitoring.*

Main contribution of the work The main contribution of the work is as follows:

- A mathematical model of the railway track is developed. With the help of this mathematical model, limiting conditions for specific trains and the particular track are found out.
- A 3D vibration sensor (ADXL335) based embedded system has been developed for capturing vibration of a railway track while a train is under motion. Vibration signals captured by this system are analysed in both time-domain and frequency-domain. These signals are used to find out safety of the train and also the general condition of the railway vehicle.
- The same signals are analyzed with advanced signal processing techniques such as Wavelet transform and Wigner-Ville transform for condition monitoring of the trains. Wheel-flat, in particular is detected by this method.
- Another embedded system with MPU6050 IMU sensor and Arduino Uno development board is developed to capture 3-axis vibration and the gyroscope signals. These signals

are appropriately correlated and statistical measures are derived to quantify the quality of different trains.

The organization of the thesis

- Chapter 1: This emphasizes the importance of condition monitoring for structures and machines. Importance of vibration signals as a health indicator is also discussed. Literature review in this field is provided.
- Chapter 2: This chapter discusses a simple method to model a railway track. Limiting conditions of a specific train and track are discussed.
- Chapter 3: In this chapter an embedded system consisting of ADXL335 and Arduino Uno development board is discussed. The vibration signals captured are analysed in both time-domain and frequency-domain. While time-domain analysis offers critical information related to the safety measure of a train, frequency-domain analysis provides information related to the condition of different components of a train.
- Chapter 4: This chapter discusses advanced signal processing techniques for the vibration signal analysis; wheel-flat fault is detected with these techniques.
- Chapter 5: This chapter discusses statistical treatment of the vibration signals.
- Chapter 6: This chapter provides a brief summary of the research work done and future scope of the work is also discussed.

2

Development of a mathematical model for a railway track using a gray-box modelling technique

Mathematical model of a system provides the relationship between the input and the output variables. There are different methods of modelling a system viz. utilizing system dynamics, black box modelling and gray-box modelling. In literature there are many works that describe modelling of a railway track using the system dynamics of a track or interaction between track and train wheel. In standard black-box modelling most of the time standard test signals such as impulse and step are used to model a system. In this chapter we discuss a simple method that uses “system subjected to a pulse input” to model a system. This approach is very helpful especially in modelling of a railway track as the track may be subjected to an impulse, step or any signal (i.e. pulse of variable length) in between depending on the speed of the train.

2.1 Introduction

Mathematical modelling of a system helps in understanding the dynamics of the system better. Modelling of a railway track has been a fascinating area for researchers since a long time. Modelling of a railway track as an electrical transmission lines system was done by few researchers such as Hill et. al. , Berova etc. [19], [20]. One of the earliest models of a railway track was presented by Timoshenko, where the rail was considered as an infinite uniform Euler beam [7]. Again according to Grassie et.al., railway track can be modelled as a track resting on a simple elastic support, track resting on a continuous, two-layer support and track resting on discrete supports [8]. Another popular approach for rail track modelling is by finite element model [10] , [15], [18], [11]. Mathematically modelling a railway track is an age old practice to calculate the stress pattern of different components. It helped in anticipating and estimating the service periods and specific values of life-spans of different components. Aim of mathematical models may be different from situations to situations. Few models aimed at studying particular problems or phenomena while few may aim at the validity of models at different frequencies. To model train and track interaction utilizing dynamic behavior, Knothe et. al. considered five subsystems as shown in fig 2.1 [9]. In this way it is needed to model different subsystems separately. Many researchers model the rail as Bernoulli-beam. In some cases the rail is modelled as a series of interconnected plates. Rail fastening system along with the rail-pads are modelled. Rail-pads are generally modelled as spring and viscous dampers. Sleepers are modelled as a Timoshenko beam of variable thickness. Although ballast can be modelled as a viscous damper it possesses non-linear parameters for different loads. In all these modelling one major problem is finding out values of different parameters. However in laboratory experiments it is possible to find out these values. Track is generally modelled as

- Track resting on a simple elastic support
- Track resting on a continuous, two-layer support and
- Track resting on discrete supports

as described by Grassie [8]. Track resting on a simple elastic support can be represented as shown in fig. 2.2.

Santos et. al. in their paper proposed the concept of the convolution kernel [23]. The rail was exposed to a vertical excitation that moves along the rail. The response was described by means of a point of deflection. This deflection was obtained by a convolution integral. The convolution kernel is the impulse response of the track, which depends on time and the excitation location. To model a railway track mainly two types of dynamic models are

found in the literature; they are: distributed sleeper model and discrete sleeper model [23], [8]. The distributed sleeper model is shown in fig. 2.3 and discrete model is shown in fig. 2.4 [8]. As described by Santos et al. for the convolution method with variable kernel, the point deflection of the rail, $y(t)$ is calculated by means of the convolution product of the rail impulse response (the convolution kernel) by the excitation force $y_1(t) = \int_0^t h_{12}(t - \tau) F_2(\tau)$. Where $y_1(t)$ is the deflection at point 1, $h_{12}(t)$ describes the deflection at point 1 on the rail due to a unit impulse force F_2 applied to another point 2. As described by Dahlberg, theoretical modelling of railway track and sub-structure can be done as modelling for static loading and modelling for dynamic loading [13]. For static loading modelling either the track structure is represented by a beam on an elastic foundation wherein the substructure is represented as a spring-damper system or the track structure is modelled in detail by using a finite-element model. For dynamic loading, modelling techniques are classified as frequency-domain and time-domain modelling. Frequency domain method is like inserting an irregular strip between rail and the wheel and then the strip is forced to move between the wheel and the rail so that the strip will excite both the wheel and the rail. Displacements of the track and the vehicle are calculated by the numerical integration method for time domain modelling. The track can be modelled by finite elements and the vehicle is modelled by using a mass spring damper system. Ferreira et al. in their paper they have categorized mathematical modelling of the railway track in three main categories [12]. In one end they mentioned a microscopic model that deals with the forces on specific track components such as rail, sleeper and ballast etc. These models are used for design purposes based on engineering judgment or empirical evidence. On the other hand there are macro models that are used for maintenance and planning. These models involve a higher level of details such as track force analysis. Between these two models there exist another level of models that are concerned with the components deterioration based on the microscopic models. Tatsuo Oyama et. al. in their work proposed an optimal railway track maintenance strategy by developing discrete optimization mathematical programming models [24]. They measured track surface irregularities transitions and thereby proposed a probabilistic degradation model by logistic distribution. Based on this they predicted track maintenance operation effects and thereby designing probabilistic restoration model and finally optimal track maintenance schedule is found out by designing optimal track maintenance scheduling model by an all-integer linear programming model.

For system identification of structures two methods are available viz. Forced Vibration Testing (FVT) and Ambient Vibration Testing (AVT) [21]. Many works based on FVT can be seen for the dynamics analysis of bridges [52], [50], and a few for railway vehicle and track analysis [32], [67], [68]. This paper presents a mathematical model for railway track

system using gray-box technique. For this purpose, a second order LTI system has been considered and using pulse input the output is derived. The output obtained is utilized to relate with the experimental vibration data captured from the field experimentation on train belong to North-East Frontier Railway (NFR) of India. The model is authenticated using both experimental and theoretical data. The criteria for model validation has been used as the nearness of experimental and theoretical data. The key contributions to the railway track modelling is summarized in the table 2.1.

2.2 Modelling of Railway track system

A second order LTI model has been adopted to develop a model of a railway track system. A pulse signal is applied to the second order LTI model and its output response has been determined. However it has been reported that the frequency above 50Hz represents the characteristic vibration of the track and below 50Hz represents the characteristic vibration of a train (consisting of bogie and engine) [69]. The scheme for the development of the railway track system depicted in the fig. 2.5. System identification technique is applied to find out the system; the identified system would replace the general second order LTI system. The vibration obtained would contain properties of both the train and the track. Therefore the signal needed to be filtered properly to detect vibrations only from the railway track. The following assumptions are made to suit the real time scenario for the development of a mathematical model for the railway track system.

- As one sensor is connected on the fishplate of the track, the train will input a pulse to the track at that point.
- The pulse starts at $t = 0sec$ and ends at $t = Tsec$
- Length of the pulse(T) will depend on the speed of the train.
- The track system can be considered as a second order underdamped ($\zeta < 1$) LTI system. (It can be considered as a 2nd order system as the most commonly found model of a railway track is “an infinite Euler beam on Continuous support [8]”) Again it is an underdamped system as the ballast (working as a viscous damper) supposed to absorb energy.

Mathematical derivations Laplace Transform of a pulse is given by $A[\frac{1}{s} - \frac{e^{-sT}}{s}]$, where A is the magnitude of the pulse, T is the length of the pulse. A second order LTI system

Table 2.1 Key contributions to the railway track modelling

Sl. no.	Author	Year	Moelling technique	Summary of the key findings
1	Timoshenko	1926	An infinite uniform Euler beam	Different statistical and dynamic stress patterns on rail are analysed
2	Grassie et. el.	1982	Track resting on a simple elastic support, track resting on a continuous, two-layer support and track resting on discrete supports	Study to calculate both the response of the track alone and the contact force between a moving wheel and the rail.
3	Thompson	1991	Finite element	Study of the source of noise in railways
4	Hill et. el.	1993	Transmission lines system	Different impedances and admittances for a single-track, power-rail electrified railway are obtained
5	Dong et. el.	1994	Finite element	The dynamic interactions between the railway vehicle and track is studied
6	Santos et. el.	1995	Convolution kernel	Study of the loading pattern on the railway track
7	Luo et. el.	1996	Finite element	Study of the dynamic response of railway ballast excited by forces from the moving train at different speeds
8	Berova	1997	Transmission lines system	The work described the investigation of railway track circuit performance with the help of mathematical modelling
9	Knothe et. el.	2007	Considered five subsystems to understand the dynamic behaviour of the railway train and track system.	Study of the sufficiently high frequencies that becomes significant frequencies for the track's dynamic behavior.
10	Kacimi et. el.	2013	3D finite element	Study of the ground induced vibration due to the passage of a single high speed train locomotive

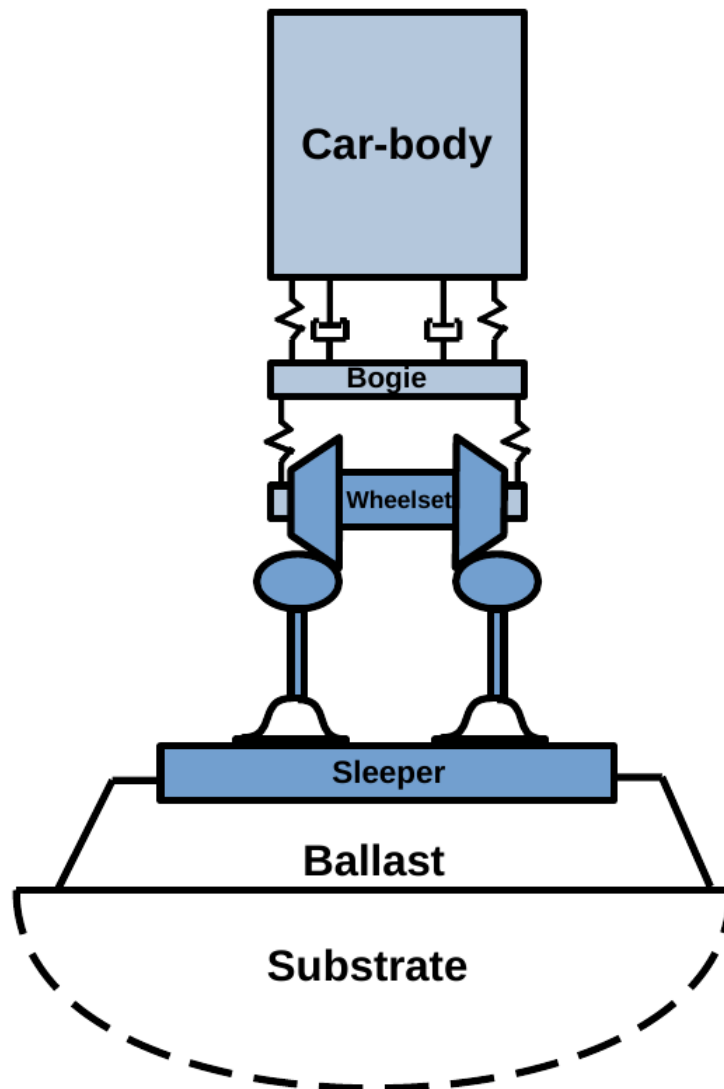


Fig. 2.1 Five subsystems of the vehicle/track system.

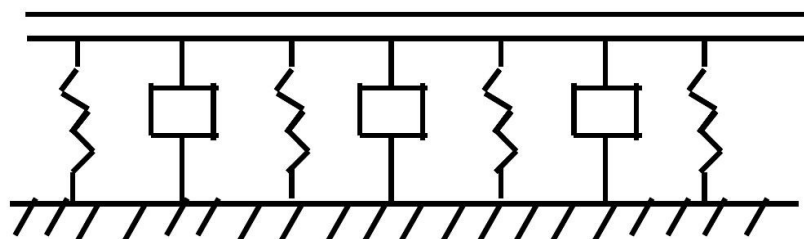


Fig. 2.2 Track resting on a simple support.

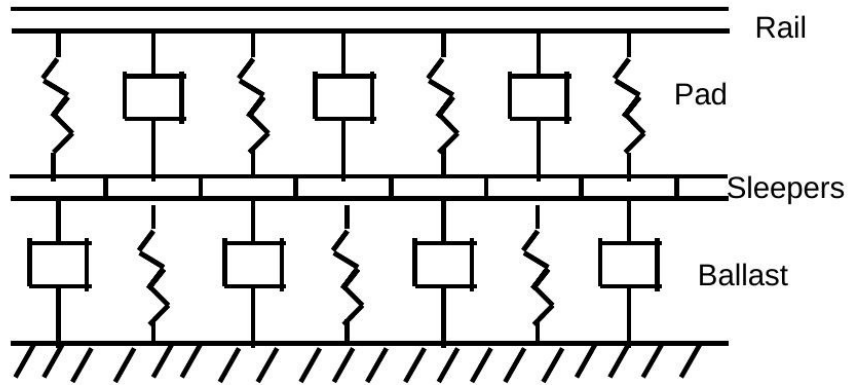


Fig. 2.3 Distributed sleeper model

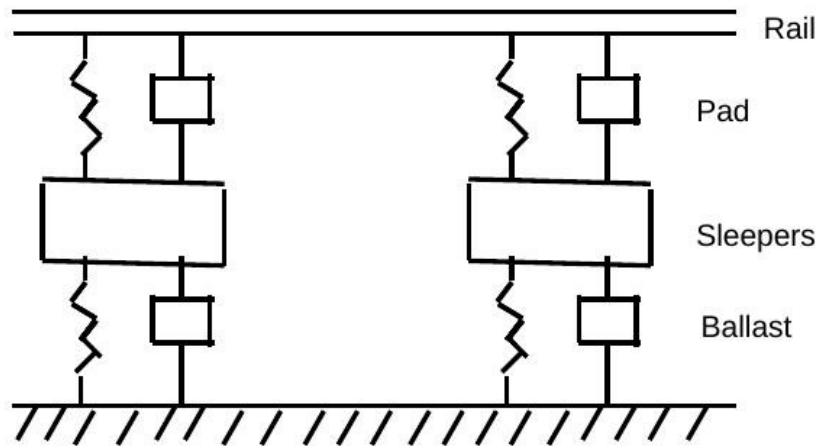


Fig. 2.4 Discrete sleeper model

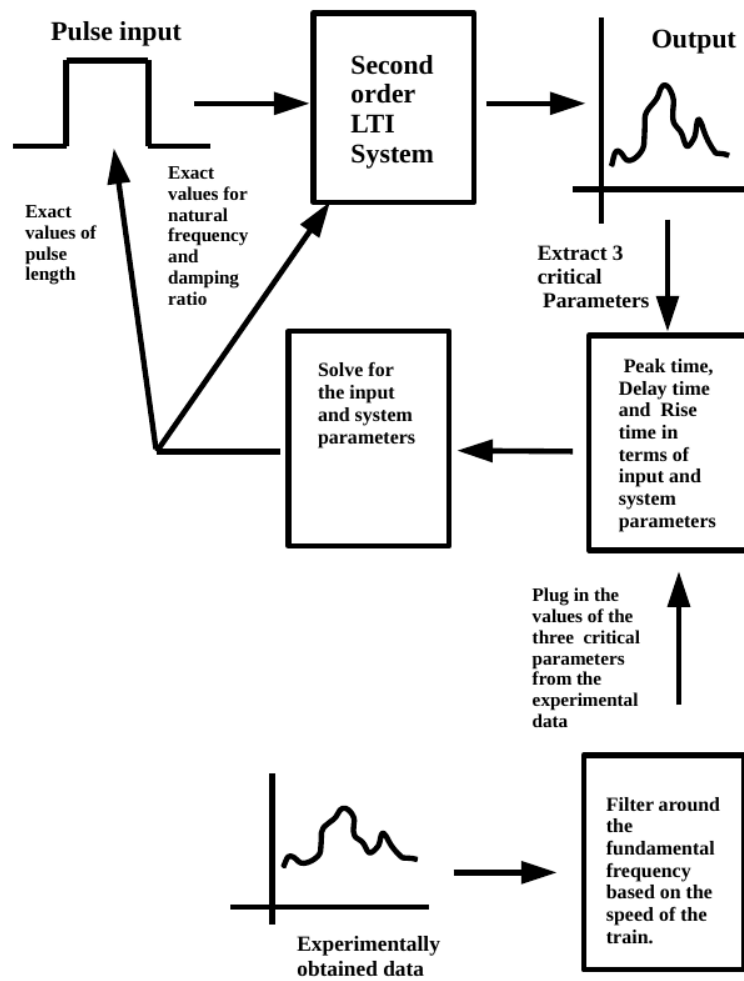


Fig. 2.5 Scheme adopted for development of model for railway track system

in Laplace domain can be represented as $\frac{\omega_n^2}{s^2 + 2\zeta\omega_n s + \omega_n^2}$, where $\zeta = \text{damping ratio}$ and $\omega_n = \text{natural frequency}$ of the system. Therefore the output of a second order LTI system subjected to a pulse input in Laplace domain can be represented as the multiplication of the input and the system transfer function.

$$C(s) = A\left[\frac{1}{s} - \frac{e^{-sT}}{s}\right]\left[\frac{\omega_n^2}{s^2 + 2\zeta\omega_n s + \omega_n^2}\right] \quad (2.1)$$

The work reported in this paper utilized gray-box modelling technique to develop a mathematical model for railway track system. These three parameters namely *damping ratio* ζ , *natural frequency* ω_n and length of the *input pulse* T plays vital role in the model development process. Eq. (2.1) can be simplified and represented as

$$\begin{aligned} C(s) &= A\left[\frac{1}{s} - \frac{e^{-sT}}{s}\right]\left[\frac{\omega_n^2}{s^2 + 2\zeta\omega_n s + \omega_n^2}\right] \\ &= \frac{A}{s} \frac{\omega_n^2}{s^2 + 2\zeta\omega_n s + \omega_n^2} - \frac{A}{s} e^{-sT} \frac{\omega_n^2}{s^2 + 2\zeta\omega_n s + \omega_n^2} \\ &= \frac{A}{s} \frac{\omega_n^2}{s^2 + 2\zeta\omega_n s + \omega_n^2} \\ &\quad - \frac{A}{s} \left(1 - sT + \frac{s^2 T^2}{2!} - \dots\right) \frac{\omega_n^2}{s^2 + 2\zeta\omega_n s + \omega_n^2} \\ &= A\left[T \frac{\omega_n^2}{s^2 + 2\zeta\omega_n s + \omega_n^2} + \frac{T^2}{2} \frac{\omega_n^2}{s^2 + 2\zeta\omega_n s + \omega_n^2}\right] \\ &\quad (\text{neglecting the higher order terms}) \end{aligned} \quad (2.2)$$

Now taking the inverse Laplace Transform of Eq. (2.2) we have,

$$\begin{aligned} C(t) &= AT \frac{\omega_n}{\sqrt{1 - \zeta^2}} e^{-\zeta\omega_n t} \sin(\omega_n \sqrt{1 - \zeta^2} t) \\ &\quad - A \frac{T^2}{2} \frac{\omega_n^2}{\sqrt{1 - \zeta^2}} e^{-\zeta\omega_n t} \sin(\omega_n \sqrt{1 - \zeta^2} t - \theta) \\ &\quad (\text{where, } \theta = \cos^{-1} \zeta \text{ and } \zeta < 1) \end{aligned} \quad (2.3)$$

2.2.1 Determination of peak time t_p

As first peak of the curve ($c(t)$) will be a maxima (either local or global) ; the derivative of the curve equated to zero should yield the peak condition i.e.

$$\frac{d}{dt}c(t) = 0 \quad (2.4)$$

Putting the values of $c(t)$ in Eq. (2.4) and simplifying we obtain,

$$\begin{aligned} A.T. \frac{\omega_n^2}{\omega_d} \frac{d}{dt} [e^{-\zeta \omega_n t} \{ \sin(\omega_d t) - \frac{T}{2} \omega_n \sin(\omega_d t - \theta) \}] &= 0 \\ \implies e^{-\zeta \omega_n t} \{ \omega_d \cos(\omega_d t) - \frac{T}{2} \omega_n \omega_d \cos(\omega_d t - \theta) & \\ - \zeta \omega_n \sin(\omega_d t) + \frac{T}{2} \zeta \omega_n^2 \sin(\omega_d t - \theta) \} &= 0 \\ \implies \omega_d \cos(\omega_d t) - \zeta \omega_n \sin(\omega_d t) - \frac{T}{2} \omega_n \omega_d \cos(\omega_d t - \theta) & \\ + \frac{T}{2} \zeta \omega_n^2 \sin(\omega_d t - \theta) &= 0 \\ \implies \omega_n \sqrt{1 - \zeta^2} \cos(\omega_d t) - \zeta \omega_n \sin(\omega_d t) & \\ - \frac{T}{2} \omega_n \omega_n \sqrt{1 - \zeta^2} \cos(\omega_d t - \theta) + \frac{T}{2} \zeta \omega_n^2 \sin(\omega_d t - \theta) &= 0 \end{aligned} \quad (2.5)$$

Again $\cos(\theta) = \zeta$ and $\sin(\theta) = \sqrt{1 - \zeta^2}$. Therefore, Eq. (2.5) can be written as

$$\begin{aligned} \omega_n \sin(\theta) \cos(\omega_d t) - \cos(\theta) \omega_n \sin(\omega_d t) & \\ - \frac{T}{2} \omega_n^2 \sin(\theta) \cos(\omega_d t - \theta) + \frac{T}{2} \zeta \omega_n^2 \sin(\omega_d t - \theta) &= 0 \\ \implies -\omega_n \{ \sin(\omega_d t - \theta) \} - \frac{T}{2} \omega_n^2 \{ \sin(\theta - (\omega_d t - \theta)) \} &= 0 \\ \implies \frac{T}{2} \omega_n \{ \sin(\omega_d t - 2\theta) \} = \sin(\omega_d t - \theta) & \end{aligned}$$

Taking $\omega_d t - \theta = X$;

it is found that $\frac{T}{2} \omega_n \{ \sin(X - \theta) \} = \sin(X)$

$$\begin{aligned}
&\therefore \frac{T}{2} \omega_n \{ \sin(X) \cos(\theta) - \cos(X) \sin(\theta) \} = \sin(X) \\
&\left\{ \frac{T}{2} \omega_n \cos(\theta) - 1 \right\} \sin(X) = \cos(X) \sin(\theta) \\
&\left\{ \frac{T}{2} \omega_n \cos(\theta) - 1 \right\} \tan(X) = \sin(\theta) \\
&\implies \tan(X) = \frac{\sin(\theta)}{\frac{T}{2} \omega_n \cos(\theta) - 1} \\
&\implies X = \tan^{-1} \left\{ \frac{\sin(\theta)}{\frac{T}{2} \omega_n \cos(\theta) - 1} \right\} \\
&\implies \omega_d t - \theta = \tan^{-1} \left\{ \frac{\sqrt{1 - \zeta^2}}{\frac{T}{2} \zeta \omega_n - 1} \right\} \\
&\implies t = \frac{1}{\omega_d} \left\{ \tan^{-1} \left(\frac{\sqrt{1 - \zeta^2}}{\frac{T}{2} \zeta \omega_n - 1} \right) + \theta \right\}
\end{aligned}$$

Hence the peak time t_p is

$$t_p = \frac{1}{\omega_n \sqrt{1 - \zeta^2}} \left\{ \tan^{-1} \left(\frac{\sqrt{1 - \zeta^2}}{\frac{T}{2} \zeta \omega_n - 1} \right) + \cos^{-1} \zeta \right\} \quad (2.6)$$

where $T =$ pulse width, $\zeta =$ damping ratio and $\omega_n =$ natural frequency of the system.

2.2.2 Calculation of Rise Time t_r

At rise time (t_r) the output is exactly equal to the input i.e $c(t_r) = A$, in this case.

$$\begin{aligned}
c(t_r) &= A.T \frac{\omega_n}{\sqrt{1 - \zeta^2}} \cdot e^{-\zeta \cdot \omega_n t_r} \sin(\omega_n \sqrt{1 - \zeta^2} t_r) - \\
&A \cdot \frac{T^2}{2} \frac{\omega_n^2}{\sqrt{1 - \zeta^2}} \cdot e^{-\zeta \cdot \omega_n t_r} \sin(\omega_n \sqrt{1 - \zeta^2} t_r - \theta) = A \\
&\implies T \frac{\omega_n}{\sqrt{1 - \zeta^2}} \cdot e^{-\zeta \cdot \omega_n t_r} \sin(\omega_n \sqrt{1 - \zeta^2} t_r) - \\
&\frac{T^2}{2} \frac{\omega_n^2}{\sqrt{1 - \zeta^2}} \cdot e^{-\zeta \cdot \omega_n t_r} \sin(\omega_n \sqrt{1 - \zeta^2} t_r - \theta) = 1
\end{aligned}$$

$$\implies T \frac{\omega_n^2}{\omega_d} . e^{-\alpha t_r} (\sin(\omega_d t_r) - \frac{T}{2} \omega_n \sin(\omega_d t_r - \theta)) = 1 \quad (2.7)$$

where $\alpha = \zeta . \omega_n = \text{damping factor}$ and $\omega_d = \omega_n \sqrt{1 - \zeta^2} = \text{damped natural frequency}$

$$\implies \sin(\omega_d t_r) - \frac{T}{2} \omega_n \sin(\omega_d t_r - \theta) = \frac{\omega_d}{T \omega_n^2} e^{\alpha t_r} \quad (2.8)$$

Assuming a fast system, t_r will be small.

$$\begin{aligned} \therefore \omega_d t_r - \frac{T}{2} \omega_n (\omega_d t_r - \theta) &= \frac{\omega_d}{T \omega_n^2} \{1 + \alpha t_r\} \\ \implies t_r \left\{ \omega_d - \frac{T}{2} \omega_n \omega_d - \alpha \frac{\omega_d}{T \omega_n^2} \right\} &= \frac{\omega_d}{T \omega_n^2} - \frac{T}{2} \omega_n \theta \\ \implies t_r &= \frac{\omega_n \sqrt{1 - \zeta^2} - \frac{T^2}{2} \omega_n^3 \cos^{-1} \zeta}{T \omega_n^3 \sqrt{1 - \zeta^2} \left\{ 1 - \frac{T}{2} \omega_n \right\} - \zeta \omega_n^2 \sqrt{1 - \zeta^2}} \end{aligned} \quad (2.9)$$

2.2.3 Calculation of Delay Time t_d

At delay time (t_d) the output is exactly equal to the half of the input i.e $c(t_d) = 0.5A$, in this case.

Following the procedure for calculation of Rise time , we get delay time as

$$t_d = \frac{0.5 \omega_n \sqrt{1 - \zeta^2} - \frac{T^2}{2} \omega_n^3 \cos^{-1} \zeta}{T \omega_n^3 \sqrt{1 - \zeta^2} \left\{ 1 - \frac{T}{2} \omega_n \right\} - 0.5 \zeta \omega_n^2 \sqrt{1 - \zeta^2}} \quad (2.10)$$

Now there are three equations - (2.6), (2.9) and (2.10) and three unknowns; they are *damping ratio* ζ , *natural frequency* ω_n and the *pulse length* T . So plugging in values of peak time t_p delay time t_d and rise time t_r from experimentally obtained data it is possible to solve the three equations to determine the parameters ζ, ω_n and T .

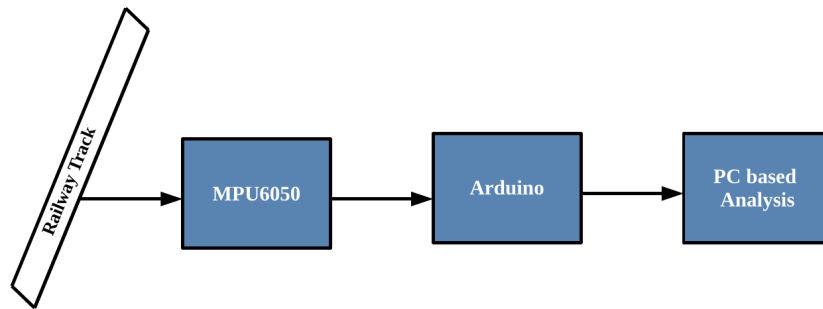


Fig. 2.6 Block diagram for extracting vibration signals from the railway track

2.3 Experimental Results and validation of the model

MPU6050, an Inertial Measurement Unit (IMU) is interfaced to the Arduino Uno microcontroller based embedded system. The MPU6050 combines a 3-axis gyroscope, a 3-axis accelerometer and a Digital Motion Processor (DMP) to process the collected measurements. IMUs are widely used in various applications due to its low cost and easy implementations. MPU6050 is a Micro-Electro-Mechanical Systems (MEMS) sensor connected to the I^2C module of the microcontroller. In this configuration, the microcontroller works as a master while the sensor is the slave. Master generates the start-conditions, sends the address of the slave device, reads data from the slave device and then generates the stop conditions [70]. The accelerometer and the gyroscope of the MPU6050 are user-programmable with gyroscope full range of ± 2500 /s, ± 5000 /s, ± 10000 /s, and ± 20000 /s while the accelerometer full scale range of $\pm 2g$, $\pm 4g$, $\pm 8g$, and $\pm 16g$. Moreover, the MPU6050 contains 6 16-bit analog-to-digital converters (ADCs) for digitizing the outputs. The Arduino Uno based embedded system with the MPU6050 as the sensor system is used to record 3-D vibrations of the railway track, while a train is under motion over the track. A laptop is used to pull and store vibration data captured by the embedded system through its USB port. The scheme for data collection is as shown in fig. 2.6

The North East Frontier Railway (NFR) authority, Maligaon, Assam, India provided facility to carry out the experiments on railway track under the supervision of their authorized persons in accordance to their rule. The NF Railway authority permitted the capture of vibrations of a railway track located at Chandmari, Guwahati, Assam, India. The experimental setup used for the purpose of capturing vibration signals of railway track at Chandmari is shown in fig. 2.7. The MPU6050 sensor was firmly attached on the fishplate of the joint of two railway tracks as advised by NF Railway authority. Figure 2.8 shows the orientation of the sensor axis with reference to the railway track. The orientation of the sensor is made



Fig. 2.7 Experimental set-up for capturing 3-D vibration signals from railway tracks.

in such a way that the X-axis is parallel to the railway track, Y-axis is perpendicular to the railway track and the Z-axis is perpendicular to the ground.

Figure 2.9 shows raw and filtered signals for Rajdhani Express collected by the scheme.

The filtered signal along with the key parameters are presented in fig. 2.11.

The baseline is considered as zero level value as the vibration signal generated by the wheel has been recorded by the sensor, where there is a possibility of recording of the vibration data by the sensor may start at a negative value. Therefore rise time and delay time is calculated considering the time taken from some initial negative value (-0.0175) to reach 0 of the output. Also only the first peak is considered, because as the vibration is produced by the first wheel, the vibration due to the second wheel will appear before the vibration due to the first wheel dies down i.e settling down.

Accordingly, the delay time t_d is calculated as 0.2527 sec, rise time t_r as 0.467 sec and peak time t_p as 1 sec. This clearly justifies our assumption of a fast system i.e delay time t_d and rise time t_r are small compared to 1. Now there are three equations for delay time t_d , rise time t_r and peak time t_p with three unknowns pulse length T , natural frequency ω_n and damping ratio ζ . Solving these equations the system can be modelled as $\frac{\omega_n^2}{s^2 + 2\zeta\omega_n s + \omega_n^2}$, where s is the Laplace variable, ω_n is the natural frequency and ζ is the damping ratio. Values of ω_n and ζ can be put by solving the equations (2.6), (2.9) and (2.10).

Again, vibration data of another train, the Kamrup Express is considered for further analysis. The filtered vibration signal and the key parameters are shown in figures 2.12 and 2.13.

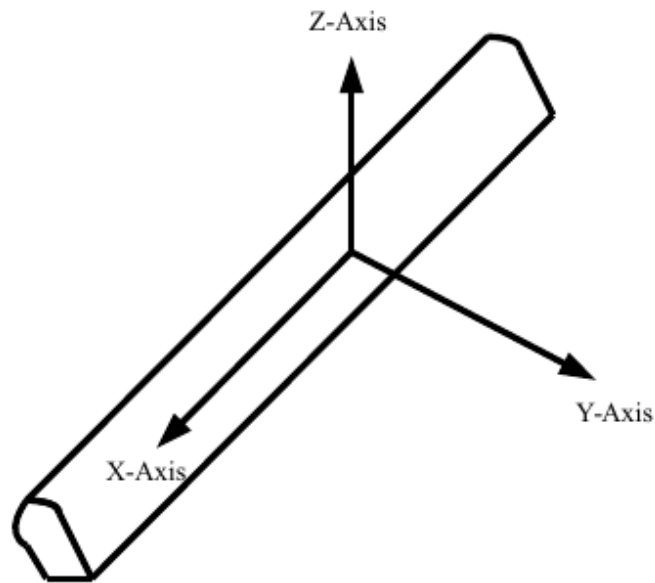


Fig. 2.8 The orientation of the MPU6050 sensor axis with reference to the railway track

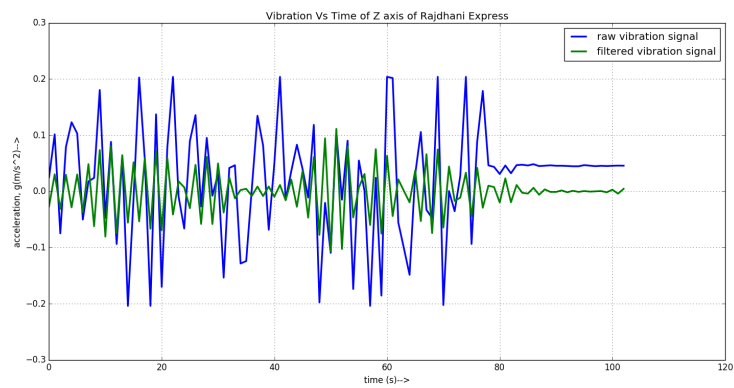


Fig. 2.9 Vibration signal of Z axis of Rajdhani Express

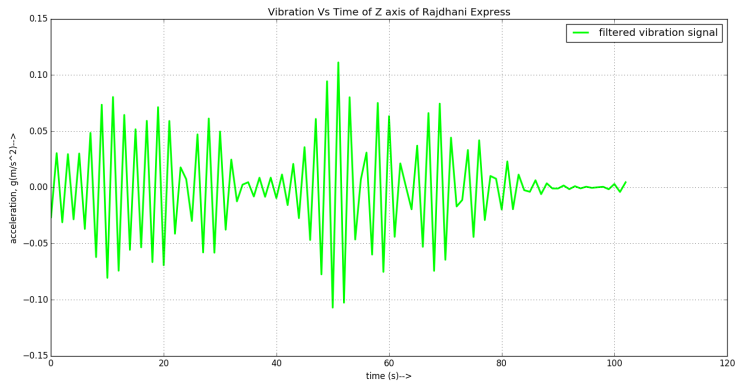


Fig. 2.10 Filtered Vibration signal of Z axis of Rajdhani Express

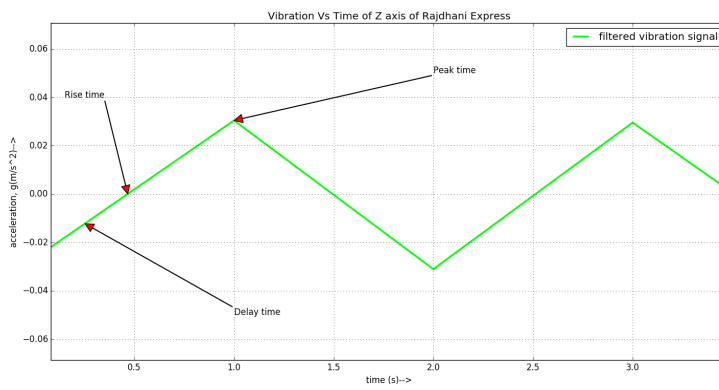


Fig. 2.11 Filtered Vibration signal of Z axis of Rajdhani Express with Key Parameters



Fig. 2.12 Filtered Vibration signal of Z axis of Kamrup Express

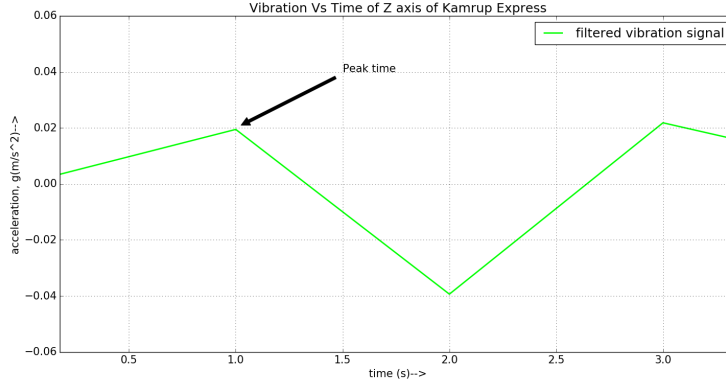


Fig. 2.13 Filtered Vibration signal of Z axis of Kamrup Express with Key Parameters

2.4 Discussion

It has been observed from the equations (2.6), (2.9) and (2.10), the expressions for delay time t_d , rise time t_r and peak time t_p contain the term T (pulse length). This pulse length is inversely proportional to the speed of the train. For slow moving train pulse length will be very long (ideally step input) and for a fast moving train the pulse length will be short (ideally impulse input).

From equation (2.6), equation for peak time t_p

$$t_p = \frac{1}{\omega_n \sqrt{1 - \zeta^2}} \left\{ \tan^{-1} \left(\frac{\sqrt{1 - \zeta^2}}{\frac{T}{2} \zeta \omega_n - 1} \right) + \cos^{-1} \zeta \right\}$$

From experimental data of Rajdhani as well as Kamrup Express, it is found that, $t_p = 1$,

$$\begin{aligned} \therefore \frac{1}{\omega_n \sqrt{1 - \zeta^2}} \left\{ \tan^{-1} \left(\frac{\sqrt{1 - \zeta^2}}{\frac{T}{2} \zeta \omega_n - 1} \right) + \cos^{-1} \zeta \right\} &= 1 \\ \text{or } \frac{1}{\omega_d} \left\{ \tan^{-1} \left(\frac{\sin(\theta)}{\frac{T}{2} \alpha - 1} \right) + \theta \right\} &= 1 \\ \implies \frac{\sin(\theta)}{\frac{T}{2} \alpha - 1} &= \tan(\omega_d - \theta) \\ \implies \frac{T}{2} \alpha - 1 &= \frac{\sin(\theta)}{\tan(\omega_d - \theta)} \end{aligned}$$

$$\implies T = \frac{2}{\zeta \omega_n} \left\{ \frac{\sin(\theta)}{\tan(\omega_d - \theta)} + 1 \right\} \quad (2.11)$$

Eq. (2.11) is the general expression for the pulse length (T) of the train running on the railway track located at Chandmari, Guwahati, Assam, India, when considered the vibration produced by the Rajdhani Express.

Now, to determine the condition for the speed limit of a train it is necessary to consider a step function for slow moving trains, whereas an impulse is considered for a fast moving train. The expression for peak time is given by [71]

$$t_p = \frac{\pi}{\omega_n \sqrt{1 - \zeta^2}}$$

Comparing with the equation (2.6), we have

$$\begin{aligned} t_p &= \frac{1}{\omega_n \sqrt{1 - \zeta^2}} \left\{ \tan^{-1} \left(\frac{\sqrt{1 - \zeta^2}}{\frac{T}{2} \zeta \omega_n - 1} \right) + \cos^{-1} \zeta \right\} \\ &= \frac{\pi}{\omega_n \sqrt{1 - \zeta^2}} \\ \implies \tan^{-1} \left(\frac{\sqrt{1 - \zeta^2}}{\frac{T}{2} \zeta \omega_n - 1} \right) + \theta &= \pi \\ \implies \tan^{-1} \left(\frac{\sin(\theta)}{\frac{T}{2} \zeta \omega_n - 1} \right) + \theta &= \pi \\ \implies \frac{T}{2} \zeta \omega_n - 1 &= \frac{\sin(\theta)}{\tan(\pi - \theta)} \end{aligned}$$

$$\implies T = \frac{2}{\zeta \omega_n} \left\{ \frac{\sin(\theta)}{\tan(\pi - \theta)} + 1 \right\} \quad (2.12)$$

Equation (2.12) is the expression for the track under condition when the train moves very slow i.e step input. To find the limiting value we can compare equations (2.11) and (2.12). Comparing these two equations we find that $\omega_d = \pi$.

$$\therefore \omega_n \sqrt{1 - \zeta^2} = \pi \quad (2.13)$$

Therefore when the concerned train i.e Rajdhani Express runs over the track at the Chandmari railway track very slowly, this condition ($\omega_n \sqrt{1 - \zeta^2} = \pi$) must be maintained.

For a fast moving train, input is considered as an impulse. A second order system subjected to an impulse input, the expression for peak time is given by [71]

$$t_p = \frac{\theta}{\omega_n \sqrt{1 - \zeta^2}} \quad (2.14)$$

Comparing with the equation (2.6), we have

$$\begin{aligned} t_p &= \frac{1}{\omega_n \sqrt{1 - \zeta^2}} \left\{ \tan^{-1} \left(\frac{\sqrt{1 - \zeta^2}}{\frac{T}{2} \zeta \omega_n - 1} \right) + \cos^{-1} \zeta \right\} \\ &= \frac{\theta}{\omega_n \sqrt{1 - \zeta^2}} \\ \text{or } &\frac{1}{\omega_n \sqrt{1 - \zeta^2}} \left\{ \tan^{-1} \left(\frac{\sqrt{1 - \zeta^2}}{\frac{T}{2} \zeta \omega_n - 1} \right) + \theta \right\} \\ &= \frac{\theta}{\omega_n \sqrt{1 - \zeta^2}} \\ \implies &\tan^{-1} \left(\frac{\sqrt{1 - \zeta^2}}{\frac{T}{2} \zeta \omega_n - 1} \right) = 0 \\ \implies &\sin(\theta) = 0 \\ \implies &\sqrt{1 - \zeta^2} = 0 \end{aligned}$$

$$\implies \zeta = 1 \quad (2.15)$$

Hence this condition ($\zeta = 1$) must be satisfied for fast moving train. By intuition also we can say that when the system is subjected to an impulse input, damping should be high, in this case it should be atleast 1.

2.5 Conclusion

This chapter proposes a simple yet powerful method to model a railway track. It has been shown that a track can be modelled as a second order LTI system. Further, the limiting condition for a specific train (Rajdhani Express) has been demonstrated, when it is running

over the track. It is also found that if the train is fast moving the damping ratio should be high ; at least critically damped ($\zeta = 1$) and when the train is moving slow the condition to be maintained is $\omega_n \sqrt{1 - \zeta^2} = \pi$.

3

Condition monitoring of NFR trains with measurements from a single wayside 3D vibration sensor

This chapter discusses the development of a simple one sensor based system to achieve condition monitoring of NFR (Northeast Frontier Railway, India) trains. Vibration of a railway track under train in motion provides important information about the train. To capture the vibration of a track under train in motion, vibration sensor ADXL335 is selected, as it is a reliable vibration sensor. Moreover ADXL335 shows insignificant effect of temperature on its measurements. Therefore it is considered to be suitable for measurement of vibration of a railway track under train in motion, because the temperature experienced by the sensor would vary during the train in motion as well as due to change in weather condition. To capture and store vibration data, an embedded system has been developed using an Arduino Uno board. ADXL335 sensor is interfaced to the Arduino Uno board and software has been developed to capture 3D vibration of a railway track under train in motion. The captured data is transferred and stored in a laptop which is interfaced to the Arduino Uno board through USB port. The vibration data stored in the laptop is utilized to analyse the condition of the train using signal processing techniques. Time-domain and frequency-domain analysis of the

vibration signals captured by ADXL335 installed in a railway track have been carried out to determine the condition of a train in motion. It has been observed that the time-domain analysis can provide information about slip and derailment tendency of a train, whereas frequency domain analysis can provide conditions of different components of a train.

3.1 Introduction

A large population in India, is dependent on trains for their commute. A large number of trains ply regularly to and from their respective destinations. Although many health monitoring systems are available, they are costly. The condition monitoring system of rolling stock infrastructure of Indian railways is not developed yet. The Indian railways intends to install "On Board Condition Monitoring System" (OBCMS) and working on it since 2015. It is a huge project that requires to install the sensors on 250,000 wagons, 50,000 coaches and 10,000 locomotives at a cost of Rs. 1.13 billion [72–74]. The major problems with On Board Condition Monitoring System are - (i) huge number of sensors will lead to a complex sensor network, (ii) installation of sensors at different positions of the wagons will lead alternation of the wagons especially in the suspension, axle and bearing systems, (iii) data communication will be difficult as the sensors will be in constant motion; utilizing internet is again difficult as the signal strength fluctuates a lot in the railway routes, (iv) Huge cost, (v) Would require a lot of time for alteration of the existing structures and then installing the sensors.

Most of these problems can be easily bypassed by shifting the focus from "on board monitoring systems" to "Wayside (track-side) health monitoring systems". Utilising wayside health monitoring following convenience can be achieved - (i) number of sensors drastically reduced, as once installed, one system can be utilised to monitor any number of trains that runs over the track, (ii) no need to change any existing infrastructure of wagon or the track as the sensor can be nicely fitted into existing structure, mostly on the fishplate of the track, (iii) data communication complexity reduces as the sensors are stationary, (iv) time and cost both reduces as the number of sensors required reduces drastically.

Traditionally track-side health monitoring systems are used for wheel-impact load detection, continuous monitoring of wheel profile, bogie performance etc [39]. Derailment of trains is one of the major causes of accidents in Indian Railways. These accidents are caused due to poor mechanical condition of either the train's moving system (Locomotive, Wagon) or the improper condition of railway track (Railway track, fish plate, sleeper etc.). Therefore, it is necessary to develop a reliable on-line monitoring system to determine operating condition of railway track and the train to collect information about their operating conditions. Study shows that from 2009 to 2015 there were 803 railway accidents in India. These accidents

killed 620 people and 1855 people were injured. Out of these 803 accidents, 47% were due to the derailment of the trains [75]. The causes of derailment are different for low speed derailment and high speed derailment. According to Liu, below 10 mph major causes of derailment are improper train handling, braking operations and improper use of switches. Whereas, above 25 mph major causes of derailment are bearing failure, broken wheel, axle and journal defects [33]. Hence, it becomes necessary to monitor the condition of the trains and tracks, especially for fast moving trains. When a train moves on a rail, it creates a dynamic force pattern on the ground and it depends on soil composition of the ground, rail track condition and moving system of the train [28]. Nature of vibration of a rail track could offer important information for on line condition monitoring of a train's moving system and/or the improper condition of a railway track. Wheel defects such as eccentric wheels, unbalanced wheel, wheel flats etc., creates variation on track support systems due to irregular placing of sleepers which are in turn placed upon irregular support of stone ballast are well known faults and contribute to the stress field present in the ground below and beside the train. Azoh also mentioned that Rail irregularities, wheel defects and variation stiffness due to the discrete support of rail are the origin of vibration induced by train [16]. Again, many other parameters like power output, fuel efficiency etc, also produce interactive force between the wheel and the rail and these interactive forces varies on the velocity of the railway vehicle [[17], [69]]. In recent years, the fault diagnosis of railways has been a major thrust area of research. Faults such as tread flat leads to periodic jumping of the vehicle over the track as the wheel (tread flat) makes impact on the track [36]. This will further enhance the damage of the wheel. Hence it becomes a necessity to detect this fault at the earliest. While most of the literature describe application of Hilbert-Huang Transform (HHT) to detect this fault [[56], [59]], again, some work prefer Frequency Slice Wavelet Transform [36].

In this work, a simple time-domain and frequency-domain based method has been investigated to determine condition of a train using the measurements of a railway track vibrations(3D), under train in motion. The precise selection of sensor for measurement of vibration ensures error free measurements, which is an important criteria for sensor based measurement system[76], [77]. For this purpose, ADXL335 sensor is used to capture the 3-D vibration of a railway track. The real time data from ADXL335 sensor is captured by Arduino 328 Uno microcontroller based embedded system. The real time data captured by the embedded system are transferred to a laptop for storage and analysis. The real time 3-D vibration signals and speed of a train are used for quantifying the defects/faults of a train. For this purpose, the real time vibration signals of railway track are analysed using signal processing techniques, where, the power components for selected frequency band

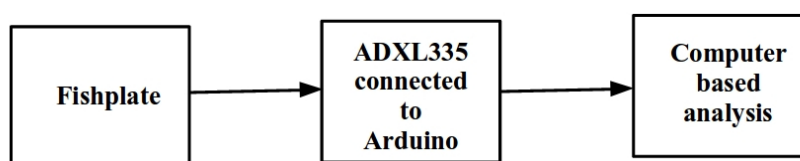


Fig. 3.1 Block diagram for extracting vibration signals from the railway track

are determined. Again, vibrations of two directions (X-Z and Y-Z) are co-related and these correlated signals are used to determine the power components for selected frequency.

3.2 Scheme for capturing vibration of a railway track using ADXL335 sensor:

The functional block diagram adopted for condition monitoring for trains' moving system and/or the improper condition of railway track is depicted in fig. 4.1.

A 3-axis accelerometer ADXL335 is interfaced to the Arduino Uno microcontroller based embedded system to record 3-D vibration of railway track, while moving a train over it. A laptop is used to pull and store vibration data captured by the embedded system through its USB port. The ADXL335 is a small, thin, low power, complete 3-axis accelerometer with signal conditioned voltage outputs. The product measures acceleration with a minimum full-scale range of ± 3 g. ADXL335 has been designed with an innovative temperature compensation circuit, as a result, there is no quantization error or non monotonic behavior of the sensor. The temperature hysteresis is very low (typically less than 3 mg over the -25°C to $+70^{\circ}\text{C}$ temperature range), therefore the sensor is convenient for outdoor application where temperature variation is significant due to weather condition as well as temperature variation of the track will occur during the train in motion due to the frictional effect. It can measure the static acceleration of gravity in tilt-sensing applications, as well as dynamic acceleration resulting from motion, shock, or vibration. The sensor is fixed to the fishplate of the track as advised by the NFRA authority.

The North East Frontier Railway (NFR) authority, Maligaon, Assam, India provided facility to carry out the experiments on railway track under the supervision of their authorised persons in accordance to their rule. The NF Railway authority permitted the capture of vibrations of a railway track located at Chandmari, Guwahati, Assam, India. The experimental setup used for the purpose of capturing vibration signals of railway track at Chandmari is



Fig. 3.2 Experimental set-up for capturing 3-D vibration signals from railway track.

shown in fig. 4.2. The ADXL335 sensor was firmly attached on the fishplate of the joint of two railway tracks as advised by NF Railway authority. Fig. 4.3 shows the orientation of the sensor axis with reference to the railway track. The orientation of the sensor is made in such a way that the X-axis is parallel to the railway track, Y-axis is perpendicular to the railway track and the Z-axis is perpendicular to the ground.

NFR authority advised to carry out the studies on five different trains, they are —(i) Kamrup express (ii) Kopili express, (iii) Kolangpar express, (iv) Rajdhani express and (v) Rajendra Nagar Capital express. Because, these five trains represent five different categories of trains with different allowable speeds and can be classified into 5 different grades, based on their operational performance.

3.3 Information about the trains:

Kamrup express (KA-Exp) is one of the major trains of NFRA that connects Howrah (West Bengal) and Dibrugarh(Assam). It covers 1582 km with an average speed of 42 kmph (26 mph). As explained by Xiang Liu et.al as the speed of the train increases the derailment due to equipment failure increases compared to derailment due to other factors like human and track conditions. As the speed of this train is high (26 mph) it is very important to analyse the health of this train to avoid accidents due to equipment failure. This train is recently awarded an ISO certificate that quantifies it to be of a very good quality train. Kopili express (KO-Exp) is a fast train that runs within Assam and connects Nagaon and Guwahati and

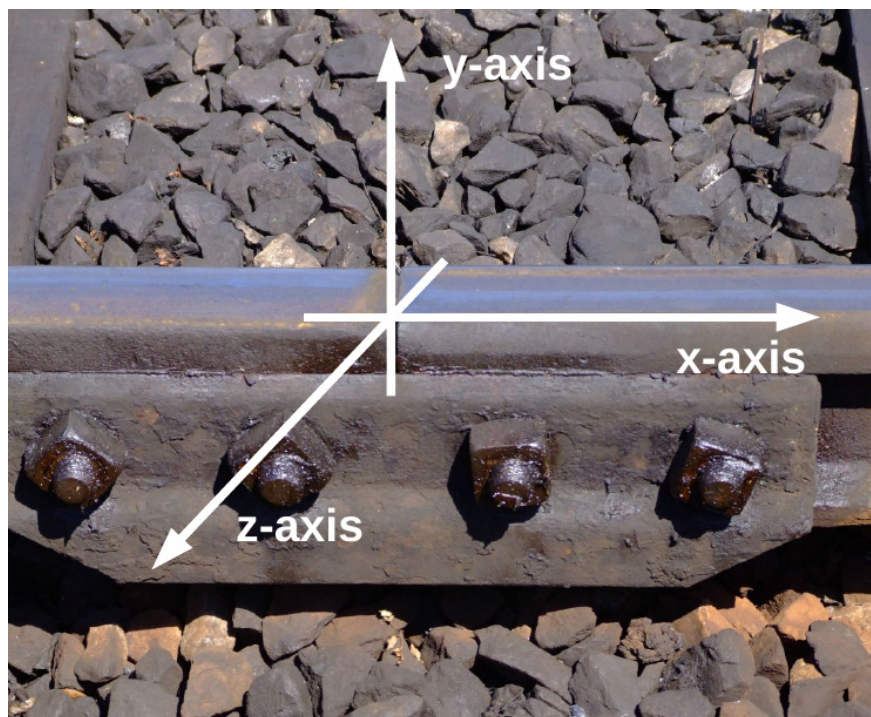


Fig. 3.3 The orientation of the ADXL335 sensor axis with reference to the railway track

completes 116 km run at an average speed of 43 kmph. As explained above health analysis of this train is very necessary owing to its speed. Kolongpar express (KLP-Exp) connects Mairabari of Assam to Guwahati. It covers 160 km at an average speed of 32 kmph. Rajdhani express (RJ-Exp) (Dibrugarh) is one of the premier trains of NFRA and it covers 2434 km at an average speed of 65 kmph. There was an incident of derailment of this train on 25 June 2014 in Chhapra, Bihar that killed four people and injured eight. Condition monitoring of this kind of high speed train is of utmost importance as small hitch in the equipment can magnify due to speed and may result in fatal accidents. Rajendra Nagar Capital express (RJN-Exp) connects Patna, Bihar to Guwahati, Assam. It covers 949 km at an average speed of 42 kmph.

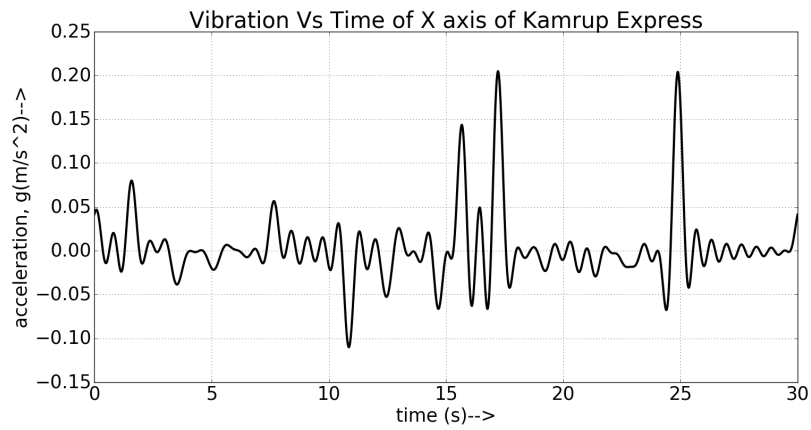
3.4 Experimental results and analysis:

Figure 3.4 shows the vibration(acceleration) vs time graph for Kamrup Express. Horizontal axis represents the time in second and Vertical axis represents the vibration data from the sensor after proper signal conditioning in all the 3-axes. Various information from these waveforms can be extracted. Figures from 3.5 to 3.8 shows vibration(acceleration) vs time characteristics of Kopili, Kolongpar, Rajdhani and Rajendra Nagar Capital Express respectively.

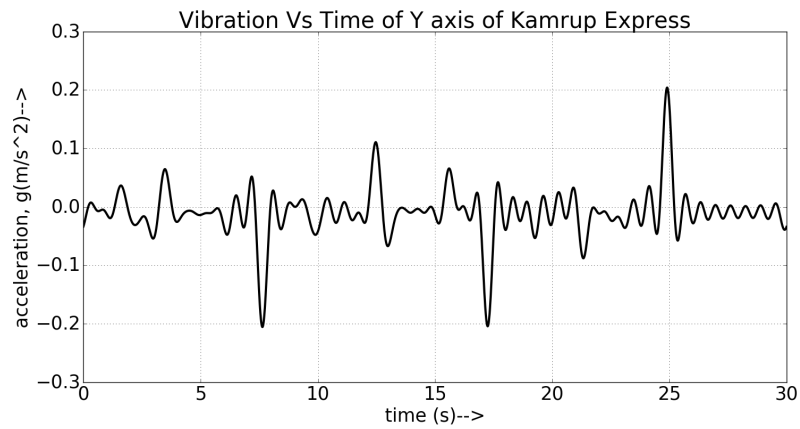
3.4.1 Information from time-domain analysis:

Analysis of vibration signals in time domain is mostly focussed on Principal Component Analysis (PCA), and it's variants [51], [60]. Another popular method of analysing time domain data is Kurtosis analysis [54]. Apart from these another method is to create time-domain features to be further analysed by Artificial Intelligence, Machine learning etc. [42], [65]. Compared to the techniques present in the literature, here a fairly simple technique is used to interpret X and Y axis vibration. X-axis and Y-axis vibrations are very important to analyse specially for railways from a safety point of view. As uneven or non-periodical vibration in the X-axis can be a measure of relative slip between the train and track. Similarly an uneven or non-periodical vibration in the Y-axis can be a measure of tendency of derailment. To quantify these, the following algorithm is proposed:

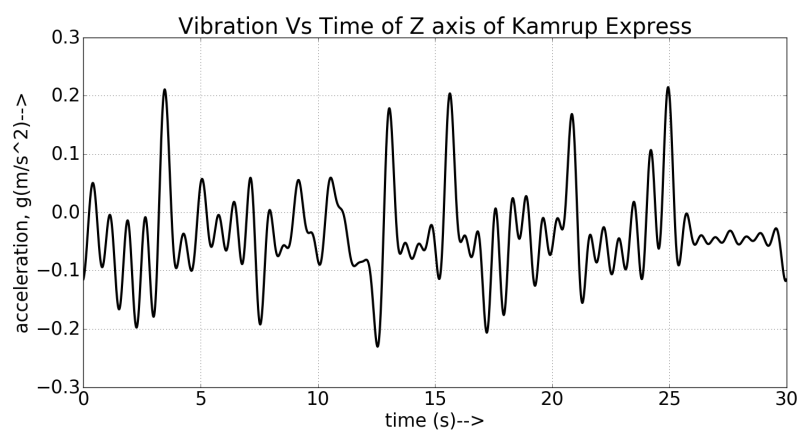
1. RMS value of the vibration in the direction of x-axis for a fixed period of time (say $1T$ seconds) are calculated.
2. If $(|x(t)| - r.m.s \text{ value of the vibration}) \geq \text{threshold}$, it is a instant of slip, threshold to be determined empirically.



(a) Vibration Vs Time of Kamrup Express: X-Axis

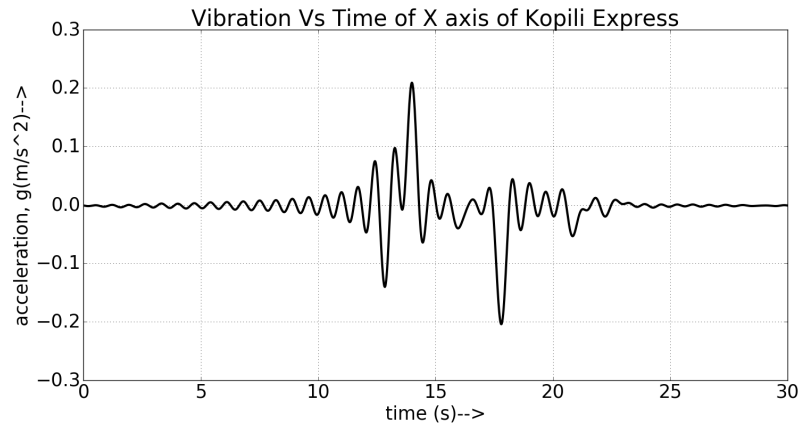


(b) Vibration Vs Time of Kamrup Express: Y-Axis

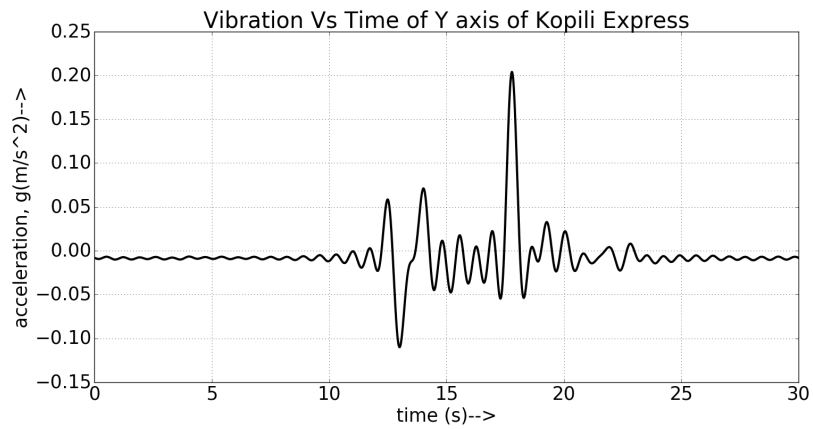


(c) Vibration Vs Time of Kamrup Express: Z-Axis

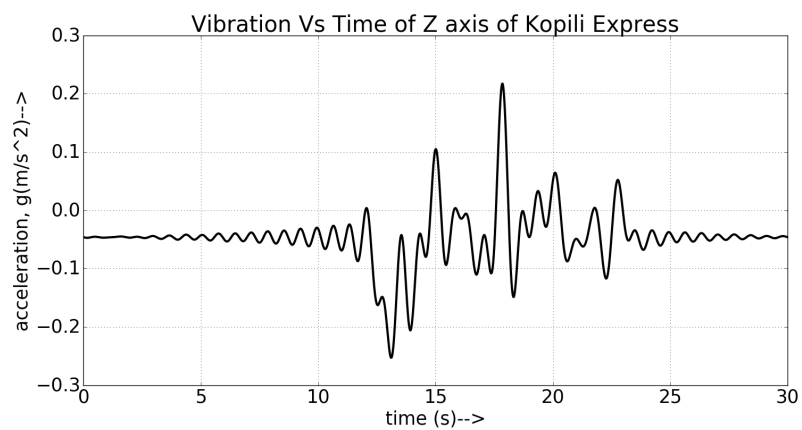
Fig. 3.4 Vibration Vs Time of Kamrup Express



(a) Vibration Vs Time of Kopili Express: X-Axis

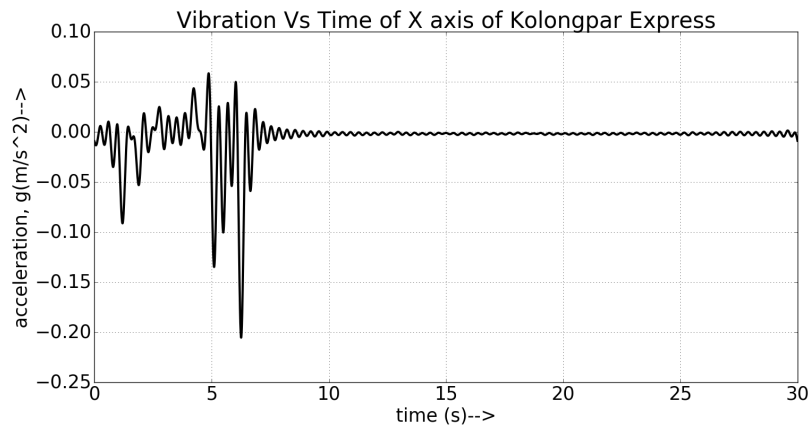


(b) Vibration Vs Time of Kopili Express: Y-Axis

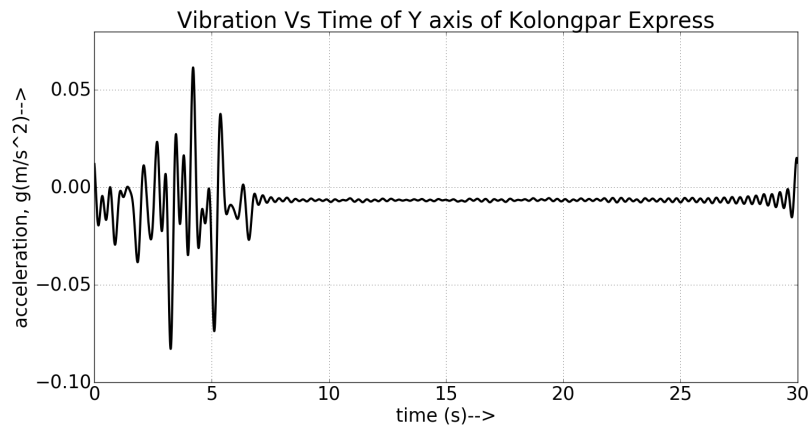


(c) Vibration Vs Time of Kopili Express: Z-Axis

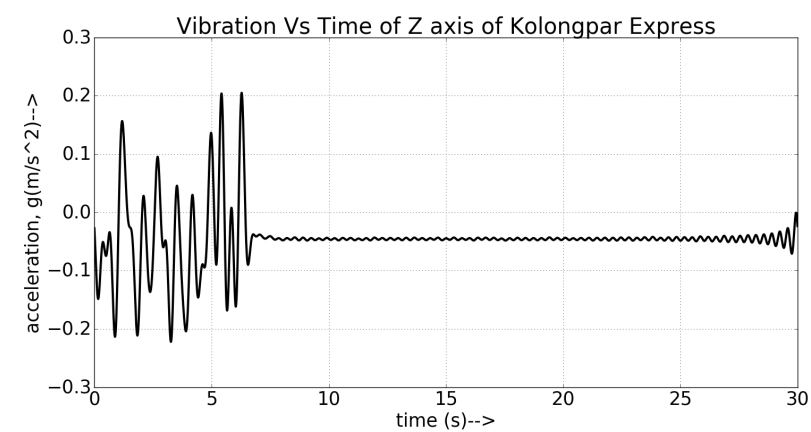
Fig. 3.5 Vibration Vs Time of Kopili Express



(a) Vibration Vs Time of Kolongpar Express: X-Axis

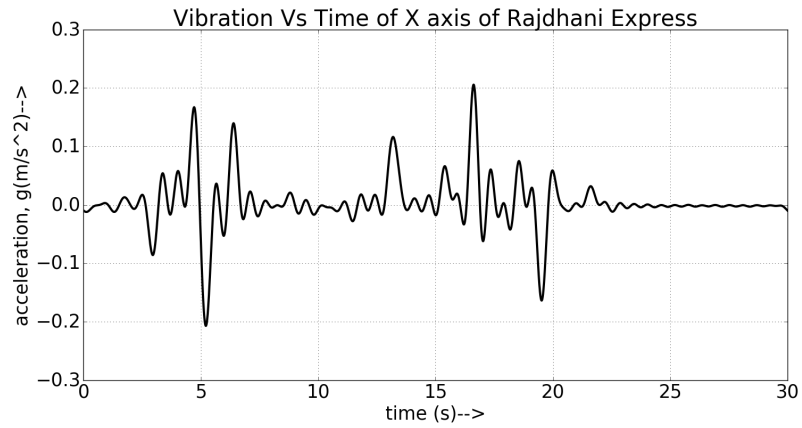


(b) Vibration Vs Time of Kolongpar Express: Y-Axis

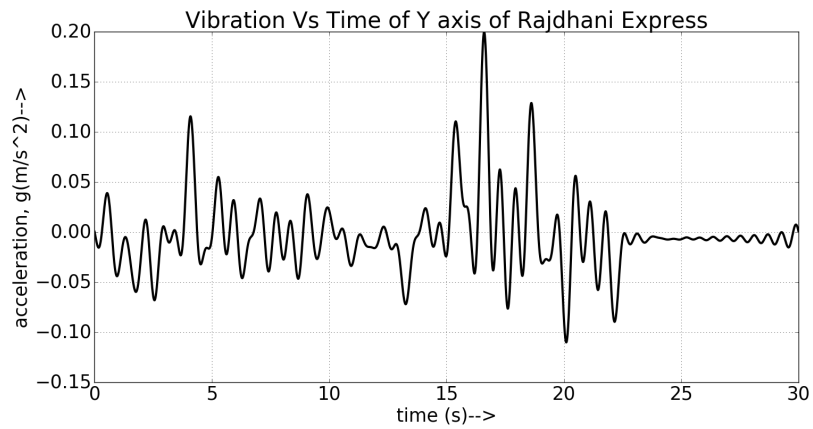


(c) Vibration Vs Time of Kolongpar Express: Z-Axis

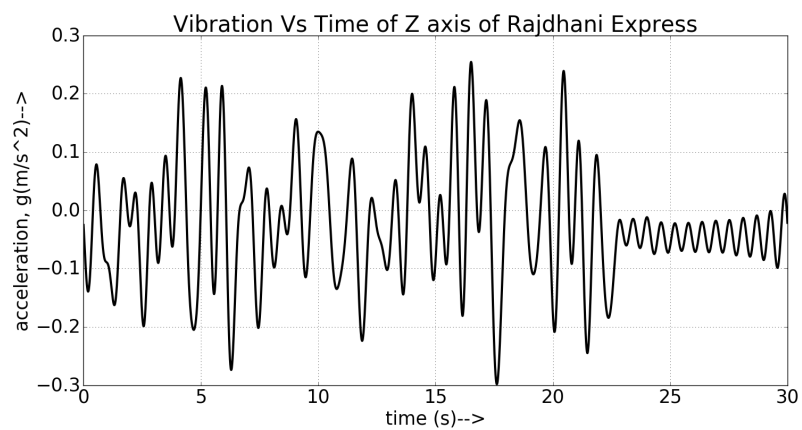
Fig. 3.6 Vibration Vs Time of Kolongpar Express



(a) Vibration Vs Time of Rajdhani Express: X-Axis

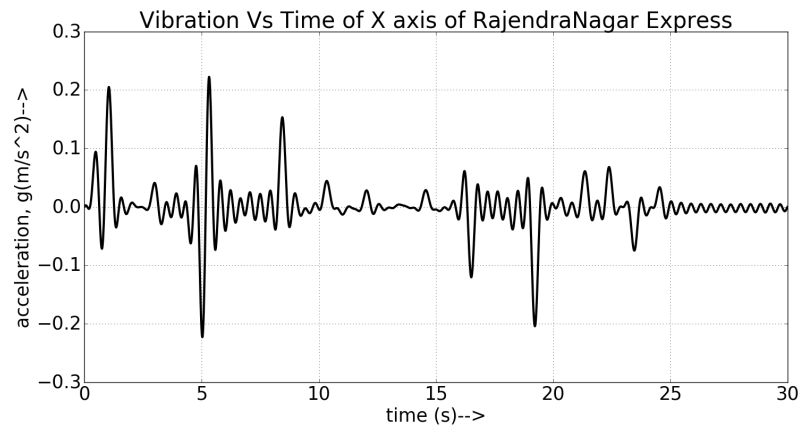


(b) Vibration Vs Time of Rajdhani Express: Y-Axis

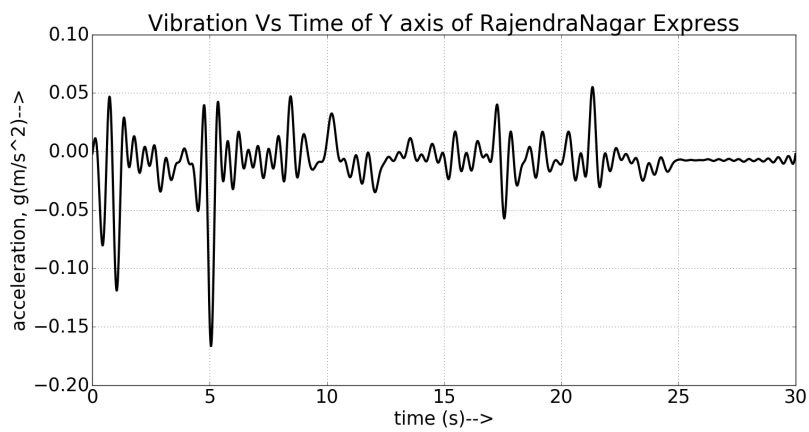


(c) Vibration Vs Time of Rajdhani Express: Z-Axis

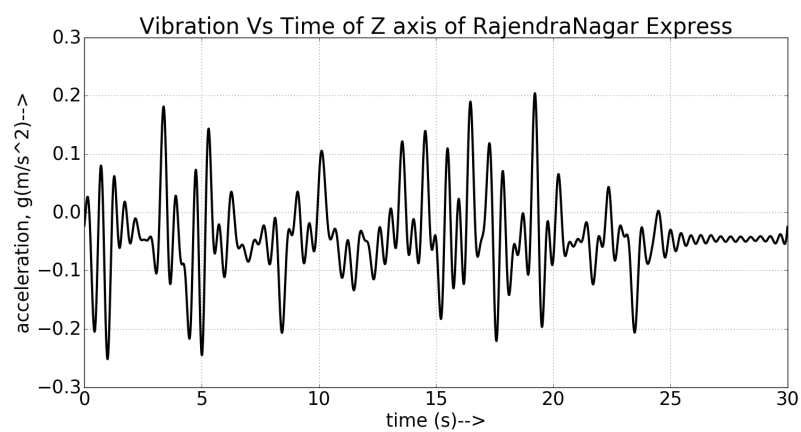
Fig. 3.7 Vibration Vs Time of Rajdhani Express



(a) Vibration Vs Time of Rajendra Express: X-Axis



(b) Vibration Vs Time of Rajendra Express: Y-Axis



(c) Vibration Vs Time of Rajendra Express: Z-Axis

Fig. 3.8 Vibration Vs Time of Rajendra Express

Table 3.1 Slip tendency and derailment tendency

Sl.No.	Train	Average Speed of the train (kmph)	Instant of slips	Instants of derailment tendency
1	Kamrup Express	42	2	0
2	Kopili Express	43	0	2
3	Kolongpar Express	32	2	2
4	Rajdhani Express	65	0	0
5	Rajendra Nagar Capital Express	42	0	4

3. Similar algorithm could be used for determining derailment tendency in the y-axis direction.

Here the threshold taken is 5 times the r.m.s value, time considered is 30 sec and accordingly the result is as shown in the table 3.1. Root Mean Square (r.m.s.) value of an a.c. signal is the effective value of the signal. Therefore, r.m.s. value can also be considered as the steady state value, of a decaying sinusoid. Extending this to a rapidly varying signal such as vibration, r.m.s. value can be considered as the steady state value of the signal. Here the vibration signals of the x-axis and y-axis are considered. The r.m.s. values of these two vibration signals can be considered as the steady state values of these two signals. If there is an instant where the instantaneous magnitude is more than 5 times the r.m.s value, then this instantaneous magnitude of the signal can be considered as an impulse. This can be explained with the help of the figure 3.9. Here a pulse of width T and height 1/T is considered such that the area under the pulse is unity. Keeping the area of the pulse constant, if the width is reduced to half, the height rises to 2/T. Similarly reducing the width to one fourth, height rises to 4 times the original height. Any more rise in the height can be viewed as an impulse as the width would be further reduced. In the present analysis, the time scale is in seconds. Therefore if an pulse of width 1 sec and height 1 r.m.s value, is considered and above arguments are applied, 4 times the r.m.s value is associated with 0.25 seconds so that the area is unity. Thus 5 times the r.m.s value at any given instant can be considered as an impulse. In the analysis of x-axis and y-axis vibration, these impulses may be seen as unwanted occurrences and therefore may be considered as instants of slips and derailment tendencies respectively.

It has been observed from table 3.1, that although the Rajdhani express possesses the highest average speed, still its slip and derailment tendencies are zero whereas Kolongpar express possess least average speed but it has some tendencies of slip and derailment. From

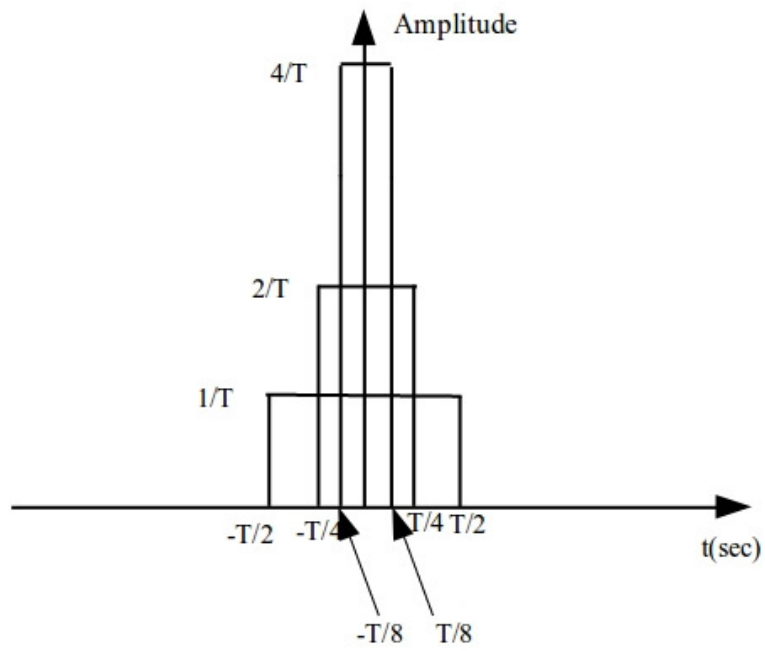


Fig. 3.9 Concept of an impulse

Table 3.2 Power w.r.t Frequency analysis: X-axis

SI No	Train	Equivalent Power (watt)				
		frequency band (0-10 Hz)	frequency band (11-20 Hz)	frequency band (21-30 Hz)	frequency band (31-40 Hz)	frequency band (41-50 Hz)
1	KA-Exp	0.0191959	0.0275451	0.0235695	0.0289769	0.0123937
2	KO-Exp	0.0193217	0.0264800	0.0085777	0.0280528	0.0153028
3	KLP-Exp	0.0074484	0.0013602	0.0031284	0.0015782	0.0020494
4	RJ-Exp	0.0150945	0.0356127	0.0285931	0.0288910	0.0154726
5	RJN-Exp	0.0117320	0.0106172	0.0124066	0.0157163	0.0269102

derailment tendency column, it can be said that Kamrup and Rajdhani are the safest while Rajendra Nagar Capital express is the least safe among the five. Hence the experimental result matches with the observed conditions of the trains that is discussed in section IV.

3.4.2 Information from frequency domain analysis:

In literature it is mentioned that the different frequency bands have different information regarding the components of the train-track system [69]. The total average power of a train calculated over a frequency range of the vibration signal can be expressed as:

$$p = \sum_{f_1}^{f_2} |c_k^2| \quad (3.1)$$

Where C_k is the coefficient of the Fourier Transform and f_1 and f_2 are start and end frequencies respectively.

Tables from 3.2 to 3.4 summarize power of different trains for different frequency bands. For the unit of power, it is noted that the signal captured is voltage. It is assumed that the signal is passed through a 1Ω resistor (as standard in signals and systems textbooks [78]); therefore the unit of power in this case is watt.

Total power of the trains: Total power p can be calculated as:

$$p = \sqrt{p_x^2 + p_y^2 + p_z^2} \quad (3.2)$$

Table 3.3 Power w.r.t Frequency analysis Y-axis:

SI No	Train	Equivalent Power (watt)				
		frequency band (0-10 Hz)	frequency band (11-20 Hz)	frequency band (21-30 Hz)	frequency band (31-40 Hz)	frequency band (41-50 Hz)
1	KA-Exp	0.0283628	0.0250795	0.0355176	0.0224921	0.0205089
2	KO-Exp	0.0102689	0.0145361	0.0170792	0.0096148	0.0056743
3	KLP-Exp	0.0001830	0.0007241	0.0006482	0.0004964	0.0018521
4	RJ-Exp	0.0217776	0.0155402	0.0181767	0.0129091	0.0216623
5	RJN-Exp	0.0041240	0.0030603	0.0023146	0.0065929	0.0055731

Table 3.4 Power w.r.t Frequency analysis Z-axis:

SI No	Train	Equivalent Power (watt)				
		frequency band (0-10 Hz)	frequency band (11-20 Hz)	frequency band (21-30 Hz)	frequency band (31-40 Hz)	frequency band (41-50 Hz)
1	KA-Exp	0.0804690	0.0842628	0.0727922	0.0877441	0.0774075
2	KO-Exp	0.0657289	0.0303902	0.0328026	0.0272098	0.0272171
3	KLP-Exp	0.0143683	0.0109733	0.0222704	0.0146527	0.0374704
4	RJ-Exp	0.0835180	0.1052653	0.1698987	0.1506657	0.1210481
5	RJN-Exp	0.0351622	0.0320230	0.0297571	0.0480538	0.0708138

Table 3.5 Total Power from Frequency analysis

SI No	Train	Equivalent Power (watt)				
		frequency band (0-10 Hz)	frequency band (11-20 Hz)	frequency band (21-30 Hz)	frequency band (31-40 Hz)	frequency band (41-50 Hz)
1	KA-Exp	0.0874539	0.0921300	0.0843548	0.0951030	0.0810317
2	KO-Exp	0.0692753	0.0428492	0.0379643	0.0402464	0.0317356
3	KLP-Exp	0.0161852	0.0110810	0.0224984	0.0147458	0.0375720
4	RJ-Exp	0.0876205	0.1122076	0.1732441	0.1539529	0.1239407
5	RJN-Exp	0.0372964	0.0338757	0.0323228	0.0509866	0.0759593

Table 3.6 Power calculations of different trains along X-Z directions

SI No	Train	Equivalent Power (watt)				
		frequency band (0-10 Hz)	frequency band (11-20 Hz)	frequency band (21-30 Hz)	frequency band (31-40 Hz)	frequency band (41-50 Hz)
1	KA-Exp	0.1547204	0.1602695	0.1543397	0.1575361	0.1623435
2	KO-Exp	0.0978272	0.0964842	0.0968943	0.0922040	0.0925974
3	KLP-Exp	0.0549084	0.0565561	0.0499748	0.0537572	0.0513343
4	RJ-Exp	0.1686879	0.1681257	0.1830112	0.2034626	0.1973378
5	RJN-Exp	0.0920142	0.0939117	0.0910631	0.0935497	0.1009353

Table 3.7 Power calculations of different trains along Y-Z directions are tabulated below:

SI No	Train	Equivalent Power (watt)				
		frequency band (0-10 Hz)	frequency band (11-20 Hz)	frequency band (21-30 Hz)	frequency band (31-40 Hz)	frequency band (41-50 Hz)
1	KA-Exp	0.1472782	0.1463560	0.1779980	0.1481666	0.1681321
2	KO-Exp	0.0755703	0.0797833	0.0797560	0.0749607	0.0774284
3	KLP-Exp	0.0294609	0.0315399	0.0274707	0.0309160	0.0293441
4	RJ-Exp	0.1957497	0.1865890	0.2091912	0.1951999	0.2305419
5	RJN-Exp	0.0786349	0.0789375	0.0880515	0.0848541	0.0817337

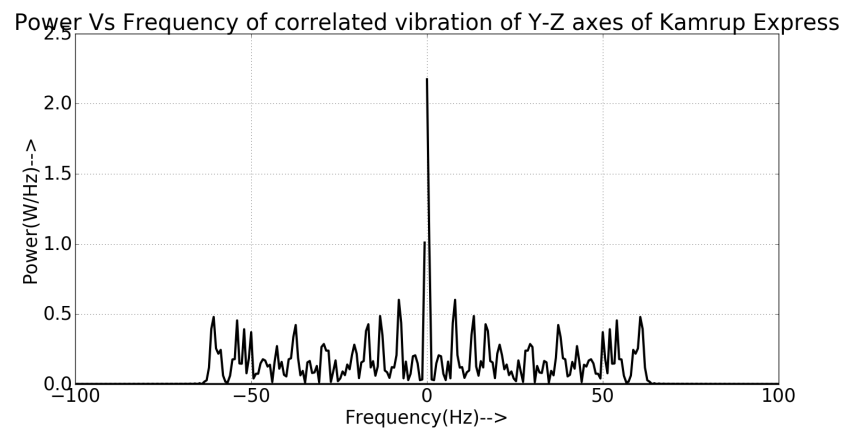
For power contents in combined direction we find correlation in the two directions by the following formula:

$$r_{xy}(k) = \sum_{-\infty}^{\infty} x(n)y(n) \quad (3.3)$$

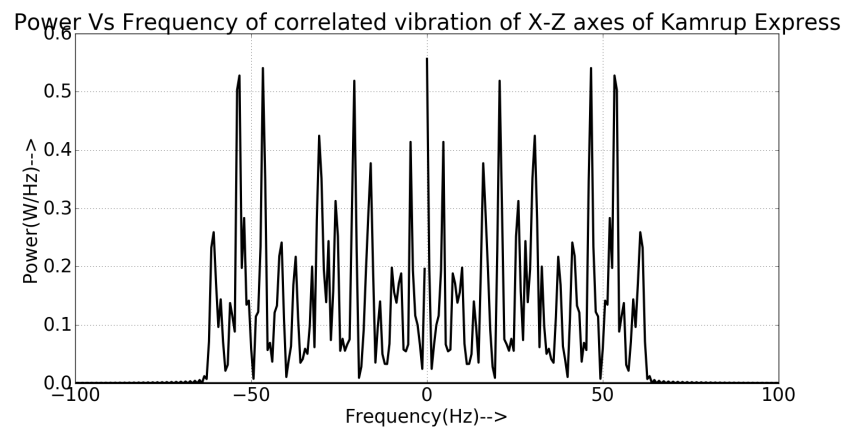
The Fourier Transform of $r_{xy}(k)$ from the Wiener Khintchine theorem is given by

$$s_{xy}(f) = \sum_{-\infty}^{\infty} r_{xy}(k)e^{-j2\pi kf} \quad (3.4)$$

which is the required cross Power Spectral Density. Thus the power contents in X,Y,Z and YZ and ZX directions are calculated. Figure 3.10 shows the cross power spectrum of Kamrup Express. Similar cross PSD profiles are obtained for the other trains. Power calculation of different trains along X and Z directions are tabulated in 3.6. Power calculation of different trains along Y and Z directions are tabulated in 3.7



(a) Power Vs Frequency of Kamrup Express: Y-Z Axes correlation



(b) Power Vs Frequency of Kamrup Express: X-Z Axes correlation

Fig. 3.10 Cross Power Spectrum Density for Kamrup Express

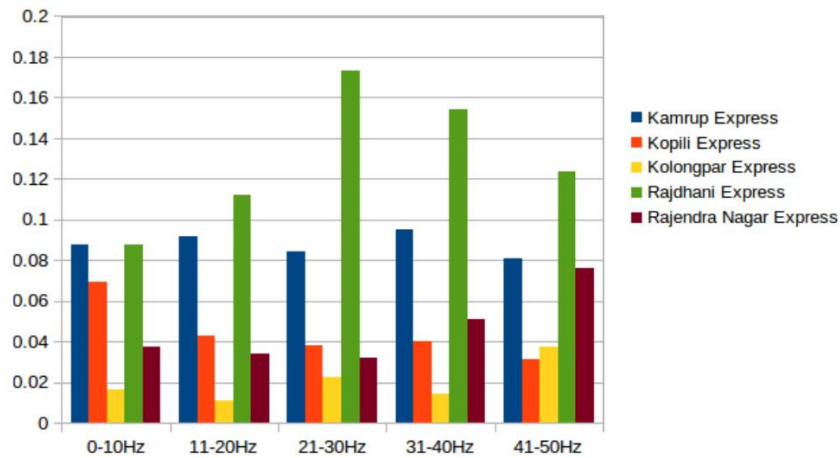


Fig. 3.11 Total power of different trains at different frequency bands

To monitor the condition or health of the train, essentially the health of different components of the train is needed to find out. Here a few important components of the train —bogie and locomotive are considered. Major components which are very essential from a safety point of view are wheel, primary suspension, secondary suspension, unsprung mass and axle. Vibrations at different frequencies carry information regarding different components of the train-track system. The information regarding the suspension between the car body and bogie also known as secondary suspension can be obtained by the vibration resonance below 10 Hz. Vibrations below 5 Hz can be interpreted to obtain information regarding the wheels of the train. Primary suspension i.e. the suspension between bogie and wheel is a very important component of the system and the information regarding this can be obtained by vibrations of frequency between 10 to 30 Hz. Above 50 Hz the rail response and ground vibration becomes independent of each other [69]. Between 30 to 40 Hz equivalent wheel-gearbox-axle-propulsion motor mass i.e. unsprung mass information can be extracted.

As discussed above Rajdhani express is of premier category and Kamrup express is an ISO certified train. These two trains are at better health compared to the other three. This can be confirmed by data tabulated in Table 3.5 for which we can visualize data as given in figure 3.11 . Different shades of gray represents different trains as indicated in the side of the figure.

Frequency band 0-10 Hz represents energy due to wheel and secondary suspension. Here as can be seen from the figure 3.11, energy from Kamrup express and Rajdhani express is high compared to the other three trains viz. Kopili, Kolongpar and Rajendra Nagar. This can be interpreted as wheel and secondary suspension i.e. suspension between car body and bogie in good condition. More energy from the secondary suspension can be interpreted as more vibrations from the secondary suspension and hence less vibration of the car body

and increased passenger comfort. Information regarding the suspension between bogie and wheel is obtained from an energy band of 10-30 Hz. As seen from the figure-3.11, here also Rajdhani and Kamrup express shows a very high energy dissipation compared to the other three. This can be interpreted as the primary suspension of these two trains are better equipped to handle uneven track conditions. Because of this, these trains are much more stable even at higher speeds compared to the other three. Information regarding the unsprung mass i.e. equivalent wheel-gearbox-axle-propulsion motor mass can be obtained from the frequency band 30-40 Hz. This frequency band also shows a similar trend of Rajdhani and Kamrup being better than the other three trains.

3.5 Discussion

It has been observed that with a simple 3D vibration sensor system preliminary condition monitoring of trains is possible. In countries like India, where there are huge numbers of local trains (covering distances within a city) ply daily, this system can be easily implemented because installing sophisticated on board monitoring systems would demand a lot of time and money.

3.6 Conclusion

In this chapter a 3D vibration sensor based embedded system has been developed for capturing vibration of a railway track during train in motion. The 3D vibration sensor ADXL335 has been used for the purpose of capturing vibration of a railway track. Arduino Uno board has been used as the core of the embedded system to interface ADXL335 for capturing vibration data on real time basis and to transfer the same to a laptop through USB port. The stored vibration signals are analysed using signal processing techniques namely time-domain and frequency-domain analysis. It has been observed that the time-domain analysis offers critical information related to the safety measure of a train in terms of slip and derailment tendencies. Whereas frequency-domain analysis provides information related to the condition of different components of a train such as wheel and suspension system.

4

Linear and Quadratic Time-Frequency Analysis of Vibration for Fault Detection and Identification of NFR Trains

This chapter discusses a simple sensor based system that detects and identifies faults of a train. Four different trains are considered for analysis as suggested by the North-East Frontier Railway(NFR) authorities. For this purpose, an embedded system containing ADXL335 sensor is used to capture the vibration of a railway track during movement of a train over the track. The embedded system transfers the captured signals from ADXL335 to a laptop. These signals are processed using linear time-frequency transform(Wavelet transform) in conjunction with quadratic time-frequency transform(Wigner-Ville transform)to find out if there are any faults and thereby quantify the quality of the moving trains. Wheel-flat fault is detected for one train with the wheel position and the bogie number. This is a low cost technique as the method involves only one ADXL335 sensor, an Arduino development board and the software used for the analysis is python which is an open source and platform independent software.

4.1 Introduction

Derailment of trains is a common issue in India. According to Factly report, from 2009 to 2015, there were 803 railway accidents in India. Out of these 803 accidents, 47% were due to the derailment of the trains [75]. Wheel-set defects are most likely to cause these accidents, compared to the faults of other components of the vehicle [31]. Although several work had been done in condition monitoring, fault detection and identification of train and tracks, improvement in the wayside condition monitoring is required by implementing appropriate signal analysis methodologies [[35], [37]]. In recent years, the fault diagnosis of railways has been a major thrust area of research. Faults such as tread flat leads to the periodic jumping of the vehicle over the track, as the wheel (tread flat) makes impact on the track [36]. This further enhances the damage of the wheel. Hence it becomes a necessity to detect this fault at the earliest. While most of the literature describes the applications of the Hilbert-Huang Transform (HHT) to detect this fault [56], [59], some work preferred Frequency Slice Wavelet Transform [36]. In a notable work by Papaelias et.al., presence of the wheel damage and its severity is detected by simple time-domain features, such as Root Mean Square (RMS) value and frequency-domain technique, such as Fast Fourier Transform (FFT) [35]. Similarly Bracciali et. al. used the energy and the cepstrum analysis of the vibration signal for wheel flat detection. The system used by them detects the occurrence of the wheel-flat in a bogie but unable to detect the exact defective wheel [26]. Different preferred methods are observed for fault detection in signal analysis in different domains. In time-domain, Wei et. al. had reported the use of one promising method known as Consensus Principle Component Analysis (CPCA). CPCA was adopted by them for their work in fault detection of rail vehicle suspension systems [34]. Principal Component Pursuit (PCP) is another popular method for fault detection [51]. Along with the time-domain analysis, another popular method is Multivariate Statistical Process Control (MSPC). Jin et. al. compared various MSPC based models for detecting abnormality in bearings by analysing the vibration signal produced by the bearings [60]. In another method, time-domain features such as RMS value, crest factor, impact factor, kurtosis etc. are used as the input to some classifier and thereby used for fault detection [42], [65]. In frequency domain method, Power Spectral Density (PSD) is preferred, as it helps in determining patterns and thereby the faults. Frequency domain methods are predominant in system identification and fault analysis of mechanical structures [[22],[58],[79],[80]]. Again combining the time-domain features with the frequency can be used as another method such as Kurtogram analysis and Improved Spectral Kurtosis(ISK) analysis [[54], [57]]. For stationary signals, individual time-domain or individual frequency-domain analysis is sufficient for information extraction. However, when non-stationary signals are analysed, the time-frequency domain is preferable

for information extraction , especially for fault detection [81]. Wavelet transform in its different variations and/or in conjunction with other techniques are popular methods for fault detection, as many literature can be seen following this approach [[82], [57], [55], [61]]. Li et. al. had discussed the fault detection and classification of a Medium Voltage Direct Current (MVDC) Shipboard Power System (SPS) through Wavelet Transform Multi-Resolution Analysis (WTMRA) technique with Artificial Neural Network(ANN) [82]. The WT-MRA and Parseval's theorem were used for feature extraction and ANN was used for classification by Chen et. al. in their experimentation with Fault Detection and Identification (FDI) of rotating machinery [57]. In their paper, it was described how Improved Spectral Kurtosis (ISK) in conjunction with Adaptive Redundant Multiwavelet Packet (ARMP) can be used for FDI. The shortcoming of Kurtosis analysis is that when periodic faults occur, the Kurtosis analysis becomes less effective and can be mitigated by extracting the sensitive frequency band, which is generated by incorporating an additional evaluation index to the spectral kurtosis and multi-wavelet. For de-noising of the vibration signal, Empirical Wavelet Transform (EWT) is used and then signal processing techniques such as calculating the Kurtosis value and the envelope spectrum are used for the fault detection [55].

In the present work, a combination of linear and non-linear time-frequency domain analysis is proposed to detect and identify the faults of a train. One of the remarkable properties of the wavelet transform is that it can indicate the presence of impulses in a vibration signal. The wavelet coefficients generated can be classified based on some threshold, and selected as fault features of a machine. However the problem of selecting the threshold or any other such criteria that qualifies the wavelet coefficients as fault features remains open [83]. An excellent solution to this problem is provided by Mallat et. al that utilises Lipschitz exponents to classify the wavelet components [84]. Using the non-linear time-frequency domain analysis such as Wigner-Ville transform and Cohen's class of time-frequency distribution, a precise localization of the frequency of these impulses in the time-domain can be achieved [85]. Analysis of these locations of impulses and their duration in time-scale are indications of faults in the system. Once this is computed the faults may be detected by simply visualizing the 3D representation of the time-frequency course of the amplitude spectrum. For the wavelet transform analysis, selection of the wavelet is done on the work presented in [86]. Schukin et al. presented the selection of "impulse" wavelet as the optimized wavelet to detect impulses. Wavelet transform would detect the presence of all the impulses generated by faults. Wigner-Ville transform would confirm whether these impulses are due to the train vibration or noise as well as the presence of wheel-flat and their position.

For data acquisition purpose, a single ADXL335 based embedded system is designed. ADXL335 sensor is used to capture the 3D vibrations of a railway track. The real time data

from ADXL335 sensor is captured by an Arduino 328 Uno microcontroller board. The data captured by the system and transferred to a laptop for storage and analysis. Compared to the existing literature, the present work

- uses *optimized wavelet* to find impulses and
- uses Wigner-Ville transform to confirm whether these impulses are due to the train vibrations or noises and find the presence of wheel-flat fault precisely at the bogie number and the wheel position.

4.2 Theoretical background

In this section a brief review of the Wavelet transform optimized for local extrema detection (presence of impulses in the vibration signal) and Wigner-Ville transform for localization of the faults are presented.

4.2.1 Wavelet transform optimized for local extrema detection

The foundation work of extrema detection is from the classical paper by Mallat et. al. while the optimization of the wavelet is from the paper by Schukin et. al.

Let us consider a wavelet $\theta(t)$. $\theta(t)$ is double differentiable and satisfy $\int_{-\infty}^{\infty} \theta(t) = 1$, t is the time. Two other wavelets may be derived, from this wavelet as :

$$\Psi^a(t) = \frac{d\theta(t)}{dt}; \int_{-\infty}^{\infty} \Psi^a(t) = 0 \quad (4.1)$$

$$\Psi^b(t) = \frac{d^2\theta(t)}{dt^2}; \int_{-\infty}^{\infty} \Psi^b(t) = 0 \quad (4.2)$$

If the function $\xi_p(t)$ represents $\frac{1}{p}\xi(\frac{t}{p})$, then the wavelet transform of a signal $f(t)$ with scaling-factor p and time t , computed with the above mentioned wavelets (4.1) and (4.2) can be represented as:

$$W_p^a f(t) = f(t) * \Psi_p^a(t) \quad (4.3)$$

$$W_p^b f(t) = f(t) * \Psi_p^b(t) \quad (4.4)$$

where "*" represents the convolution.

Now it can be derived that

$$W_p^a f(t) = f(t) * \left(p \frac{d\theta_p}{dt}\right)(t) = p \frac{d}{dt} (f(t) * \theta_p)(t) \quad (4.5)$$

and

$$W_p^b f(t) = f(t) * \left(p^2 \frac{d^2\theta_p}{dt^2}\right)(t) = p^2 \frac{d^2}{dt^2} (f(t) * \theta_p)(t) \quad (4.6)$$

The Wavelet Transform(WT) $W_p^a f(t)$ represents the first derivative of the signal $f(t)$ smoothed with a scale factor p i.e it can indicate the presence of local extrema in the wavelet surface and Wavelet Transform $W_p^b f(t)$ represents the second derivative of the signal $f(t)$ smoothed with a scale factor p that can dictate the local maxima or minima on the wavelet surface.

Second order systems are very common and higher order systems may be suitably assumed to follow the characteristics of a second order system by virtue of its dominant poles. A second order system subjected to an impulse at t_0 would produce a response of the form

$$f(t) = A_0 e^{-\xi \omega_n (t-t_0)} \sin(\omega_d (t-t_0)) \quad (4.7)$$

Where, A_0 is the initial amplitude, ξ is the damping ratio, ω_n is the natural frequency and ω_d is the damped frequency of oscillation such that $\omega_d = \omega_n \sqrt{1 - \xi^2}$. The mother wavelet selected is the 'impulse' based on the paper [86] and is given by $\Psi(t) = e^{2\pi j \omega_0 t - 2\pi |t|}$. ω_0 is the carrier frequency of the wavelet. From the above representation

$$\Psi_p^a f(t) = p \frac{d}{dt} (f(t) * \theta_p)(t) \quad (4.8)$$

Notations represent the meanings as discussed above. Here, f is the output from the system containing impulse at t_0 i.e $f(t) = A_0 e^{-\xi \omega_n (t-t_0)} \sin(\omega_d (t-t_0))$ and θ is the wavelet i.e $\theta(t) = e^{2\pi j \omega_0 t - 2\pi |t|}$. To compute the convolution, the two functions are multiplied in the Laplace domain which led to the following result:

$$\frac{A_0 e^{\xi \omega_n t_0}}{p(s + \frac{2\pi}{p}(j\omega_0 - 1))} \left[\cos(\omega_d t_0) \frac{\omega_d}{(s + \xi \omega_n)^2 + \omega_d^2} - \sin(\omega_d t_0) \frac{s + \xi \omega_n}{(s + \xi \omega_n)^2 + \omega_d^2} \right]$$

In the above representation s is the Laplace variable and also the $|t|$ of the $\theta(t)$ is relaxed to t as the reflected version of the signal is needed for the convolution. To complete the wavelet transform, this result is to be differentiated i.e multiplying with s in the Laplace domain and multiplying with the scale-factor p . Accordingly, the following result is obtained :

$$\frac{sA_0 e^{\xi \omega_n t_0}}{s + \frac{2\pi}{p}(j\omega_0 - 1)} \left[\cos(\omega_d t_0) \frac{\omega_d}{(s + \xi \omega_n)^2 + \omega_d^2} - \sin(\omega_d t_0) \frac{s + \xi \omega_n}{(s + \xi \omega_n)^2 + \omega_d^2} \right]$$

This equation may be equated to 0 to obtain the local extrema in the wavelet surface that would represent a singularity or impulse in this case.

$$\frac{sA_0 e^{\xi \omega_n t_0}}{s + \frac{2\pi}{p}(j\omega_0 - 1)} \left[\cos(\omega_d t_0) \frac{\omega_d}{(s + \xi \omega_n)^2 + \omega_d^2} - \sin(\omega_d t_0) \frac{s + \xi \omega_n}{(s + \xi \omega_n)^2 + \omega_d^2} \right] = 0$$

$$\implies \tan(\omega_d t_0) = \frac{\omega_d}{s + \xi \omega_n} \quad (4.9)$$

Eq. (4.9) shows that at point of singularity time domain information in the form of t_0 and frequency domain information in the form of s is available. Also the damped frequency of oscillation ω_d and rate of attenuation $\xi \omega_n$ are present. While t_0 would give presence of an impulse at that instant, the damped frequency of oscillation ω_d and rate of attenuation $\xi \omega_n$ would give its progression. The term $s + \xi \omega_n$ is very important as it shows that $\xi \omega_n$, the rate of attenuation in the frequency domain while preserving the time information of impulse occurrence at t_0 .

4.2.2 Wigner-Ville transform for localization of impulses

The Wigner-Ville transform of a signal $f(t)$ is defined as

$$WVT_f(t, \omega) = \int_{-\infty}^{\infty} f(t + \frac{\tau}{2}) \bar{f}(t - \frac{\tau}{2}) e^{-j\omega\tau} d\tau \quad (4.10)$$

where \bar{f} represents the complex conjugate of f and ω represents frequency. A second order system subjected to an impulse at t_0 would produce a response of the form $f(t) = A_0 e^{-\xi\omega_n(t-t_0)} \sin(\omega_d(t-t_0))$. And f is considered accordingly. Therefore the Wigner-Ville transform of f is

$$\begin{aligned} WVT_f(t, \omega) = & \int_{-\infty}^{\infty} A_0 e^{-\xi\omega_n(t-t_0+\frac{\tau}{2})} \sin(\omega_d(t-t_0+\frac{\tau}{2})) \\ & (-A_0 e^{-\xi\omega_n(t-t_0+\frac{\tau}{2})} \sin(\omega_d(t-t_0+\frac{\tau}{2}))) e^{-j\omega\tau} d\tau \end{aligned} \quad (4.11)$$

Since $\sin(\omega t)$ can be considered as the imaginary part of $e^{j\omega t}$ the conjugate part of the Wigner-Ville transform is simply taken as the negative of the f . Also since the time t will only progress in the positive direction from t_0 , the limit can be changed from 0 to ∞ . Continuing the computations

$$\begin{aligned} WVT_f(t, \omega) = & \int_0^{\infty} (-\frac{A_0^2}{2} e^{-2\xi\omega_n(t-t_0)} (\cos(\omega_d\tau) - \\ & \cos(\omega_d(t-t_0)))) e^{-j\omega\tau} d\tau \\ = & \frac{A_0^2}{2} e^{-2\xi\omega_n(t-t_0)} \left\{ \frac{\cos(\omega_d(t-t_0))}{j\omega} \right. \\ & \left. - \pi(\delta(\omega + \omega_d) + \delta(\omega - \omega_d)) \right\} \end{aligned} \quad (4.12)$$

Eq. (12) clearly shows that information in both time and frequency domain is preserved as it can be seen that the presence of the impulse in the frequency domain indicated at $\pi(\delta(\omega + \omega_d) + \delta(\omega - \omega_d))$ and its progression in time domain indicated by $(t - t_0)$.

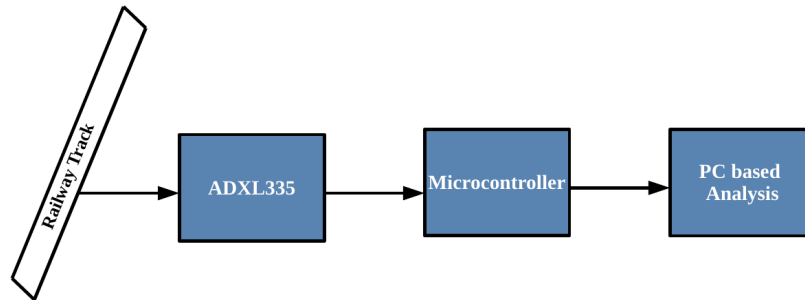


Fig. 4.1 Block diagram representation of the scheme to capture vibration signals generated by a train while in motion over a track.

4.3 Capturing of the vibration signal generated by a train running over a track, using an ADXL335 sensor

The functional block diagram adopted for data acquisition is depicted in fig. 4.1.

ADXL335, a 3-axis accelerometer is interfaced to the Arduino Uno development board to record vibration of trains running over a track. A laptop is used to pull and store vibration data captured by the embedded system through its USB port. ADXL335 measures acceleration with a full-scale range of ± 3 g. It can measure the static acceleration of gravity in tilt-sensing applications, as well as dynamic acceleration resulting from motion, shock, or vibration. The sensor is fixed to the fish-plate of the track as advised by the NFR authority.

The NFR authority, Maligaon, Assam, India provided a facility to carry out the experiments on a live railway track under the supervision of their authorised personnels in accordance with their guidelines. The NFR authority permitted us to capture vibrations of the railway track located at Chandmari, Guwahati, Assam, India. The experimental set-up used for the purpose of capturing vibration signals of the railway track at Chandmari is shown in fig. 4.2. The ADXL335 sensor was firmly attached on the fish-plate of the joint of two railway tracks as advised by NFR authority. Fig. 4.3 shows the orientation of the sensor axes with reference to the railway track. The orientation of the sensor is made in such a way that the X-axis is parallel to the railway track, Y-axis is perpendicular to the railway track, parallel to the ground and the Z-axis is perpendicular to the ground.

NFR authority advised us to carry out the studies on four different trains, they are —(i) Rajdhani Express (ii) Kamrup Express (iii) Kolongpar Express and (iv) Kopili Express, as these four trains represent four different categories of trains with different allowable



Fig. 4.2 Experimental set-up for capturing vibration signals from the railway track.

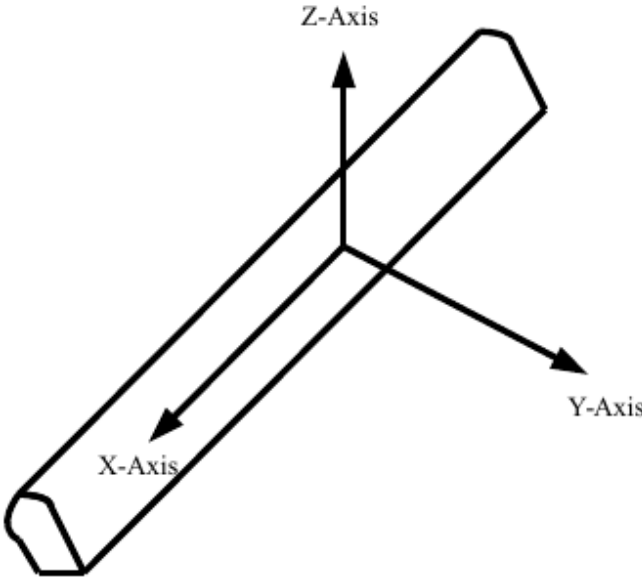


Fig. 4.3 The orientation of the ADXL335 sensor axes with the reference to the railway track.

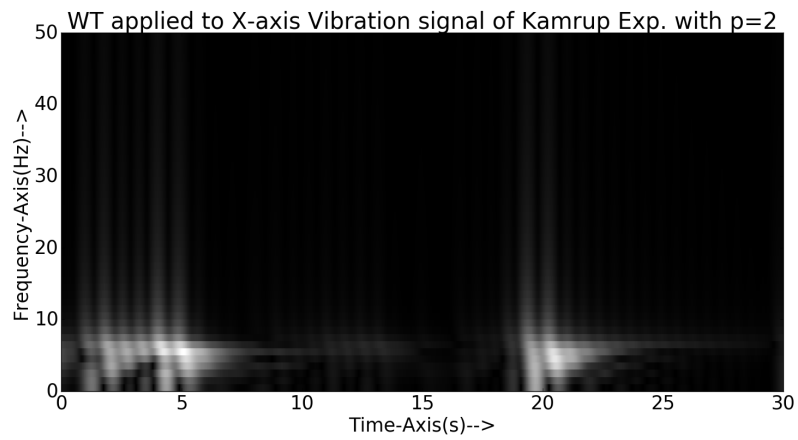
speeds. The Rajdhani Express is one of the premium trains in the NFR and enjoys the best of maintenance thereby maintaining excellent health, whereas Kamrup Express is an ISO certified train and enjoys relatively good health whereas the trains like Kolongpar Express and Kopili Express are of average health.

4.4 Experimental results and analysis:

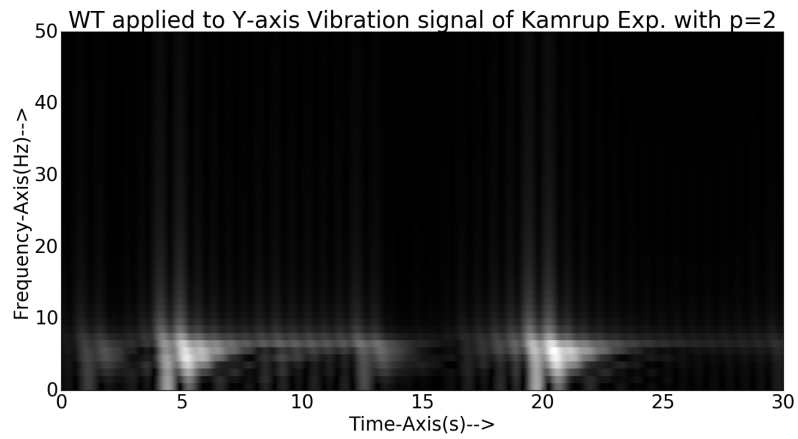
Vibration signals were captured at 200 samples/s for 30 sec as the range of frequency under study is 0-50 Hz. Since, the signal was sampled at 200 samples/s, thus the high frequency noise was easily eliminated. The major concern for the noise is due to the sensor. ADXL335 introduces Gaussian white noise but intensity is very low. The noise is proportional to the square root of the accelerometer bandwidth and in the range of $\frac{\mu g}{\sqrt{Hz}}$. Thus this can be neglected, when vibration due to large structure such as train moving over a track is considered. Moreover lower frequency components are of interest as information regarding the train is availed through the low frequencies. Hence, an external filter was avoided in the scheme. Below 50 Hz, the health condition of different parts of the vehicle can be captured [40]. Major components which are very essential from a safety point of view are wheel, primary suspension, secondary suspension, unsprung mass and axle. Vibrations at different frequencies carry information regarding different components of the train-track system. The information regarding the suspension between the car body and bogie also known as secondary suspension can be obtained by the vibration resonance below 10 Hz. Vibrations below 5 Hz can be interpreted to obtain information regarding the wheels of the train. Primary suspension i.e. the suspension between bogie and wheel is a very important component of the system and the information regarding this can be obtained by vibrations of frequency between 10 to 30 Hz. Between 30 to 40 Hz equivalent wheel-gearbox-axle-propulsion motor mass i.e. unsprung mass information can be extracted [69].

From the experiments, it was found that Z-axis vibrations were more prominent as compared to the X or the Y-axis vibrations; so for analysis only Z-axis vibrations are considered. Wavelet transform applied to the X, Y and Z-axis vibration signals of Kamrup Express is shown in fig. 4.4. As seen from the fig. 4.4, the Z-axis vibration is more prominent compared to the other two axes.

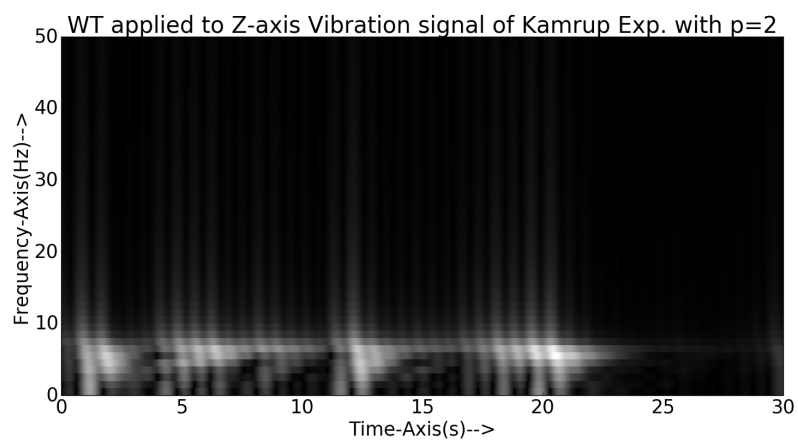
At first, the Rajdhani Express was considered for analysis. The z-axis vibration of the Rajdhani Express is as shown in fig. 4.5.



(a)



(b)



(c)

Fig. 4.4 (a) Wavelet Transform applied to X-axis vibration signal of Kamrup Express with $p=2$. (b) Wavelet Transform applied to Y-axis vibration signal of Kamrup Express with $p=2$. (c) Wavelet Transform applied to Z-axis vibration signal of Kamrup Express with $p=2$.

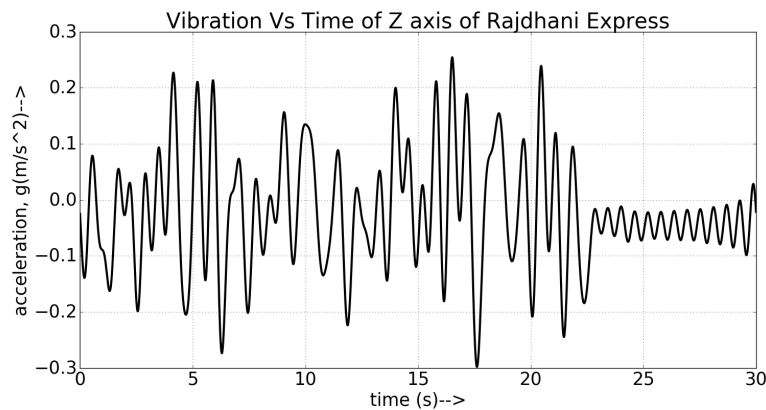
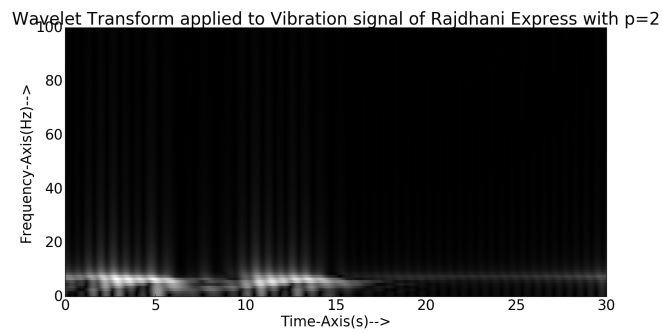


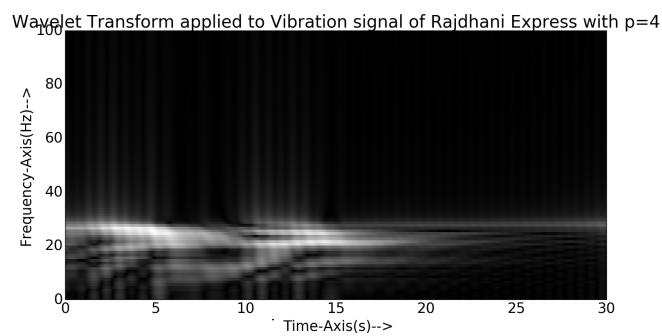
Fig. 4.5 Vibration(Acceleration) of Rajdhani Express in Z-axis.

4.4.1 Information from wavelet transform

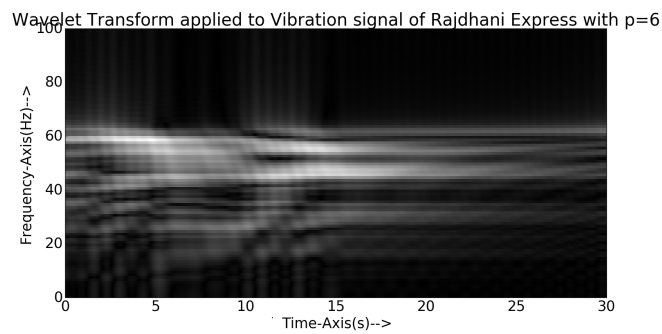
Wavelet Transform is applied to the vibration signal as discussed in the section II A. To capture various impulses at various frequencies different values of scaling-factor p is used. The spectrum in fig. 4.6a is limited to 15 s due to the value of p . If the value of p is low, the spectrum is compressed in the both time and frequency axes. The spectrum shown in fig. 4.6a is with the p value equal to 2. However, with higher p values such as $p=6$ and 8, the spectrum spreads for the entire time-scale. It is found that to capture impulses in the frequency range of 0-50 Hz, the p value from 2-6 is useful. With $p=2$, as shown in fig. 4.6 (a), short bursts of energies can be seen in the frequency range of 0-6 Hz in 0-8 s and again in frequency range of 0-6 Hz but in 10-14 s. Therefore it can be inferred that there are low frequency impulses in these time periods. With $p=4$, impulses present in higher frequencies (0-26 Hz in this case) can be seen. However the burst of energies seem to be continuous and spread out in time i.e although there are impulses it may be because of the random noise. The spreading of spectrum in time-axis increases with the increasing values of p as can be seen from fig. 4.6 (c) and (d) with $p=6$ and $p=8$ respectively. With $p=8$ the wavelet transform spreads out in both time and frequency. The impulses due to faults are expected to be sudden bursts of energy repeated periodically and not to spread out in time. This trend seems to be evident with $p=2$ while with higher values of p it becomes difficult to distinguish between noise and the impulses generated by the faults of the train. Therefore some confirmatory measures are required to firmly ascertain about the presence of the faults. Hence, Wigner-Ville transform is applied for further processing.



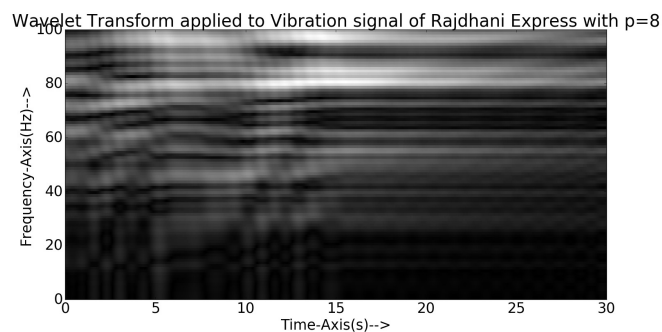
(a)



(b)



(c)



(d)

Fig. 4.6 (a) Wavelet Transform applied to vibration signal of Rajdhani Express with $p=2$. (b) Wavelet Transform applied to vibration signal of Rajdhani Express with $p=4$. (c) Wavelet Transform applied to vibration signal of Rajdhani Express with $p=6$. (d) Wavelet Transform applied to vibration signal of Rajdhani Express with $p=8$.

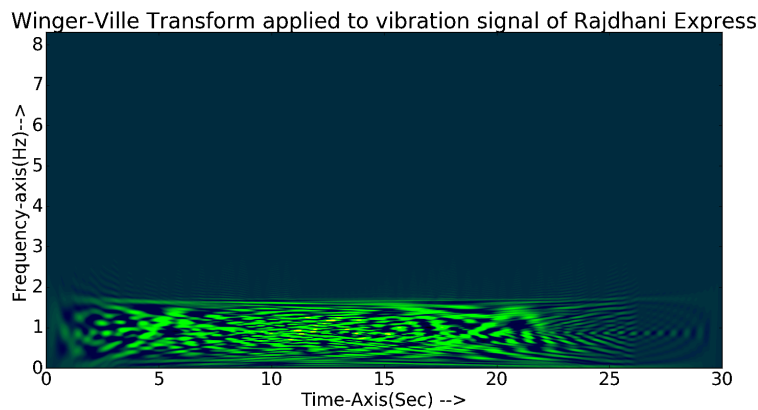


Fig. 4.7 Wigner-Ville transform applied to vibration signal of Rajdhani Express.

4.4.2 Information from Wigner-Ville transform

Wigner-Ville transform is shown in fig. 4.7. It is seen that although there are repeated patterns of energy in the lower frequency range of 0-5 Hz in wavelet transform, the energy distribution is more or less continuous in Wigner-Ville transform. Therefore this distribution of energy may be because of noise and not necessarily due to faults.

Similar procedure is carried out for the rest of the trains viz. Kamrup Express, Kolongpar Express and Kopili Express. They showed the similar characteristics in the wavelet transform, however in some cases, especially in Wigner-Ville transform some peculiar spectrum can be noticed. In the case of Kolongpar express there is a greater concentrated burst of energy only at 5.5 s which can be seen in fig. 4.10. Since this concentrated energy in the lower frequency i.e. below 5 Hz, this is a wheel-flat fault. In the case of Kopili Express, although the spectrum is short compared to that of Rajdhani or Kamrup, there is no such sudden burst of energy as Kolongpar Express. This is shown in fig. 4.11 and this train can be classified as in better health compared to Kolongpar Express. Similarly no wheel-flat is detected for Kamrup express as shown in fig. 4.9.

Referring to the fig. 4.8, the sensor is activated when the first wheel crosses the fish-plate where the sensor is connected. The length of a bogie is 23.56 m. In case of Kolongpar express the sudden burst of energy is at 5.5 s. The average speed of Kolongpar express is 32 kmph. The distance covered by the train in 5.5 s is 44.88 m. Adding length of the Centre Buffer Coupler 1.067m, the occurrence of the burst of energy is at 1.82th (44.88/24.627) bogie. As the number is 1.82, the occurrence is at the second bogie, again since it is greater than 1.5, the occurrence is towards the end of the bogie. Therefore the last wheel of the 2nd bogie of the Kolongpar Express is suffering from wheel-flat. No Wheel-flat is detected for

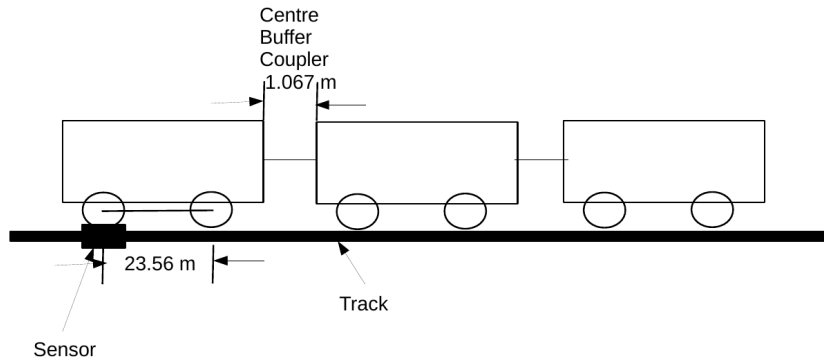


Fig. 4.8 Wheel-flat detection by calculating the distance and occurrence of the burst of energy.

Table 4.1 Detection of wheel-flat.

Sl No	Train	Avg. speed (kmph)	No. of bogies	Wheel-flat location
1	Rajdhani Exp.	65	18	No wheel-flat detected
2	Kamrup Exp.	42	12	No wheel-flat detected
3	Kopili Exp.	43	9	No wheel-flat detected
4	Kolongpar Exp.	32	8	Last wheel of 2nd bogie

rest of the trains. These along with some details of the trains such as average speed and no. of bogies (on the day of experiment) are summarized in table 4.1.

4.5 Discussion

From experiments, it is found that to capture impulses with wavelet transform in the frequency range of 0-50 Hz, the scaling factor p ranging from 2 to 6 are useful and accordingly applied to 4 different trains. They show similar trends of short impulses at low frequency range of 0-10 Hz with $p=2$. The spectrum spreads out as the p value increases. Since the wavelet used is optimized to capture impulses, it has captured a lot of impulses which may be also due to the random noise. As a confirmatory measure, Wigner-Ville transform is used. For

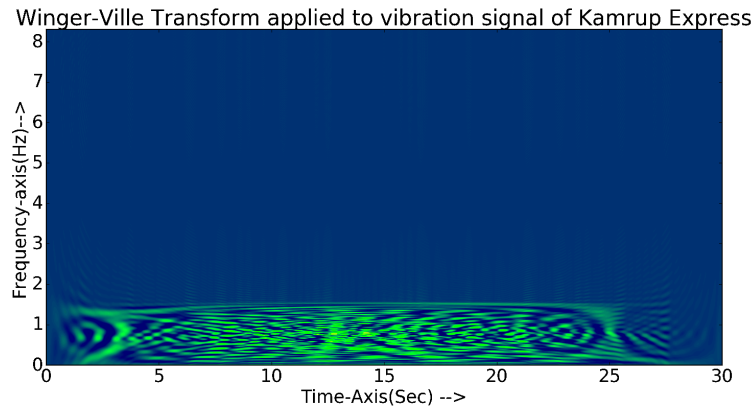


Fig. 4.9 Wigner-Ville transform applied to vibration signal of Kamrup Express.

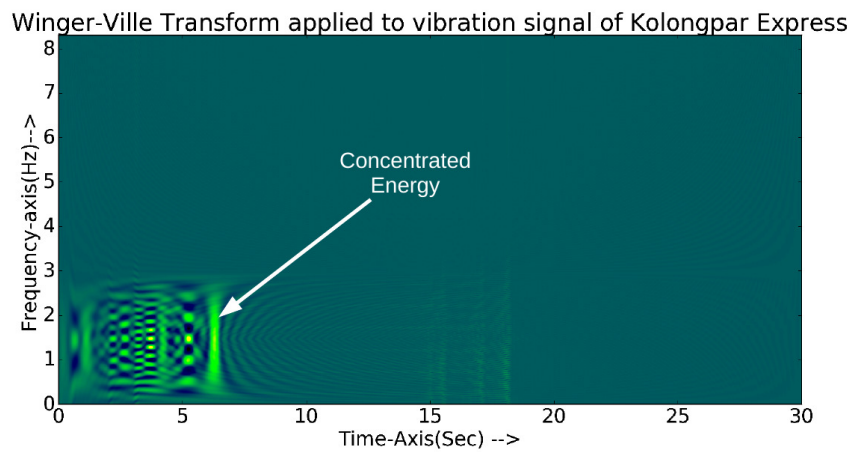


Fig. 4.10 Wigner-Ville transform applied to vibration signal of Kolangpar Express.

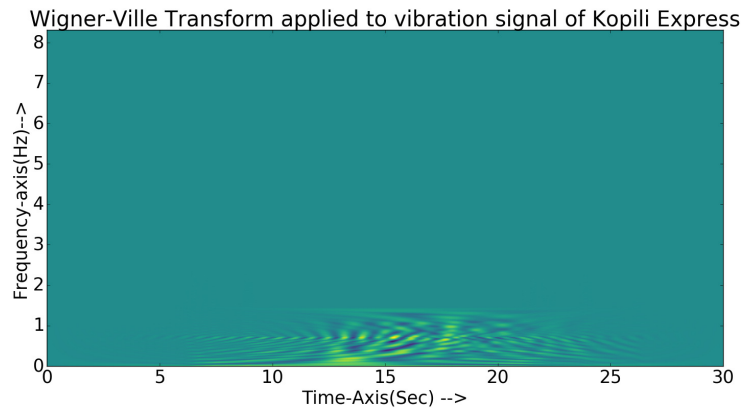


Fig. 4.11 Wigner-Ville transform applied to vibration signal of Kopili Express.

Rajdhani Express and Kamrup Express an uniform spectrum is noticed, therefore the impulses indicated by the wavelet may be because of the noise. However there is a sudden burst of energy for Kolangpar Express indicating wheel-flat type of fault. Wigner-Ville transform did not catch any high frequency energy. Therefore although wavelet transform indicated presence of impulses at different frequencies it could not be confirmed by the Wigner-Ville transform and this may be the further direction to this particular research. Wheel-flat fault for Kolangpar Express with wheel position and bogie number is also detected. Although it seems that the Wigner-Ville transform alone is sufficient to detect the wheel-flat fault, there is a major disadvantage of Wigner-Ville transform that it produces cross-frequency components (unfiltered). To observe the cross-frequency components in Wigner-Ville transform, fig. 4.7 and fig. 4.6 can be considered. As can be seen in fig. 4.6 (a), the spectrum has started dying from 15 s onwards, whereas in fig. 4.7, there are prominent spectrum components between 15 s to 20 s. This is a cross-frequency component that Wigner-Ville transform has produced. Again Wigner-Ville transform in this analysis had not caught frequency components above 3 Hz. Hence, with only Wigner-Ville transform a lot of information regarding the vehicle especially that of Primary and Secondary suspensions will be missed. The information regarding the primary suspension can be obtained from 10-30 Hz band while the information regarding the secondary suspension can be obtained from 5-10 Hz band [67]. Therefore, analysis in both linear and non-linear time-frequency is required. Hence, it is proposed to detect the impulses first with linear time-frequency transform like Wavelet transform and then to confirm the presence with the quadratic time-frequency transform like Wigner-Ville transform.

4.6 Conclusion

Four trains of NFR viz. Rajdhani Express, Kamrup Express, Kolongpar Express and Kopili Express are analysed for fault detection. For this purpose, vibration generated by the train when running over a track is captured by ADXL335 vibration sensor connected to the fish-plate of the track. The development board used was Arduino Uno. The captured vibration signals were analysed with linear time-frequency technique wavelet transform and quadratic time-frequency technique Wigner-Ville transform. Wavelet transform captures the impulses present whereas the Wigner-ville transform confirms whether they are due to vibration of the train or due to random noise. Also Wigner-Ville transform captured the wheel-flat of the trains. It can be concluded that although wavelet transform is most widely used for detecting impulses in the vibration signals, the smoothing factor p affects the results over different frequency ranges. With increasing p , the spectrum spreads in both time and frequency domain and therefore, it is difficult to detect impulses. With lower value of p , it is difficult to catch the higher frequency impulses. Again Wigner-Ville transform produces cross terms, therefore all the energy distribution is not reliable. Moreover the noise present tends to produce a continuous spectrum especially in the wavelet transform. However combining these two techniques, conclusions can be drawn about presence of impulses in the signals as well as wheel-flats and thereby detect different faults. As final comments, it is worthwhile to mention that the data acquisition had been carried out in a limited time frame, as allowed by the NFR authority. The data acquisition had to be carried out on a live environment while a train moves over a track. As such the data acquisition could be carried out for only a limited number of times. To generalise this work, more data acquisition is needed. However the work presented here proves to be useful for fault detection and can be extended in further research for robust detection of any number of faults in the train vehicles. However, it is to be noted that the technique described is quite inexpensive and the method is capable of approximating the state of the health of a train vehicle. This method can be used as a first step towards health monitoring of trains in countries like India, where a huge number of trains (including local, metro, intercity, long distance etc.) ply regularly. By simply installing one sensor based system on a track, the health of all the trains running over that track can be monitored. This is of immense potential.

5

Health Monitoring of a few Passenger Trains Using Statistical Measures and Graph Signal Processing

Health monitoring is an important activity for proper maintenance of a structure and it's been an active research topic among the researchers. Vibration analysis is one of the prime methods to estimate the health of a structure or a system. This chapter presented here describes an approach for estimating the health condition of a train by extracting statistical measures and Graph Signal Processing(GSP) of vibration signals generated by a train under motion and captured by an Inertial Measurement Unit (IMU) MPU6050. These signals are the characteristics of a train and were captured during the movement of the train over a track. While statistical treatment provided a relative health estimation among the trains, GSP provided an absolute health estimation of the trains when compared against a standard database.

5.1 Introduction

Railway safety is a major concern, especially in a country like India, where a large number of trains ply daily. Periodical maintenance of the railway vehicles becomes easier if they can be categorised. By proper maintenance, best health of the railway vehicle and the track can be ensured. This would reduce the risk of accident, mainly due to the derailment which mostly occurs due to the bad conditions of the track or the bad conditions of the major vehicle components such as the wheels and the suspension systems. The best way to ensure the health of a mechanical system is to ensure that there is no fault. Most of the faults can be detected and isolated by analysing the signature vibration signals generated by the system. Vibration analysis has been the mainstay of fault diagnosis [87], [88]. Traditional way of detecting fault is to analyse statistical indicators such as Root Mean Square (RMS), Crest Factor (CF), Kurtosis etc. Many authors had applied these techniques to find fault in a mechanical system, especially that of the bearings [89], [62], [63]. These time-domain features are very helpful, when one needs to track a particular machine for degradation. However, for comparing two systems, based on the time-domain features obtained from the vibration signal, these features need some improvement. Higher order features such as skewness, kurtosis, entropy etc. are calculated from probability distribution. As the vibration signals generated by trains under motion over a track are random in nature, they do not fit any particular probability distribution. To calculate these higher order features, Empirical Cumulative Distribution Function (ECDF) can be utilized. In most of the cases these ECDFs are quite similar, although the original vibration signals from which these ECDFs are obtained are different. This makes characterizing the systems based on these features become difficult and improving these features become desirable. Condition monitoring, characterization or classification of systems depends on the features it generates. Better features enable one to carry out these tasks easily. Features selection is a process that requires care, however once selected, the features should be distinctive and sharp enough so that the classification or characterization can be done easily. Again the difference between two lower order features such as mean or rms value, generated by the similar systems such as two similar trains are quite small. Hence it is necessary to improve upon the features so that the next task of classifying or quantifying the similar systems becomes easier. Again many authors describe these features as the input to an artificial intelligent system for condition monitoring [43], [45], [47]. Improving upon these features would make the learning process faster. Sensor fusion, as it is known for combining data of different sensors for improving features has been discussed by few authors [90], [91].

The Indian railways tracks are fixed on precast RCC Sleeper using fishplate. Therefore, this type of railway track not only vibrates when a train moves over it, the angular motion

of the track is also experienced. Therefore, it is necessary to capture both vibrations and angular velocities of a track to quantify the quality of trains. The work reported in this paper, an MPU6050 was used to capture the acceleration and the angular velocity of a railway track while a train in motion. Arduino Uno development board was used to interface MPU6050 and a laptop through the USB port for capturing MPU6050 signals while a train was in motion. The acceleration and the angular velocity of a train were analysed in time-domain, where the angular velocity and the vibration (represented as velocity derived from acceleration) were correlated. Analyses were carried out to find the proper combination of signals that to be correlated for better extraction of the features of a train while under motion. The time-domain features viz. skewness, RMS, kurtosis, mean, standard deviation, variance, crest factor, form factor, peak to peak value and entropy of the accelerometer signal, the gyroscope signal and the correlated signals were calculated. Based on these features, three trains of the North-East Frontier Railway (NFR) had been categorized.

While these statistical parameters provided a nice way of classifying and comparing the trains amongst each-other, it was relative. So it was desired to have some kind of quantification of the train health in terms of some absolute numbers. The statistical parameters of the vibration signals generated by the trains were compared with statistical parameters of a railway vibration database by means of a graph. The ten statistical parameters Mean, Std. Dev, RMS, Variance, peak to peak value, crest factor, form factor, skewness, kurtosis and Entropy of the database were considered as the nodes of the graph. To utilise the GSP technique the graph was supplied with the vibration signal of the database and the different trains. The average value of the statistical parameters constitute the signal on the graph that to be processed. The Graph Fourier transform was used to quantify the trains which confirmed the quantification done by correlating the 3D vibration and gyroscope signals. The major contribution of this work can be summarized as , improvement of time domain statistical features by correlation, using these features for quantification of the health of different trains, representing a vibration signal by a graph with these parameters as the nodes of the graph and finally using this graph to process vibration signals for quantification of the health of the trains.

5.2 MPU6050 measurements of the different trains under study

A simple Arduino based system has been configured to capture the vibration and the angular velocity of a train, which is generated when the train moves over a railway track. The sensor MPU6050 is interfaced to an Arduino Uno card to capture vibration and the angular velocity of a railway track. It is necessary to adapt proper placement arrangement of a

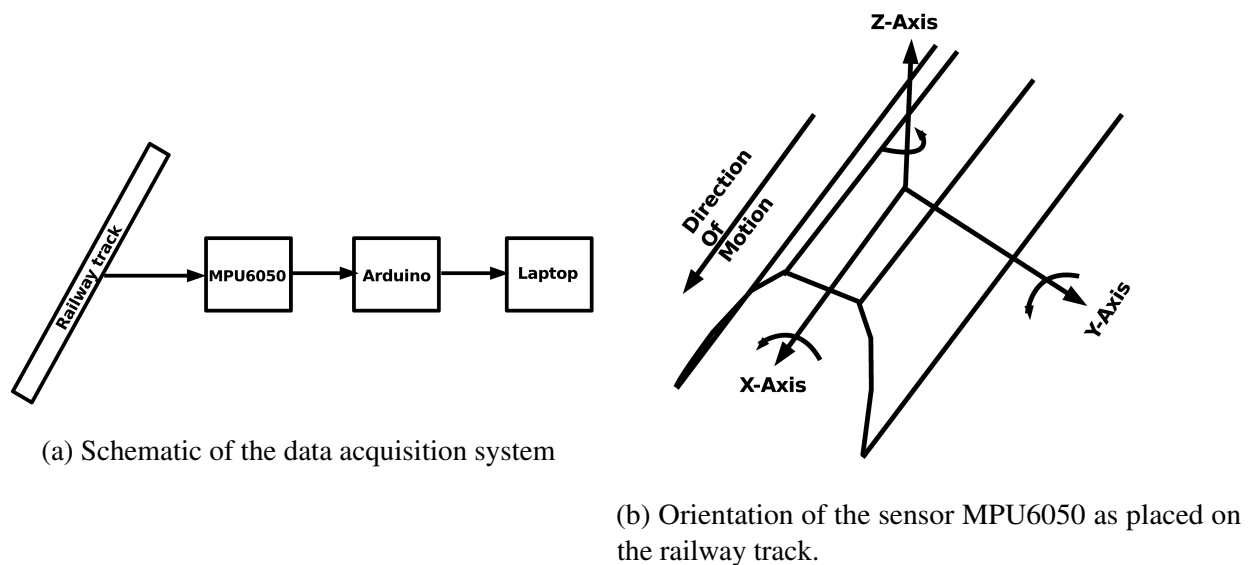


Fig. 5.1 Vibration signal acquisition and sensor orientation

sensor to enhance the durability and functioning of the sensor [77]. The MPU6050 sensor was placed on the wayside of the track's fishplate to ensure consistent performance and protect it from possible impact due to environmental changes. MPU6050 is an integrated 6-axis motion tracking device that combines a 3-axis gyroscope, 3-axis accelerometer along with a Digital Motion Processor. It has in-built analogue-to-digital converters (ADC), with operating software that takes care signal processing of the captured signals and to deliver digital output signals with lowest possible noise. The sensor is one of the most reliable one as it passes through a number of tests before its release. Moreover its robust nature to noise and temperature stability makes the sensor very desirable. For capturing the signals by Arduino Uno card, a library programme developed by Mr. Jeff Rowberg is used. This library manipulates the Digital Motion Processor (DMP) and provides "Real world Acceleration" along with other data values. Combination of this programme and the lowest noise offered by the MPU6050 eliminates traditional difficulties of sensing such as noise, extracting the true values from the raw data etc. Arduino based system has a software platform that allows incorporation of in-built software prototype for data acquisition from MPU6050 sensor and store the data (vibration and the angular velocity) in the Laptop. The function block diagram of the measurement scheme is shown in Fig.5.1 (a). Fig. 5.1 (b) shows the orientation of the sensor MPU6050, when placed on the track.

5.3 Time-Domain Features

The lower order features such as RMS, mean, standard deviation, variance etc extracted from the captured vibration and the angular velocity from MPU6050 over a period of time are used to quantify the quality of a train. As such, if one wants to compare the condition of a particular train over a period of time, these features can be of great help. Further, these features can be used to determine the quality of a train on an online basis. Again, the vibration signals generated by the train and the extracted lower order features can be stored for a particular train over a period of time and these features could be utilized for determining qualitative deterioration of the train for the period under investigation. For example, an increase in RMS value is an indication of increasing faults [46]. Some time-domain features such as form factor and crest factor are independent of the size but dependent on the shape of the signal. Therefore these features are useful for comparing two similar systems. However these features are not good enough for critical analysis, as these features will vary quickly with the variations in mean, RMS or standard deviation. Since the built of the trains, their operating range, speed etc. will be different; these will affect the shape of the vibration signals and effectively change these features. To overcome these limitations, features such as skewness, kurtosis and entropy are utilized. These features are derived from the moments of the signal, that constitute the probability density function (PDF) of the signal, hence these features are relatively independent of the factors such as built of the train, speed, operating range etc.

5.3.1 Definitions and mathematical formulae of the time-domain features considered

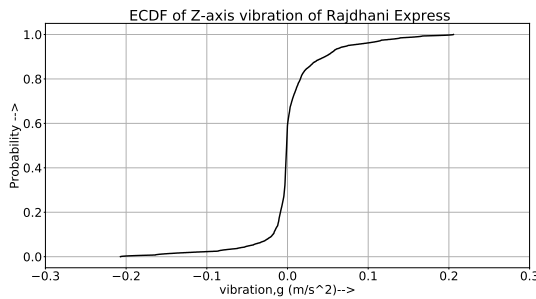
If $x(n)$ is a signal series, the statistical features considered in this work and their mathematical formulae are listed in tab 5.1

5.4 Experimental results and analysis

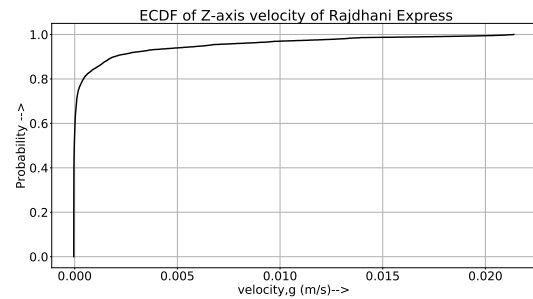
The authority of NFR permitted the experiments on a limited number of trains. In this study three trains are considered, viz. Kamrup Express, Rajdhani Express and Kolongpar Express. The experiments were carried out for a restricted period of time under constant supervision of security and administrative persons of NFR. Kamrup Express is one of the important trains of NFR that connects Howrah (West Bengal) and Dibrugarh(Assam). Rajdhani express (Dibrugarh) is one of the premier trains of NFR and it covers 2434 km at an average speed of

Table 5.1 Time-domain features

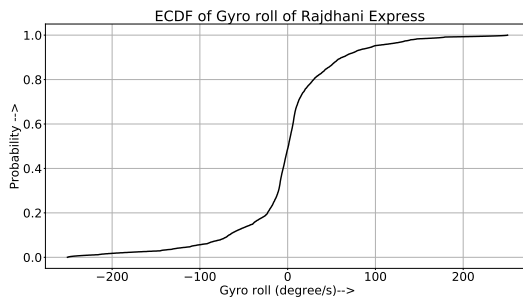
SI No	Features	Formula	Remarks
1	Mean	$\mu = \frac{\sum_{n=1}^N x(n)}{N}$	$n = 1, 2, 3, \dots, N$ are the data points
2	Std. Dev	$\sigma = \sqrt{\frac{\sum_{n=1}^N (x(n) - \mu)^2}{N-1}}$	$n = 1, 2, 3, \dots, N$ are the data points [92]
3	RMS	$X_{rms} = \sqrt{\frac{\sum_{n=1}^N x(n)^2}{N}}$	$n = 1, 2, 3, \dots, N$ are the data points [92], [53]
4	Variance	$v = \frac{\sum_{n=1}^N (x(n) - \mu)^2}{N-1}$	
5	Peak to Peak value	$max(x(n)) - min(x(n))$	
6	Crest Factor	$\frac{PositivePeak}{RMS}$ [44]	Standard deviation divided by RMS value [53].
7	Form Factor	$SF = \frac{\sqrt{\frac{1}{N} \sum_{n=1}^N x(n)^2}}{\frac{1}{N} \sum_{n=1}^N x(n) }$	Modification is done in calculating mean by considering the absolute values of the signal sequence. [66]
8	Skewness	$Sk = m_3 - 3m_2m_1 + 2m_1^3$	m_1 is the first moment coefficient, m_2 is the second moment coefficient and m_3 is the third moment coefficient [49].
9	Kurtosis	$Ku = m_4 - 3m_2^2 - 4m_3m_1 + 12m_2m_1^2 - 6m_1^4$	where m_1 is the first moment coefficient, m_2 is the second moment coefficient, m_3 is the third moment coefficient and m_4 is the fourth moment coefficient[49].
10	Entropy	$E_{Sh} = \sum_{i=1}^N x_i \log \frac{1}{x_i}$	Shannon entropy is considered [64]



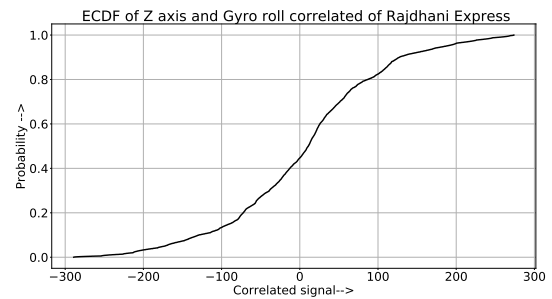
(a) ECDF of the Z-axis vibration (acceleration) of the Rajdhani Express



(b) ECDF of the Z-axis vibration (velocity) of the Rajdhani Express



(c) ECDF of the Gyro roll of the Rajdhani Express.



(d) ECDF of the Z-axis vibration and Gyro roll correlated signal of the Rajdhani Express.

Fig. 5.2 ECDFs of Rajdhani Express.

65 kmph. Kolongpar express connects Mairabari of Assam to Guwahati. These three trains were suggested by NFR authority to carry out the experiments as they have different range of travel distances with different speeds and they come under different category trains according to NFR classifications.

Six different signals viz. X, Y and Z axes vibration (acceleration from the accelerometer) and X, Y and Z axes gyroscope signal (angular velocity) for each of the trains were captured and stored in a laptop. Before analysis, the vibration signal i.e acceleration obtained from the MPU6050 had to be converted to the velocity, so that the proper correlation between the accelerometer and the gyroscope signals could be carried out. Again for some features viz. skewness, kurtosis and entropy Empirical Cumulative Distribution Function (ECDF) had been calculated. As an example, Fig. 2 shows the ECDFs of Z-axis vibration, Z-axis vibration in terms of velocity, Gyro roll angle and ECDF of correlated signal of Z-axis vibration velocity and gyro roll angle, generated by the Rajdhani Express.

Another important aspect at this point was to select the axes to be correlated for proper meaningful results. As there are 6 different signals, 15 correlations would have been possible, but might not yield meaningful results. This issue is discussed in the following subsection.

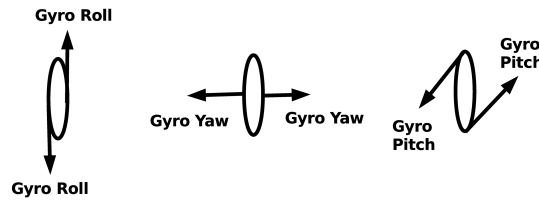


Fig. 5.3 Gyroscope orientation

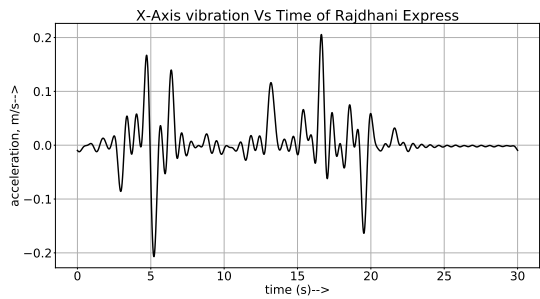
For correlation, both the signals must be of the same dimension. Therefore it was necessary to convert the acceleration signal of the accelerometer to velocity such that it could be correlated with the angular velocity of the gyroscope. Trapezoidal rule was utilized for numerical integration to obtain velocity from the acceleration samples.

5.4.1 Selecting proper signals for correlation

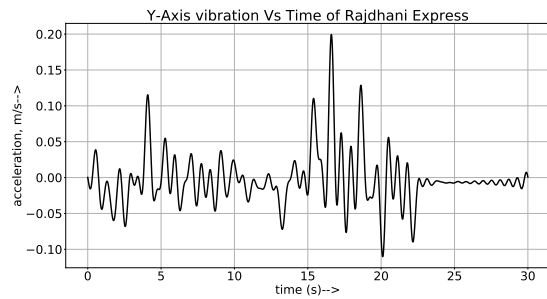
The aim of the correlation of various signals is to find out the condition of a train. By analysing the Z-axis vibration, health of the train can be estimated along with the comfort level, whereas the X and Y axes analysis should indicate safety of the train [67]. Fig. 5.3 shows the gyroscope orientation when the X-axis of the accelerometer is horizontal and passing through the center of the ellipse. Analysing this figure, it can be seen that correlating Gyro roll with the Z-axis of the accelerometer will give better insight into the Z-axis vibration of the train. Similarly Gyro yaw with X-axis and Gyro pitch with Y-axis should be correlated.

5.4.2 Signal analysis

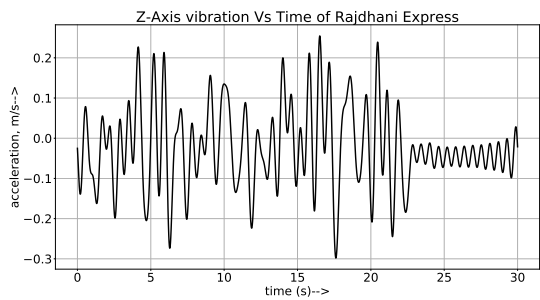
The vibration signal collected for Rajdhani Express is depicted in the following figures. Fig. 5.4 shows the 3-axis vibrations in terms of the acceleration due to gravity (g), of the Rajdhani Express. Fig. 5.5 shows the gyroscope signal obtained from Rajdhani Express. The acceleration signals thus obtained had been converted to velocity signals using the trapezoidal rule of numerical integration. The velocity signals thus obtained are shown in Fig. 5.6. The velocity signals were correlated with the gyro angles as discussed in the previous subsection and the results obtained are shown in Fig. 5.7. Similar analyses were carried out for the rest of the trains.



(a) X-axis vibration of Rajdhani Express



(b) Y-axis vibration of Rajdhani Express



(c) Z-axis vibration of Rajdhani Express

Fig. 5.4 The 3-axis vibrations of Rajdhani Express

5.4.3 Calculation of the time-domain features

The time-domain features viz. skewness, RMS, kurtosis, mean, standard deviation, variance, crest factor, form factor, peak to peak value and entropy were calculated for the vibration (velocity), the gyroscope and the correlated signals. First of all, Rajdhani express was considered and the results obtained are tabulated in table 5.2. Similarly the time-domain features of the Kamrup and the Kolongpar Express were obtained and are tabulated in table 5.3 and table 5.4 respectively. The comparison of the time domain features of the three trains along the X-Axis and Yaw correlated signal are tabulated in table 5.5. Similarly, comparison of the time domain features of the three trains along the Y-Axis and Pitch ; Z-Axis and Roll correlated signals are tabulated in tables 5.6 and 5.7 respectively.

5.5 Graph Signal Processing on the vibration signal

Graph Signal Processing (GSP) is an emerging area of the signal processing technique. In this work, GSP is used to quantify the health condition of the different trains. The first step necessary for GSP is to create the proper graph that captures the relationships between the different nodes.

Table 5.2 Time-domain features of Rajdhani Express

SI No	Features	Velocity (m/s)			Angular velocity (deg/s)			Correlated		
		X-Ax	Y-Ax	Z-Ax	Roll	Yaw	Pitch	X-Ax and Yaw	Y-Ax and Pitch	Z-Ax and Roll
1	Mean	0.0009	0.0007	0.0048	-0.765	-1.1294	7.31	-12.743	27.508	20.681
2	Std. Dev	0.0029	0.0019	0.0072	62.977	54.291	49.484	83.288	52.324	197.099
3	RMS	0.003	0.002	0.0087	62.982	54.303	50.021	84.258	59.115	198.18
4	Variance	8.7249	3.5465	.00005	3966.1	2947.5	2448.7	6937.04	2737.8	38848.1
5	X_{pp}	0.0214	0.0198	0.0444	501.504	513.99	490.98	648.82	401.42	1018.99
6	CF	6.9203	9.9341	5.0524	3.9785	4.8323	5.0013	2.7896	5.0322	2.687
7	FF	3.4013	2.9494	1.7927	-82.322	-48.081	6.8428	-6.6117	2.1489	9.5825
8	Sk	4.4484	6.0905	2.2152	-0.4508	0.0229	0.9777	-0.7259	1.5668	0.1383
9	Ku	21.405	46.969	5.3917	4.0426	6.4322	8.1593	3.0875	4.3367	-0.2555
10	En	11.465	10.30	56.5	16731.3	8392.6	-91061.1163100.5	-319168.8311582.7		

Table 5.3 Time-domain features of Kamrup Express

Sl No	Features	Velocity (m/s)			Angular velocity (deg/s)			Correlated		
		X-Ax	Y-Ax	Z-Ax	Roll	Yaw	Pitch	X-Ax and Yaw	Y-Ax and Pitch	Z-Ax and Roll
1	Mean	-0.0001	0.0003	-0.0031	5.71	-	2.6444	-2.8541	4.1414	-75.187
2	Std. Dev	0.0026	0.0029	0.0048	53.467	48.061	36.866	59.827	63.719	130.53
3	RMS	0.0026	0.003	0.0058	53.771	48.091	36.961	59.895	63.854	150.642
4	Variance	6.8583	8.9547	2.3518	2858.73	2309.89	1359.12	3579.27	4060.2	17040.04
5	X_{pp}	0.0209	0.0211	0.02652	504.5	502.78	360.27	494.72	528.99	814.16
6	CF	7.6625	6.8223	3.44	4.67	5.2529	6.7682	4.1086	6.0423	1.7849
7	FF	-22.487	8.2877	-1.821	9.4159	-28.436	13.976	-20.984	15.418	-2.0035
8	Sk	5.537	5.0938	2.3294	0.6824	-0.2135	3.1853	-0.2454	2.4487	-0.249
9	Ku	33.105	26.706	5.14	6.92	9.4051	16.575	3.5454	9.6257	0.453
10	En	-5.5541	1.8131	-45.16	-79738.723253.8	-43700.241030.5	-89812.51035865.1			

Table 5.4 Time-domain features of Kolongpar Express

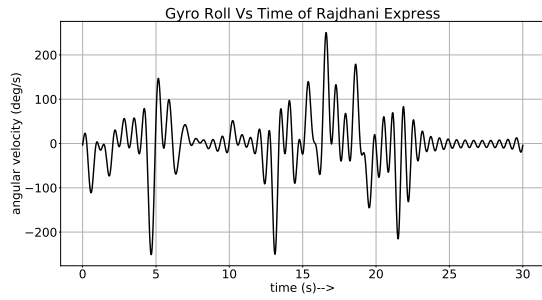
SI No	Features	Velocity (m/s)			Angular velocity (deg/s)			Correlated		
		X-Ax	Y-Ax	Z-Ax	Roll	Yaw	Pitch	X-Ax and Yaw	Y-Ax and Pitch	Z-Ax and Roll
1	Mean	0.0001	.00001	0.0017	-1.624	1.5	1.8156	2.3672	0.128	-12.7015
2	Std. Dev	0.0014	0.0002	0.0035	31.1843	30.2434	14.8615	16.7497	1.6571	45.9526
3	RMS	0.0014	0.0002	0.0039	31.2266	30.2805	14.972	16.9162	1.6621	47.6756
4	Variance	2.0418	.000000800001	0.00001	972.4662	914.6634	220.8661	280.5539	2.7461	2111.643
5	X_{pp}	0.0211	0.0034	0.0246	442.6193	374.2255	218.1555	188.78	17.6052	390.9628
6	CF	14.6223	11.6271	6.0888	8.0087	6.9242	9.3996	7.43	6.4054	3.9636
7	FF	7.58	27.6158	2.2817	-19.227	20.1832	8.2462	7.1458	12.9827	-3.7535
8	Sk	10.2259	5.0938	3.8192	1.1052	1.3124	3.1853	2.5512	2.4487	0.2078
9	Ku	120.9	64.9	15.0694	23.7358	15.8028	35.1925	16.4647	15.6776	4.5188
10	En	2.1415	-0.1440	24.4474	8868.11	-21161.24	14744.63	25923.25	1077.7	115442.21

Table 5.5 Comparison along X-Axis and Yaw correlated signal

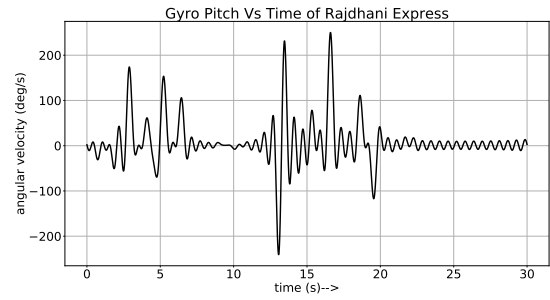
Sl. No.	Train	Mean	Std. Dev	RMS	Variance $\hat{\alpha}_{pp}$	CF	FF	Sk	Ku	En	
1	Raj- Exp	-12.74383	288	84.258	6937.04	648.82	2.7896	-6.6117	-0.72593	0.875	163100.5
2	Ka- Exp	-2.854159	827	59.895	3579.2	494.72	4.1086	-20.984	-0.24543	0.5454	41030.5
3	KOL- Exp	2.3672	16.749	16.916	280.55	188.78	7.43	7.1458	2.5512	16.464	-25923.2

Table 5.6 Comparison along Y-Axis and Pitch correlated signal

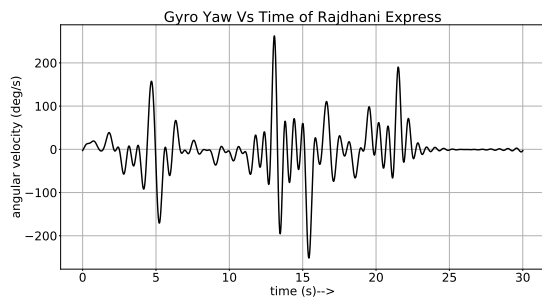
Sl. No.	Train	Mean	Std. Dev	RMS	Variance _{pp}	CF	FF	Sk	Ku	En	
1	Raj-Exp	27.508	52.324	59.115	2737.8	401.42	5.0322	2.1489	1.5668	4.3367	-319168.8
2	Ka-Exp	-75.187130.53	150.64	17040.0814.16	1.7849	-2.00352.4487	9.6257	-89812.5			
3	KOL-Exp	-12.70145.952	47.675	2111.64	390.96	3.9636	-3.753	2.4487	15.677	-10777.7	



(a) Gyroscope Roll of Rajdhani Express



(b) Gyroscope Pitch of Rajdhani Express



(c) Gyroscope Yaw of Rajdhani Express

Fig. 5.5 Gyroscope signal obtained from Rajdhani Express

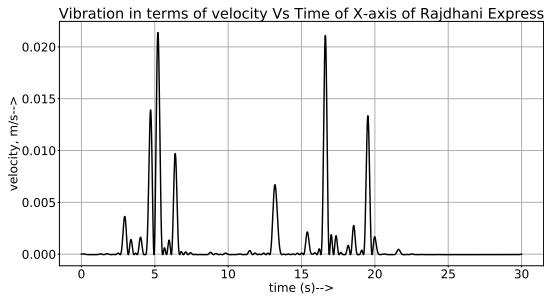
5.5.1 Mathematical analysis of Graph Signal Processing (GSP)

Preliminaries

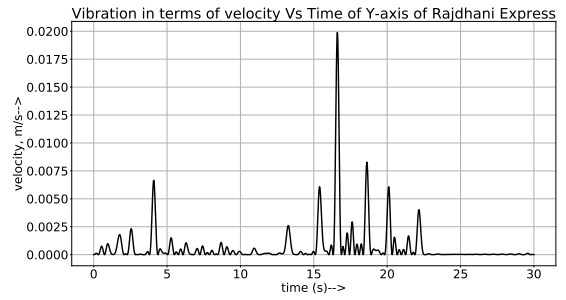
A signal is based on some “support”. For example an ac voltage is based on its time support. An image is based on the support of a grid of pixels. These supports may be considered as unweighted and un-directed graph. For the example of time varying signals , if we proceed from one hour to next hour , the hours are essentially the same but the signal generated at those particular time may be different. Similarly, if we hop from one pixel to the other on an image, the pixels may be considered as nodes of a graph with varying intensities (i.e. the generated signal). In GSP, we exploit this inherent support of a signal. In GSP, the graph topology is important. Following terms are very important for further discussion of GSP.

Adjacency matrix: Given a graph $G = (v, \epsilon, \omega)$ of N vertices, its adjacency matrix $A \in \mathbb{R}^{N \times N}$ is defined as

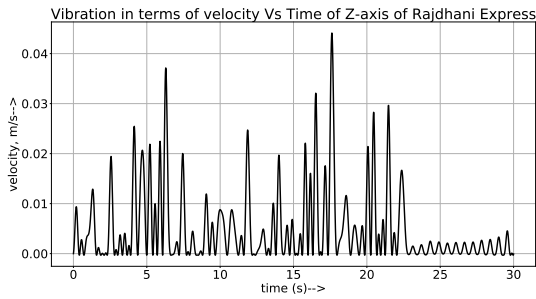
$$A_{mn} = \begin{cases} w_{mn}, & \text{if } (n, m) \in \epsilon \\ 0, & \text{otherwise} \end{cases}$$



(a) X-axis vibration in terms of velocity of Rajdhani Express



(b) Y-axis vibration in terms of velocity of Rajdhani Express



(c) Z-axis vibration in terms of velocity of Rajdhani Express

Fig. 5.6 Velocity signal obtained from Rajdhani Express

Degree of a node: The degree of a node is essentially the sum of all the weights incident on it. Given a weighted and undirected graph, the degree of a node i is defined as

$$deg(i) = \sum_{j \in N(i)} w_{ij}$$

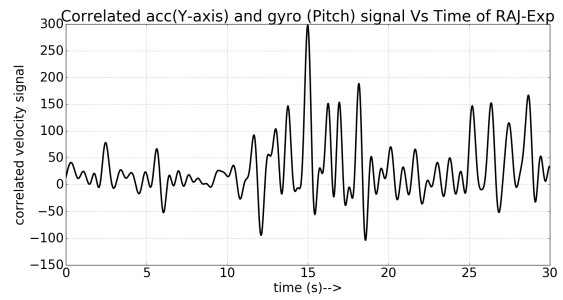
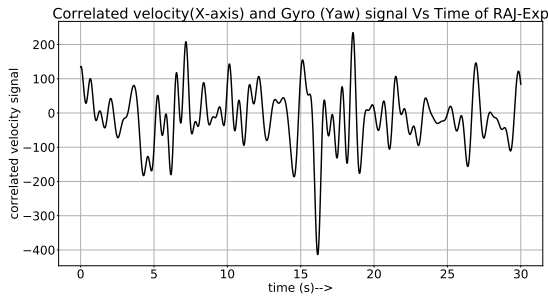
where $N(i)$ is the neighborhood of the node i and w_{ij} is the weight on the edge $(i, j) \in \mathcal{E}$. In terms of the adjacency matrix A ,

$$deg(i) = \sum_j A_{ij} = \sum_j A_{ji}$$

The degree matrix $D \in \mathbb{R}^{N \times N}$ is a diagonal matrix such that $D_{ii} = deg(i)$

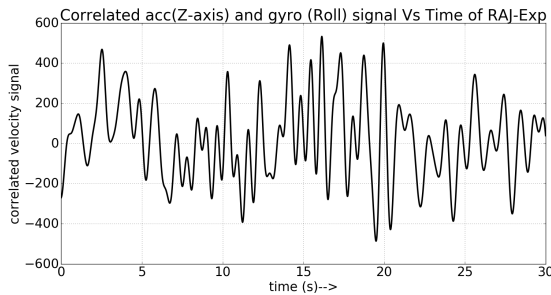
Laplacian of a graph: Given a graph G with adjacency matrix A and degree matrix D , we define Laplacian matrix $L \in \mathbb{R}^{N \times N}$

$$L = D - A$$



(a) Correlated signal , velocity (X-axis) and Yaw from the gyro of Rajdhani Express

(b) Correlated signal , velocity (Y-axis) and Pitch from the gyro of Rajdhani Express



(c) Correlated signal , velocity (Z-axis) and Roll from the gyro of Rajdhani Express

Fig. 5.7 Correlated signals obtained from Rajdhani Express

Laplacian quadratic form: The Laplacian quadratic form of signal $x = [x_0, x_1, \dots, x_N]$ is explicitly given by

$$x^T Lx = \frac{1}{2} \sum_{(i,j) \in \mathcal{E}} w_{ij} (x_i - x_j)^2$$

$x^T Lx$ quantifies the local variation of signal , and is very useful in learning graph from smooth signals.

Learning graph from smooth signals

The Laplacian quadratic form $x^T Lx$ captures the variation of the signal over the nodes. This property can be utilized in learning graph from data. A signal on graph can be considered as a smooth signal , if the Total Variation (TV) of signal over the nodes is very low. "If the nodes are related, the signal on the nodes are similar". *The Laplacian Quadratic form can be minimized subjected to certain conditions to obtain the graph from smooth signal.*

In this work, we are considering ten statistical parameters (Mean, Std. Dev, RMS, Variance, X pp (peak to peak value), CF(crest factor), FF(form factor), Sk(skewness),

Ku(kurtosis) and En (Entropy)) to be the ten nodes of a graph. Since, these nodes are correlated as they are representing vibration signal, the signal generated on the nodes are similar and can be considered as smooth signal.

The minimization criteria used here utilizes the properties of the Laplacian

- Symmetric
- Diagonal elements are strictly positive for connected graph
- Off-diagonal elements are non positive.

Graph Fourier Transform (GFT)

Eigenvalues and eigenvectors of the Laplacian:

The eigenvalues and eigenvectors of Laplacian L are denoted by λ_i and v_i . For a non zero signal x , the Laplacian quadratic form $x^T L x > 0$ i.e. L is positive semi-definite. Therefore, all eigenvalues of L are non negative for a non zero signal on a connected graph. These eigenvalues capture spectral properties of the Laplacian L and analogous to the frequency in frequency-domain transforms. This forms the basis of the GFT. A constant vector results in 0 eigenvalue (analogous to 0 frequency for dc or constant signal.)

$$[L1]_i = \sum_{j \in N(i)} w_{ij}(1 - 1) = 0$$

GFT

Given a graph G and a graph signal $x \in \mathbb{R}^N$ defined on G , let us consider a normal Graph-Shift operator $S = V \Lambda V$. Columns of $V = [v_1 v_2 \dots v_N]$ corresponds to the eigenvectors of S . Λ is a diagonal matrix containing the eigenvalues of S . Now we can define GFT of x as

$$\tilde{x} = \langle x, v_k \rangle = \sum_{n=1}^N x(n) v_k^*(n)$$

In matrix form $\tilde{x} = V^* x$

i.e GFT essentially finds the components of the signal x in the directions of v_1, v_2, \dots, v_N , where v_1, v_2, \dots, v_N are the eigenvectors corresponding to the eigenvalues $\lambda_1, \lambda_2, \dots, \lambda_N$

Following steps are executed to create the graph of a vibration signal generated by a train.

- Vibration database created by Neri et al. is considered. The database is available at <https://realvibrations.nipslab.org/> [93].

$$\begin{bmatrix}
 0 & 3.584 & 3.051 & 4.326 & 0 & 0 & 0 & 12.26 & 0 & 1.076 \\
 3.584 & 0 & 1.001 & 1.024 & 5.169 & 0 & 1.531 & 0 & 0 & 11.24 \\
 3.051 & 1.001 & 0 & 1.027 & 5.468 & 0 & 1.569 & 0 & 0 & 7.215 \\
 4.326 & 1.024 & 1.027 & 0 & 4.066 & 0 & 1.421 & 0 & 0 & 23.69 \\
 0 & 5.169 & 5.468 & 4.066 & 0 & 1.597 & 15.65 & 0 & 2.293 & 0 \\
 0 & 0 & 0 & 0 & 1.597 & 0 & 0 & 6.18 & 1.161 & 0 \\
 0 & 1.531 & 1.569 & 1.421 & 15.65 & 0 & 0 & 0 & 0 & 0 \\
 12.26 & 0 & 0 & 0 & 0 & 6.18 & 0 & 0 & 0 & 20.03 \\
 0 & 0 & 0 & 0 & 2.293 & 1.161 & 0 & 0 & 0 & 0 \\
 1.076 & 11.24 & 7.215 & 23.69 & 0 & 0 & 0 & 20.03 & 0 & 0
 \end{bmatrix} \quad (5.1)$$

- The statistical parameters under consideration viz. Mean, Std. Dev, RMS, Variance, X_{pp} (peak to peak value), CF(crest factor), FF(form factor), Sk(skewness), Ku(kurtosis) and En (Entropy) are calculated. These will represent the ten nodes of the graph.
- Karl Pearson’s correlation coefficient is calculated among the statistical parameters under consideration.
- The values of these correlation coefficients are the relations among the nodes. However, for the weight matrix, the reciprocal of the coefficients are considered, because greater the correlation coefficient, lesser should be the distance between the nodes i.e close to each-other.

Considering the database of [93], table 5.10 is prepared. The Karl Pearson’s correlation coefficient is calculated among the statistical parameters which is given by $r = \frac{\sum(x_i - \bar{X})(y_i - \bar{Y})}{n\sigma_x\sigma_y}$. The correlation coefficients are tabulated in the tab. 5.9

To construct the graph, the diagonal elements 1 of the correlation coefficient matrix is replaced with 0 so that there is no self-loop. Further all the negative coefficients are changed to 0 so that there is no connection between the respective nodes. Again strong bonding is represented by greater value of the coefficient ; however the greater value of the weight matrix will put the nodes further apart, therefore the reciprocal of the coefficients are considered except the 0 values as these are disconnected nodes. Accordingly the weight matrix is produced as shown in eq. 5.1 as a matrix.

The graph produced by the weight matrix is shown in fig. 5.8. Now the vibration signal of a train is essentially represented by its key statistical parameters as the nodes of a graph. For processing of the signal on the graph, first the signal was added to the graph. In this case, the average values of different statistical parameters were added to the nodes (which represents the different statistical parameters). The average values of the different parameters

Table 5.8 Statistical parameters of vibration signals from the database

Sl. No.	Train	Mean	Std. Dev	RMS	Variance X_{pp}	CF	FF	Sk	Ku	En	
1	1-X axis	-0.000140	0.04659	0.04659	0.00217	10.66	129.14	-332.2	1.83143	714.22	-78.71
2	1-Y axis	0.00755	0.03279	0.03364	0.00107	9.3895	154.62	4.45	6.87	2631.4	6362.48
3	1-Z axis	0.00135	0.09467	0.09468	0.00896	16.28	74.15	69.86	-1.04184	355.88	624.33
4	2-X axis	0.00108	0.029	0.029	0.00084	0.74522	12.55	26.93	0.0079	3.89	1056.04
5	2-Y axis	0.00532	0.02637	0.0269	0.00069	0.3127	5.6807	5.05	0.04555	0.49859	4844.86
6	2-Z axis	0.00163	0.06	0.06	0.00369	1.75	13.66	37.22	-0.05	5.69	1168.96
7	3-X axis	-0.000520	0.01374	0.01375	0.00018	4.5	199.52	-26.34	12.93	5459.96	-793.64
8	3-Y axis	0.00658	0.01129	0.013	0.00012	3.85456	153.02	1.99	1.26	5340.04	7716.52
9	3-Z axis	0.001749	0.02	0.02	0.00041	8.14	173.29	11.68	-13.73	10815.2	1887.44
10	4-X axis	-0.004530	0.02296	0.0234	0.000527	0.236091	4.62152	-5.160330	330.17255	0.58957	-4346.04
11	4-Y axis	0.005897	0.04437	0.04476	0.001968	0.394034	4.4412	7.5901	0.21835	0.36468	4119.79
12	4-Z axis	0.02685	0.05042	0.05713	0.00254	0.96874	7.30179	2.12728	1.031339	1.52678	17505.4336
13	5-X axis	0.000977	0.028476	0.028492	0.00081	0.237102	4.09774	29.15127	0.045615	0.012669	750.82
14	5-Y axis	0.008541	0.049936	0.050661	0.002493	0.354156	3.862317	5.93098	0.035477	-	5786.94
15	5-Z axis	0.001629	0.040121	0.040154	0.001609	0.343753	3.96625	24.64461	-0.08139	-0.09358	1387.65
16	6-X axis	-	0.021622	0.021833	0.000467	2.194618	55.019572	-7.200328	-0.198194	447.89	-
17	6-Y axis	0.011702	0.024876	0.027491	0.000618	0.890723	18.52427	2.349181	0.078783	3.26317	10438.24
18	6-Z axis	0.024296	0.100055	0.102962	0.010011	1.100563	6.046116	4.23775	2.054	7.69639	9251.7884
19	7-X axis	0.001194	0.055285	0.055298	0.003056	0.730966	6.037115	46.2832	0.052352	0.65877	454.93
20	7-Y axis	0.00686300	0.035286	0.035947	0.001245	0.398437	5.707265	5.237864	-	0.265819	3739.76
21	7-Z axis	0.000331	0.107671	0.107671	0.011593	1.935422	8.338103	325.06	-0.0896	1.352818	304.46

Table 5.9 Correlation coefficient

Statistical parameters	Mean	Std. Dev	RMS	Variance	X_{pp}	CF	FF	Sk	Ku	En
Mean	1	0.279015	0.327753	0.231157	–	–0.176	–	0.08151	–	0.92914
Std. Dev	0.279	1	0.998385	0.976124	0.1397	–	0.1913	–	0.1377	–
RMS	0.327753	0.998385	1	0.972933	0.193439	–	0.653175	–0.045771	–0.396735	0.088964
Variance	0.231157	0.976124	0.972933	1	0.182872	–	0.63722	–	–0.40107	0.138598
X_{pp}	–0.13974	0.193439	0.182872	0.245884	1	0.38372	–	0.04033	–0.289848	0.042199
CF	–	–	–	–	0.25977	1	–	–	–	–
FF	0.176045	0.37847	0.38373	0.25977	0.626071	0.06388	–	0.06829	–	0.09708
Sk	–0.191336	0.653175	0.637224	0.703331	0.208755	0.20876	–	0.161802	0.860893	–
Ku	0.08151	–0.045771	–	–	0.161802	–	–	1	–	–
En	–	–	0.04033	0.02634	0.06829	0.12958	–	0.26332	–	–
	0.13776	0.39674	0.40107	0.28985	0.435977	0.860893	–0.17318	–	1	–
	0.92914	0.088964	0.138598	0.042199	–0.097081	–	–0.192561	0.049908	–0.044103	1
					0.0719					

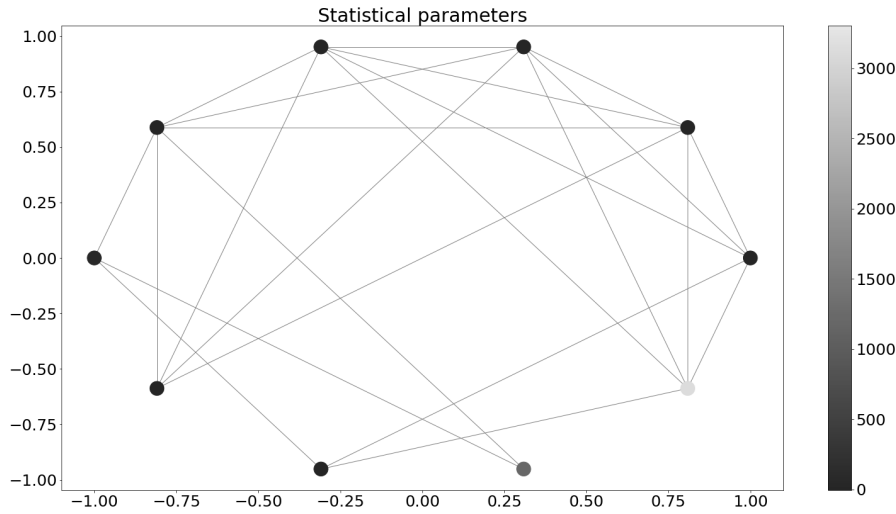


Fig. 5.8 Graph generated from the weight matrix of the statistical parameters.

from the database (Mean = 0.005, Std. Dev = 0.044, RMS = 0.045, Variance = 0.003, Peak to peak value = 3.458, Crest factor = 53.31, Form factor = -4.24, Skewness = 0.603, kurtosis = 1191.1, Entropy = 3146.01) were added to the respective nodes and then Graph Fourier Transform (GFT) is performed which gave the result as shown in fig. 5.9. The GFT of a graph signal is given by $\hat{s} = U^*s$; where, U is the Fourier basis and U^* represents the conjugate.

Similar procedure is followed to obtain the GFT of the three trains under consideration i.e Rajdhani, Kamrup and Kolongpar Express. The signal on the graph is taken as the average values of the statistical parameters. The average values of the parameters for these three trains are calculated by considering the vibration signals of the 3-axes viz. X, Y and Z. Accordingly the signal on the graph for the Rajdhani express is Mean= 0.0021, Std. Dev =0.004, RMS=0.0046, Variance= 4.09, Peak to peak value=0.0285, Crest factor=7.3, Form factor = 2.7, Skewness = 4.25, kurtosis=24.59 and Entropy=26.08. The resultant GFT plot is shown in the fig. 5.10. The signal on Kamrup express is Mean= -0.000967, Std. Dev = 0.0034, RMS = 0.0038, Variance = 6.055, Peak to peak value=0.0228, Crest factor=5.97, Form factor = -5.34, Skewness = 4.32, kurtosis=21.65 and Entropy = -16.3. The GFT is shown in fig. 5.11. The signal on Kolongpar express is Mean = 0.000603, Std. Dev = 0.0017, RMS = 0.0018, Variance = 0.6806, Peak to peak value = 0.0163, Crest factor = 10.7794, Form factor = 12.4925, Skewness = 6.3796, kurtosis = 66.95 and Entropy = 8.814966666666667. The GFT is shown in fig. 5.12.

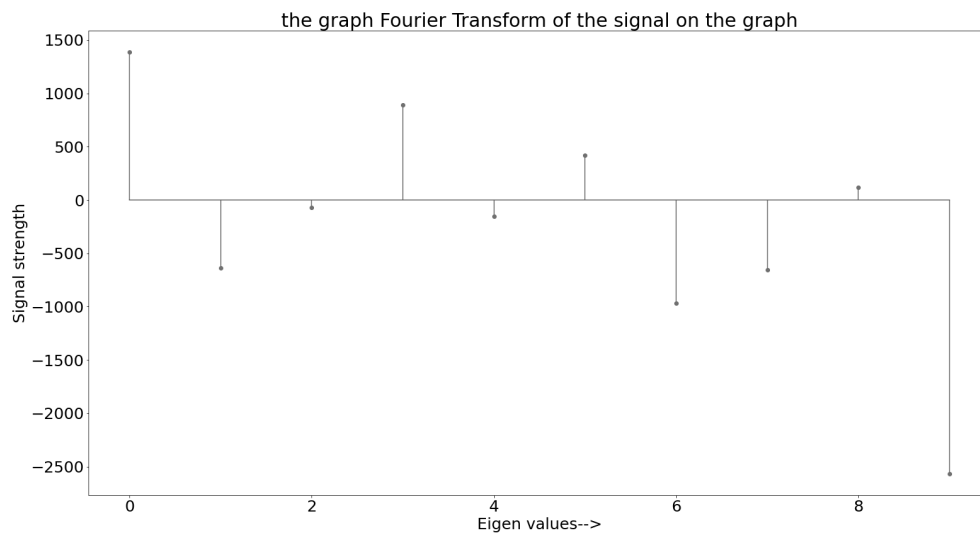


Fig. 5.9 Graph Fourier Transform (GFT) of the graph obtained from the vibration signals of the database

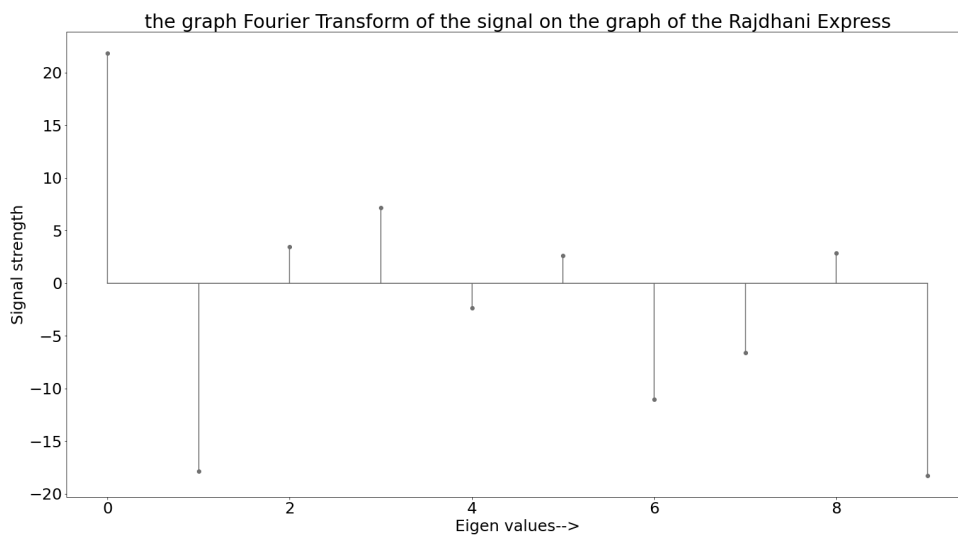


Fig. 5.10 Graph Fourier Transform (GFT) of the vibration signal on the graph of the Rajdhani Express.

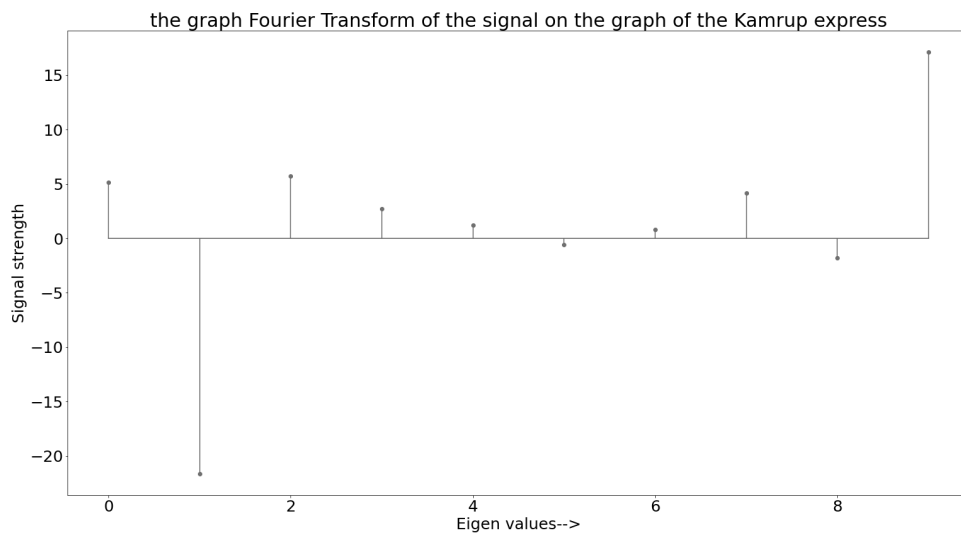


Fig. 5.11 Graph Fourier Transform (GFT) of the vibration signal on the graph of the Kamrup express.

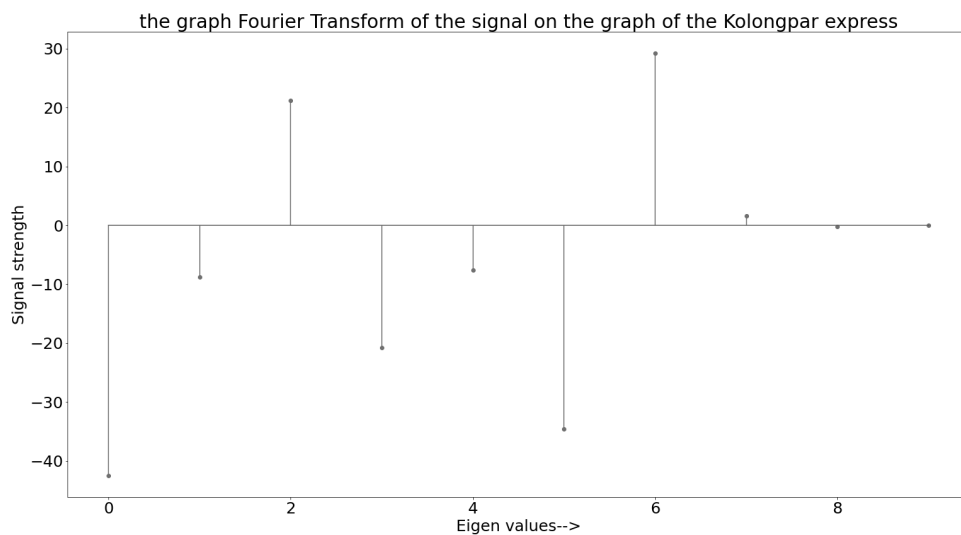


Fig. 5.12 Graph Fourier Transform (GFT) of the vibration signal on the graph of the Kolongpar express.

Table 5.10 Quantification of health condition of the trains in comparison with the database

Eigen Value	Direction of the database signal	Direction of the Rajdhani signal	Direction of the Kamrup signal	Direction of the Kolongpar signal	Value as-signed for Rajdhani	Value as-signed for Kamrup	Value as-signed for Kolongpar
0	+ve	+ve	+ve	-ve	1	1	0
1	-ve	-ve	-ve	-ve	1	1	1
2	-ve	+ve	+ve	+ve	0	0	0
3	+ve	+ve	+ve	-ve	1	1	0
4	-ve	-ve	+ve	-ve	1	0	1
5	+ve	+ve	-ve	-ve	1	0	0
6	-ve	-ve	+ve	+ve	1	0	0
7	-ve	-ve	-ve	+ve	1	1	0
8	+ve	+ve	-ve	-ve	1	0	0
9	-ve	-ve	+ve	-ve	1	0	1

For quantification of the health the direction of the signal in each eigen value is considered. If the direction of a particular eigen value signal of a particular train is the same as that of the database signal, +1 is considered and otherwise 0. Finally the total is divided by 10 as there are 10 eigen values. Accordingly we obtain **0.9 for Rajdhani**, **0.4 for kamrup** and **0.3 for Kolongpar express**. Thus the health of these three trains are quantified in the scale range of 0 to 1.

5.6 Discussion

Change in the vibration signal changes the probability distribution curve. Therefore higher order features skewness, kurtosis and entropy are good measures to compare relative health of the trains. For a good health machine, vibration analysis produces a kurtosis of 3 and skewness of 0 in ideal conditions. Whereas entropy measures the uncertainty or randomness of the signal [53]. Considering the data in table 5.5, kurtosis of Rajdhani Express is near 3, followed by Kamrup and Kolongpar Express. Hence we can say that the Rajdhani Express possesses the best of health followed by Kamrup and Kolongpar Express. Similarly in the skewness column, Kamrup Express leads with -0.2454 , followed by Rajdhani -0.7259 and Kolongpar with 2.5512 . This shows a better stability of the Kamrup express in the X-direction compared to the other two. Similar analysis can be carried out for the Y-axis

data shown in table 5.6. It shows that the Rajdhani is in very good health while Kolongpar is at bottom. To check the randomness Z-axis is considered as this axis should provide the information about the passenger comfort. To compare entropy is divided by the RMS (as the trains run at different speeds, magnitude of the vibration would be definitely different and this would normalize the fact) and we obtain the value for Rajdhani as 1573, for Kamrup 16442 and for Kolongpar 69293. Again the Rajdhani Express is much more comfortable compared to Kamrup which is relatively comfortable compared to Kolongpar Express. Hence these three trains can be categorized in three categories as Rajdhani Express as an excellent train, Kamrup Express is good while Kolongpar Express needs improvement.

Improvement in the time domain features can be easily seen from the comparison tables. If we consider table 5.2, it can be seen that skewness is close to 0 and kurtosis is close to 3 for correlated signals. However if only vibration signals for X, Y and Z axes are considered then skewness are 4.4484, 6.0905 and 2.2152 respectively while kurtosis are 21.4055, 46.9699 and 5.3917 respectively. Similar improvement can be seen for the other trains also as tabulated in tables 5.3 and 5.4.

By this it is established that time-domain features can easily be improved with simple correlations. These improved features were utilized to compare the trains. For quantifying the quality of the train a novel method employing GSP is described. This technique adds another dimension to the analysis. First it has been described how a set of vibration signals generated by a system can be effectively represented using graph with key statistical parameters as nodes of the graph. Utilizing Graph Fourier Transform (GFT) the health of the three trains were quantified as 0.9 for Rajdhani, 0.4 for Kamrup and 0.3 for Kolongpar. This outcome confirms the assumptions of the train health which were made based on the information available from NFR.

5.7 Conclusion

The work reported in this paper utilizes MPU6050 IMU sensor for capturing acceleration and angular velocity of a railway track while a train is in motion. The Arduino Uno development board was used as an interface between a laptop and MPU6050 IMU sensor to facilitate transfer of IMU signals to the laptop. The IMU signals were stored in the laptop on the real time basis while the trains were in motion. These captured signals were analysed in time-domain to extract key features to quantify the category of a train. For this purpose, vibration in terms of velocity from the accelerometer and angular velocity from the gyroscope of the MPU6050 are correlated. Selection of the signals to correlate is done in such a way that it provides meaningful features of a train. It has been found that there are tremendous

improvements in the time-domain features such as skewness, kurtosis and entropy when properly correlated in comparison to uncorrelated (accelerometer and gyroscope signals separately) signals. Also three trains of NFR viz. Rajdhani, Kamrup and Kolongpar Express are categorized on the basis of the time-domain features, which is tallying with the actual categorical representation of the train as there quality and performance concerned. Utilizing GSP, it has been shown how a set of vibration signals from a system can be used to produce a graph as the statistical parameters as nodes. GFT was utilized for quantification of the health of the three trains and promising results were obtained. For Rajdhani express a quantification of 0.9, for Kamrup 0.4 and for Kolongpar 0.3 were obtained which confirms the health condition of the trains that were available from authority.

6

Conclusion

A comprehensive study of the available literature shows that there is a dearth of reliable and effective condition monitoring systems for railway structure. This opens up a research area especially in a country like India where a huge quantity of trains operate. Literature also shows that there have been tremendous developments in on-board condition monitoring systems. However on-board condition monitoring systems come with their own disadvantages. In an on-board condition monitoring system, each train has to be mounted with a number of sensors at different positions. This leads to a lot of modifications into the existing system, such as minor or major adjustments in the structure so that sensors can be installed, communication for a large number of sensors inside the train as well as to some monitoring station. With a huge quantity of equipment, cost also raises quickly. There has been some work in wayside condition monitoring systems, most of which concentrate in finding a particular fault. Considering all these, in this work a simple, reliable and effective wayside monitoring technique is developed. The aim is to develop a simple and cost effective technique that can be installed with minimum interference to the existing structure. Also this technique enables one to gauge an overall health of the train and thereby estimating the first-hand requirement for the maintenance. Also a simple technique for mathematical modelling of a railway track is developed that enables one to find limiting conditions of any particular train and track.

This work can be extended in various ways. A comprehensive database of vibration for specific trains may be prepared and comparison of vibration signals of a particular train over the time would give the progressive deterioration of health. For ex. if the vibration signals of Rajdhani express is compared for few years, the remaining useful life can be predicted. Another extension may be to install a number of systems repeated at a certain distance. These systems may be connected to a common monitoring station by wired or wireless connection.

References

- [1] S Rao Singiresu et al. *Mechanical vibrations*. Addison Wesley Boston, MA, 1995.
- [2] Clifford F. Bonnett. *Practical Railway Engineering*.
- [3] E. Smith J. Brosseau C. Pinney B. Brickle, R. Morgan. Identification of existing and new technologies for wheelset condition monitoring: Rssb report for task t607.
- [4] RW Ngigi, Crinela Pislaru, Andrew Ball, and Fengshou Gu. Modern techniques for condition monitoring of railway vehicle dynamics. In *Journal of Physics: Conference Series*, volume 364, page 012016. IOP Publishing, 2012.
- [5] R Keith Mobley. *An introduction to predictive maintenance*. Elsevier, 2002.
- [6] Ole Døssing. Structural testing part i: Mechanical mobility measurements.
- [7] S Timoshenko. Method of analysis of statistical and dynamical stresses in rail. In *Proceedings of second international congress for applied mechanics, Zurich*, 1926.
- [8] S. L. Grassie, R. W. Gregory, D. Harrison, and K. L. Johnson. The dynamic response of railway track to high frequency vertical excitation. *Journal of Mechanical Engineering Science*, 1982.
- [9] K.L. Knothe and S.L. Grassie. Modelling of railway track and vehicle/track interaction at high frequencies. *Vehicle System Dynamics*, 1993.
- [10] R G Dong, S Sankar, and R V Dukkipati. A finite element model of railway track and its application to the wheel flat problem. *Proceedings of the Institution of Mechanical Engineers, Part F: Journal of Rail and Rapid Transit*, 1994.
- [11] C Hua Y Luo, H Yin. The dynamic response of railway ballast to the action of trains moving at different speeds. *Proceedings of the Institution of Mechanical Engineers, Part F: Journal of Rail and Rapid Transit*, 1996.
- [12] L. Ferreira and M. Murray. Modelling rail track deterioration and maintenance: current practices and future needs. *Transport Reviews*, 1997.
- [13] Tore Dahlberg. Railway track settlements - a literature review. Technical report, EU project Supertrack, 2004.
- [14] W.M. Zhai, K.Y. Wang, and J.H. Lin. Modelling and experiment of railway ballast vibrations. *Journal of Sound and Vibration*, 2004.

- [15] A.El Kacimi, P.K. Woodward, O. Laghrouche, and G. Medero. Time domain 3d finite element modelling of train-induced vibration at high speed. *Computers & Structures*, 2013.
- [16] Tse Spartan Azoh, Wolfgang Nzie Bonaventure Djeumako, and Bertin Soh Fotsing. Modeling of train track vibrations for maintenance perspectives: application. *European Scientific Journal*, 10(21):260–275, July 2014.
- [17] Rasa ŽYGIENĖ, Marijonas BOGDEVIČIUS, and Laima DABULEVIČIENĖ. A mathematical model and simulation results of the dynamic system railway vehicle wheel–track with a wheel flat. *Mokslas – Lietuvos Ateitis Science – Future Of Lithuania*, 6(5):531–537, December 2014.
- [18] D. J. Thompson. Theoretical modelling of wheel-rail noise generation. *Proceedings of the Institution of Mechanical Engineers, Part F: Journal of Rail and Rapid Transit*, 1991.
- [19] R. John Hill and David C. Carpenter. Rail track distributed transmission line impedance and admittance: Theoretical modeling and experimental results. *IEEE TRANSACTIONS ON VEHICULAR TECHNOLOGY*, 1993.
- [20] Marinna Lubomirova Berova. *Development of software tools for simulation and design of jointless track circuits*. PhD thesis, University of Bath, 1997.
- [21] R. Cantieni. Experimental methods used in system identification of civil engineering structures. In *International Operational Modal Analysis Conference*, 2004.
- [22] R. Pintelon, J. Schoukens, and G. Vandersteen. Frequency domain system identification using arbitrary signals. *IEEE Transactions On Automatic Control*, 42(12):1717–1720, December 1997.
- [23] M.A. De Los Santos, J. Martinez, and S. Cardona. A convolution application to determine the dynamic response of a railway track. *Mechanical Systems and Signal Processing*, 1995.
- [24] Tatsuo Oyama and Masashi Miwa. Mathematical modelling analysis for obtaining an optimal railway track maintenance schedule. *Japan Journal of Industrial and Applied Mathematics*, 2006.
- [25] Ján Benčat. Assessment of ground vibration from passing train. In *Third International Conference on Recent Advances in Geotechnical Earthquake Engineering and Soil Dynamics.*, volume II, pages 753–756, April 1995.
- [26] A Bracciali and G Cascini. Detection of corrugation and wheel flats of railway wheels using energy and cepstrum analysis of rail acceleration. *Journal of Rail and Rapid Transit*, 1997.
- [27] Paul G. Steets and Yan H. Tse. Conrail’s integrated automated wayside inspection. In *Proceedings of the 1998 ASME/IEEE Joint Railroad Conference*, 1998.
- [28] Sinan AL Suhairy. Prediction of ground vibration from railways. REPORT 2000: 25, SP Swedish National Testing and Research Institute , Acoustics, 2000.

- [29] Sakdirat Kaewunruen and Alex M. Remennikov. Field trials for dynamic characteristics of railway track and its components using impact excitation technique. *NDT&E International*, 2007.
- [30] S Kaewunruen and A M Remennikov. Dynamic properties of railway track and its components: recent findings and future research direction. *Insight*, 2010.
- [31] See Yenn Chong, Jung-Ryul Lee, and Hye-Jin Shin. A review of health and operation monitoring technologies for trains. *Smart Structures and Systems*, 2010.
- [32] J. Sadeghi. Field investigation on vibration behavior of railway track systems. *International Journal of Civil Engineering*, 2010.
- [33] Xiang Liu, M. Rapik Saat, and Christopher P. L. Barkan. Analysis of causes of major train derailment and their effect on accident rates. *Transportation Research Record: Journal of the Transportation Research Board*, 2289(1):154–163, January 2012.
- [34] Xiukun Wei, Ying Guo, Limin Jia, and Hai Liu. Fault detection of rail vehicle suspension system based on cpca. In *2013 Conference on Control and Fault-Tolerant Systems (SysTol)*, 2013.
- [35] Mayorkinos Papaelias, Arash Amini, Zheng Huang, Patrick Valley, Daniel Cardoso Dias, and Spyridon Kerkyras. Online condition monitoring of rolling stock wheels and axle bearings. *Journal of Rail and Rapid Transit*, 2016.
- [36] Chen Yuejian, Xing Zongyi, Li Jianwei, and Qin Yong. The analysis of wheel-rail vibration signal based on frequency slice wavelet transform. In *2014 IEEE 17th International Conference on Intelligent Transportation Systems (ITSC)*, pages 1312–1316, 2014.
- [37] Alireza Alemi, Francesco Corman, and Gabriel Lodewijks. Condition monitoring approaches for the detection of railway wheel defects. *Journal of Rail and Rapid Transit*, 2016.
- [38] F. BENEDETTO, F. TOSTI, and M. (Amir) ALANI. An entropy-based analysis of gpr data for the assessment of railway ballast conditions. *IEEE Transactions on Geoscience and Remote Sensing*, 2017.
- [39] Chunsheng Li, Shihui Luo, Colin Cole, and Maksym Spiryagin. An overview: modern techniques for railway vehicle on-board health monitoring systems. *Vehicle System Dynamics*, 2017.
- [40] Rafał Melnik and Seweryn Koziak. Rail vehicle suspension condition monitoring approach and implementation. *JOURNAL OF VIBROENGINEERING*, 2017.
- [41] Diego A Tobon-Mejia, Pierre Dersin, and Gerard Tripot. Challenges and opportunities in applying vibration based condition monitoring in railways.
- [42] Vepa Atamuradov, Kamal Medjaher, Fatih Camci, Pierre Dersin, and Pierre Dersin. Railway point machine prognostics based on feature fusion and health state assessment. *IEEE Transactions On Instrumentation And Measurement*, 2018.

- [43] Issam Abu-Mahfouz. Drilling wear detection and classification using vibration signals and artificial neural network. *International Journal of Machine Tools and Manufacture*, 2003.
- [44] A. Krishnakumari, A. Elayaperumal, M. Saravanan, and C. Arvindan. Fault diagnostics of spur gear using decision tree and fuzzy classifier. *The International Journal of Advanced Manufacturing Technology*, 2017.
- [45] B. SAMANTA and K.R. AL-BALUSHI. Artificial neural network based fault diagnostics of rolling element bearings using time-domain features. *Mechanical Systems and Signal Processing*, 2003.
- [46] Zhongjie Shen, Zhengjia He, Xuefeng Chen, Chuang Sun, and Zhiwen Liu. A monotonic degradation assessment index of rolling bearings using fuzzy support vector data description and running time. *Sensors*, 2012.
- [47] B. Sreejith, A.K. Verma, and A. Srividya. Fault diagnosis of rolling element bearing using time-domain features and neural networks. In *2008 IEEE Region 10 Colloquium and the Third ICIS, Kharagpur, INDIA December 8-10., 2008*.
- [48] N. BESSOUS, S. SBAA, and A. C. MEGHERBI. Mechanical fault detection in rotating electrical machines using mcsa-fft and mcsa-dwt techniques. *Bulletin Of The Polish Academy Of Sciences : Technical Sciences*, 2019.
- [49] Bo-Suk Yang and Kwang Jin Kim. Application of dempster–shafer theory in fault diagnosis of induction motors using vibration and current signals. *Mechanical Systems and Signal Processing*, 20(2006):403–420, 2006.
- [50] Jan Bien, Paweł Rawa, Jarosław Zwolski, J Krzyzanowski, Waclaw Skoczynski, and J Szymkowski. System for monitoring of steel railway bridges based on forced vibration tests. In *The Third International Conference on Bridge Maintenance, Safety and Management*.
- [51] Yijun Pan, Chunjie Yang, Youxian Sun, Ruqiao An, and Lin Wang. Fault detection with principal component pursuit method. In *Journal of Physics: Conference Series 659 (2015) 012035*, 2015.
- [52] Jarosław Zwolski and Jan Bień. Modal analysis of bridge structures by means of forced vibration tests. *JOURNAL OF CIVIL ENGINEERING AND MANAGEMENT*, 2011.
- [53] Wahyu Caesarendra and Tegoeh Tjahjowidodo. A review of feature extraction methods in vibration-based condition monitoring and its application for degradation trend estimation of low-speed slew bearing. *Machines*, 2017.
- [54] Wilson Wang and Hewen Lee. An energy kurtosis demodulation technique for signal denoising and bearing fault detection. *Measurement Science And Technology*, 2013.
- [55] Saeed Nezamivand Chegini and Farid Najafi Ahmad Bagheri. Application of a new ewt-based denoising technique in bearing fault diagnosis. *Measurement*, 2019.

- [56] Bo Chen, Sheng lin Zhao, and Peng yun Li². Application of hilbert-huang transform in structural health monitoring: a state-of-the-art review. *Mathematical Problems in Engineering*, 2014.
- [57] Jinglong Chen, Yanyang Zi, Zhengjia He, and Jing Yuan. Improved spectral kurtosis with adaptive redundant multi-wavelet packet and its applications for rotating machinery fault detection. *Measurement Science And Technology*, 2012.
- [58] K. F. FONG, A. P. LOH, and W. W. TAN. A frequency domain approach for fault detection. *International Journal of Control*, 81(2):264–276, February 2008.
- [59] Tian li Huang, Wei xin Ren, and Meng lin Lou. The orthogonal hilbert-huang transform and its application in earthquake motion recordings analysis. In *The 14th World Conference on Earthquake Engineering*, 2008.
- [60] Xiaohang Jin, Jicong Fan, and Tommy W. S. Chow. Fault detection for rolling-element bearings using multivariate statistical process control methods. *IEEE Transactions On Instrumentation And Measurement*, 2018.
- [61] Narendiranath Babu Thamba, H.S. Himamshu, Prabin Kumar Nayak, D. Rama Prabha, and Nishant Chiluar. Journal bearing fault detection based on daubechies wavelet. *Archives Of Acoustics*, 2017.
- [62] R. B W Heng and Mohd. Jailani Mohd Nor. Statistical analysis of sound and vibration signals for monitoring rolling element bearing condition. *Applied Acoustics*, 1998.
- [63] H.R. Martin and F. Honarvar. Application of statistical moments to bearing failure detection. *Applied Acoustics*, 1995.
- [64] Vikas Sharma and Anand Parey. Gearbox fault diagnosis using rms based probability density function and entropy measures for fluctuating speed conditions. *Structural Health Monitoring*, 2016.
- [65] Jiedi Sun, Changhong Yan, and Jiangtao Wen. Intelligent bearing fault diagnosis method combining compressed data acquisition and deep learning. *IEEE Transactions On Instrumentation And Measurement*, 2017.
- [66] C.T. Yiakopoulos, K.C. Gryllias, and I.A. Antoniadis. Rolling element bearing fault detection in industrial environments based on a k-means clustering approach. *Expert Systems with Applications*, 38(2011):2888–2911, 2011.
- [67] Jyoti Kumar Barman and Durlav Hazarika. Condition monitoring of nfr trains with measurements from a single wayside 3d vibration sensor. *IEEE Sensors Journal*, 20(8): 4096–4103, April 2019.
- [68] Jyoti Barman and Durlav Hazarika. Linear and quadratic time–frequency analysis of vibration for fault detection and identification of NFR trains. *IEEE Transactions on Instrumentation and Measurement*, 69(11):8902–8909, nov 2020. doi: 10.1109/tim.2020.2998888.
- [69] V. V. Krylov. *Noise and vibration from high-speed trains*. Thomas Telford Publishing,, 2001.

- [70] D.S. Fedorov, A.Y. Ivoylov, V.A. Zhmud, and V.G. Trubin. Using of measuring system mpu6050 for the determination of the angular velocities and linear accelerations. *Automatics & Software Enginery*, 2015.
- [71] B.S. Manke. *Linear Control Systems with MATLAB Applications*. Khanna Publishers, 1986.
- [72] BS Reporter. Indian railways to invite bids for rail health monitoring systems, October 2015. URL https://www.business-standard.com/article/economy-policy/indian-railways-to-invite-bids-for-rail-health-monitoring-systems-115102101285_1.html.
- [73] Railway Pro Communication System. Indian railways to acquire on board monitoring systems, March 2017. URL <https://www.railwaypro.com/wp/indian-railways-acquire-board-monitoring-systems/>.
- [74] Press Information Bureau. On board condition monitoring system (obcms) for rolling stock of indian railways, April 2017. URL <https://pib.gov.in/newsite/PrintRelease.aspx?relid=160685>.
- [75] Rakesh Dubbudu. Accidents in indian railways- review of the last 6 years. <https://factly.in/indian-railway-accidents-statistics-review-last-5-years/>, NOVEMBER 2016. URL <https://factly.in/indian-railway-accidents-statistics-review-last-5-years/>. Accessed on 12-09-2019.
- [76] H P Wang, P Xiang, and X Li. Theanalysis analysis on strain transfer error of fbg sensors attached on steel structures subjected to fatigue load. *STRAIN*, 52(6):522–530, 2016.
- [77] Huaping Wang, Lizhong Jiang, and Ping Xiang. Improving the durability of the optical fibre sensor based on strain transfer analysis. *Optical Fiber Technology*, 42(2018): 97–104, 2018.
- [78] Allan V. Oppenheim, Alan S. Willsky, and S. Hamid Nawab. *Signals and Systems*. PHI Learning Private Limited, 2010.
- [79] A. N. Thite, S. Banvidi, T. Ibicek, and L. Bennett. Suspension parameter estimation in the frequency domain using a matrix inversion approach. *Vehicle System Dynamics*, 49(12):1803–1822, December 2011.
- [80] D King, W B Lyons, C Flanagan, , and E Lewis 2. An optical fibre ethanol concentration sensor utilizing fourier transform signal processing analysis and artificial neural network pattern recognition. *Journal Of Optics A: Pure And Applied Optics*, 2003.
- [81] Smutny J. Analysis of vibration since rail transport by using wigner-ville transform. In *TRANSCOM 99 - 3-rd European Conference of Young Research and Science Workers in Transport and Telecommunications*, Zilina, 1999.
- [82] Weilin Li, Antonello Monti, and Ferdinanda Ponci. Fault detection and classification in medium voltage dc shipboard power systems with wavelets and artificial neural networks. *IEEE Transactions On Instrumentation And Measurement*, 2014.

- [83] Z.K. Peng and F.L. Chu. Application of the wavelet transform in machine condition monitoring and fault diagnostics: a review with bibliography. *Mechanical Systems and Signal Processing*, page 199–221, 2004.
- [84] Stephane Mallat and Wen Liang Hwang. Singularity detection and processing with wavelets. *IEEE Transactions On Information Theory*, 1992.
- [85] Jaroslav Smutny, Viktor Nohal, Daniela Vukusicova, and Herbert Seelmann. Vibration analysis by the wigner-ville transformation method. *Communications: Scientific Letters Of The University Of Zilina*, 2018.
- [86] E.L. Schukin, R.U. Zamaraev, and L.I. Schukin. The optimisation of wavelet transform for the impulse analysis in vibration signals. *Mechanical Systems and Signal Processing*, 2004.
- [87] Ruqiang Yan, Robert X. Gao, and Changting Wang. Experimental evaluation of a unified time-scale-frequency technique for bearing defect feature extraction. *Journal of Vibration and Acoustics*, 131(4), jun 2009. doi: 10.1115/1.3147125.
- [88] Ruqiang Yan and Robert X. Gao. Rotary machine health diagnosis based on empirical mode decomposition. *Journal of Vibration and Acoustics*, 130(2), feb 2008. doi: 10.1115/1.2827360.
- [89] N. Tandon. A comparison of some vibration parameters for the condition monitoring of rolling element bearings. *Measurement*, 1994.
- [90] Karl Martin Reichard, Mike Van Dyke, and Ken Maynard. Application of sensor fusion and signal classification techniques in a distributed machinery condition monitoring system. In *Proceedings of SPIE - The International Society for Optical Engineering*, 2000.
- [91] Lin Xiao, Stephen Boyd, and Sanjay Lall. A scheme for robust distributed sensor fusion based on average consensus. In *IPSN 2005. Fourth International Symposium on Information Processing in Sensor Networks, 2005.*, 2005.
- [92] Ying Zhang, Hongfu Zuo, and Fang Bai. Classification of fault location and performance degradation of a roller bearing. *Measurement*, 46(2013):1178–1189, 2013.
- [93] Igor Neri, Flavio Travasso, Riccardo Mincigrucchi, Helios Vocca, Francesco Orfei, and Luca Gammaitoni. A real vibration database for kinetic energy harvesting application. *Journal of Intelligent Material Systems and Structures*, 23(18):2095–2101, 2012.



List of publication

Journal papers

1. J. K. Barman and D. Hazarika, "Condition Monitoring of NFR Trains With Measurements From a Single Wayside 3D Vibration Sensor," in *IEEE Sensors Journal*, vol. 20, no. 8, pp. 4096-4103, 15 April 2020, doi: 10.1109/JSEN.2019.2961942.
2. J. Barman and D. Hazarika, "Linear and Quadratic Time–Frequency Analysis of Vibration for Fault Detection and Identification of NFR Trains," in *IEEE Transactions on Instrumentation and Measurement*, vol. 69, no. 11, pp. 8902-8909, Nov. 2020, doi: 10.1109/TIM.2020.2998888.
3. Hazarika, D., Barman, J.K. Development of a Mathematical Model for a Railway Track Using a Gray-Box Modelling Technique. *J. Inst. Eng. India Ser. B* 101, 667–675 (2020). <https://doi.org/10.1007/s40031-020-00489-y>

B

List of papers communicated

1. J. Barman, D. Hazarika, "Health Monitoring of a few Passenger Trains Using Statistical Measures and Graph Signal Processing," in *Sādhanā*

